Center for Cardiovascular Research, Charité, Berlin &
Max-Planck Institut for Molecular Genetics, Berlin

The human G Protein-Coupled Receptor GPR30: interaction partners and expression analysis in endothelial cells

Dissertation

zur Erlangung des akademischen Grades

doctor rerum naturalium (Dr. rer. Nat.)

im Fach Biologie

eingereicht an der

Mathematisch-Naturwissenschaftlichen Fakultät I

der Humboldt-Universität zu Berlin

von

Valeria Zazzu

Präsident: Prof. Dr. Jan-Hendrik Olbertz
Dekan: Prof. Dr. Andreas Herrmann

Gutachter/innen:

1. Prof. Dr. Patricia Ruiz Noppinger
2. Prof. Dr. Peter-Michael Kloetzel
3. Prof. Dr. Franz Theuring

Datum der mündl. Prüfung: 02.03.2011

Dedicata a Papà e Mamma

ZUSAMMENFASSUNG

Im Jahr 1997 wurden der Orphan-G-Protein-gekoppelte Rezeptor 30 (GPR30) aus menschlichen Nabelschnur-Endothelzellen (HUVECs) kloniert, die *Fluid Shear Stress* (FSS), einer mechanischen Kraft, die auf Blutgefäße wirkt, ausgesetzt waren. In dieser Studie von Takada *et al* konnte gezeigt werden, dass die Expression von GPR30 durch die FSS-Behandlung im Vergleich zu unbehandelten HUVEC-Zellen deutlich induziert wurde. Daraufhin wurde in einer Studie im dem Labor, in dem die Experimente für diese Arbeit durchgeführt wurden, die zelluläre und gewebsspezifische Expression von GPR30 in GPR30-LacZ Reportergen-Mäusen untersucht. Es konnte eine Expression von GPR30 vorwiegend in den Endothelzellen der kleinen Arterien verschiedenster Gewebetypen nachgewiesen werden.

Vor einigen Jahren wurde von zwei unabhängigen Gruppen postuliert, dass GPR30, 17-β-Östradiol (E2) direkt binden kann und dadurch rasche nicht-genomische Signale vermittelt. Im Gegensatz dazu haben verschiedene andere Veröffentlichungen gezeigt, dass E2 nicht spezifisch an GPR30 bindet. Trotz der Kontroverse, ob es sich bei GPR30 um einen Östrogenrezeptor oder um einen Orphan-Rezeptor handelt, ist bislang nichts über seine Interaktion zu anderen Proteinen und deren Wechselwirkung bekannt. Deswegen, und aufgrund der Tatsache, dass mehrere Berichte darauf hindeuten, dass GPCRs mit mehreren Proteinen (neben denen, die in der traditionellen Vorstellung mit heterotrimeren G-Proteine wechselwirken) interagieren bzw. von diesen reguliert werden, war ein Ziel dieser Arbeit, Interaktionspartner von menschlichen GPR30 zu identifizieren und folglich ein humanes vaskuläres *in vitro* Modell zu etabliren, um die potentiellen Interaktionen von GPR30 sowie die downstream-Effekte der Wechselwirkung zwischen GPR30 und den neuen Interaktionspartner des vaskulären Modells auf Transkriptebene zu evaluieren.

Ein Screening einer humanen kardiovaskulären cDNA-Bibliothek mit Hilfe des Hefe-2-Hybrid (Y2H)-Systems führte zur Identifizierung mehrerer Interaktionspartner für GPR30, darunter das PALS1-assoziierten Tight Junction-Protein (PATJ) und das FUN14 domain containing 2-Protein (FUNDC2). Durch anschließende Ko-Immunopräzipitation (CoIP)-Experimente konnte die Interaktion von GPR30 mit PATJ validiert werden. Zusätzlich wurde eine teilweise zelluläre Ko-Lokalisation gefunden. Des Weiteren konnte in dieser Arbeit die Wirkung von FSS auf die Expression von GPR30 in HUVEC-Zellen bestätigt und ebenfalls in weiteren anderen Endothelzellen gezeigt werden. So wurde eine Hoch-regulierung der Expression von GPR30 induziert durch FSS in humanen arteriellen Nabelschnul-Endothelzellen (HUAECs), humanen Aorten-Endothelzellen (HAoECs) und in humanen mikrovaskulären Endothelzellen (HMEC-1) gefunden, was darauf hindeutet, dass GPR30 in der Tat eine wichtige Rolle in der vaskulären Physiologie spielt. Abschließend wurde die Rolle von GPR30 und PATJ bei der Reaktion auf FSS auf transkriptioneller Ebene in HMEC-1-Zellen

genomweit untersucht. Interessanterweise war eine Gruppe von Genen aufgrund von FSS in Zellen, die GPR30 überexprimierten dereguliert, als alleine durch FSS. Darunter waren Gene, die zum einen eine wichtige Rolle bei verschiedenen Funktionen und der Morphogenese von Gefäßen spielen, z.B. Plexin D1 (PLXND1) und Troponin I Typ 3 (TNNI3) und zum anderen an der Entwicklung und der Funktion des endokrinen Systems beteiligt sind, z.B. der ras-related and E2-regulated growth inhibitor (RERG), der in der E2-Signalkaskade involviert ist. Zusammenfassend zeigt diese Arbeit zum ersten Mal die Interaktion von GPR30 und PATJ und beschreibt ein Modell, mit dessen Hilfe die Funktion von GPR30 in Endothelzellen weiter untersuchen könnte.

Schlagwörter: GPR30, fluid shear stress, PATJ, endothelzellen.

ABSTRACT

In 1997, the orphan G protein-coupled receptor 30, GPR30 was cloned using human umbilical vein endothelial cells (HUVECs) exposed to fluid shear stress (FSS), one of the mechanical forces acting on blood vessels. Takada *et al.* have shown that the level of GPR30 expression was markedly induced in response to FSS. Subsequently, in a study performed in the laboratory where the work for this thesis was carried out, the cellular and tissue distribution of GPR30 were investigated in GPR30-LacZ reporter mice and the expression was found predominantly in the endothelial cells of small arteries in several tissue types. GPR30, was claimed some years later to bind 17-β-estradiol (E2) directly and to mediate rapid non-genomic signalling. In contrast, various reports have indicated that E2 fails to bind GPR30 in a specific manner. Despite the controversy on whether GPR30 is an estrogen receptor or still an orphan receptor, nothing is known at present about its relation and interaction with other proteins. Therefore, also according to several reports suggesting that GPCRs interact with and are regulated by several other proteins beyond the established role of heterotrimeric G proteins, the aim of the work described in this thesis was to identify human GPR30 protein interaction partners and to establish a human vascular *in vitro* model in order to evaluate the potential role of GPR30 and the downstream effects of the interaction between GPR30 and new interaction partners in a vascular model at transcript level. The screening of a human heart cDNA library using the yeast two-hybrid (Y2H) assay led to the identification of several interaction partners for GPR30, among them PALS1-associated tight junction protein (PATJ) and the FUN14 domain containing 2 (FUNDC2). These interactions were verified by co-immunoprecipitation (CoIP) experiments and the interaction of GPR30 with PATJ could be confirmed. The effect of FSS on the expression of GPR30 was confirmed in HUVECs and was detected in other endothelial cell types. In Human Umbilical Arterial (HUAECs), Human Aortic (HAoECs) and Human Microvascular Endothelial Cells (HMEC-1) GPR30 was also found up-regulated upon FSS, suggesting that GPR30 may indeed play a key role in vascular physiology. Finally, the role of GPR30 and PATJ in the FSS response was investigated at the genome-wide transcript level in HMEC-1 cells. Interestingly, a different panel of genes was deregulated owing to FSS in cells over-expressing GPR30 compared to FSS alone. These included genes that play an important role in vascular function and morphogenesis, e.g. plexin D1 (PLXND1) and troponin I type 3 (TNNI3), and in the development and function of the endocrine system, e.g. the ras-related and E2-regulated growth inhibitor (RERG), which is involved in E2 signalling. Taken together, this study provides evidence for the first time for an interaction between GPR30 and PATJ and proposes a model to further evaluate the role of GPR30 in endothelial cells.

Keywords: GPR30, fluid shear stress, PATJ, endothelial cells.

TABLE OF CONTENTS

ABBREVIATIONS

[3H]-E2	tritium-labelled E2
AC	adenylyl cyclase
AERKO	ERα KO mice
Amot	angiomotin
AP2	adaptor protein 2
AR	ampicillin resistance
Bcl2	B-cells lymphoma 2 gene
BERKO	ERβ KO mice
BLAST	basic local alignment search tool
BT-20	breast cancer cells
cAMP	cyclic adenosine monophosphate
CaSR	calcium sensing receptor
CoIP	co-immunoprecipitation
COS-7	monkey kidney fibroblasts
DAG	diacylglycerol
DAPI	4′,6-diamidin-2-phenylindol
DAVID	database for annotation, visualization and integrated discovery
DlgA	Drosophila disc large tumor suppressor
DN	double negative
DP	double positive
ECL	extracellular loop
ECs	endothelial cells
EGF	epidermal growth factor
ERKs	extracellular signal-regulated kinases
ERs	estrogen receptors
EST	expressed sequence tag
FEG-1	flow induced endothelial G protein-coupled receptor gene-1
FSS	fluid shear stress
FUNDC2	FUN14 domain-containing 2 protein.
GABAB	gamma-aminobutyric acid class B
GDP	guanosine diphosphate
GEF	guanine nucleotide exchange factor
GFP	green fluorescent protein
GIP	GPCR-interacting proteins
GPCR-Br	G protein-coupled estrogen receptor in breast
GPCRs	G protein-coupled receptors
GPER	G protein-coupled estrogen receptor
GPR30	G protein-coupled receptor
GRKs	GPCR kinases
GTP	guanosine triphosphate

HA	haemagglutinin
HAoECs	human aortic endothelial cells
HB-EGF	heparin-binding EGF-like growth factor
HEK293	human embryonic kidney cells
HIS3	imidazoleglycerol-phosphate dehydratase
HMEC-1	human microvascular endothelial cell
HPRT	hypoxanthine-guanine phosphoribosyl transferase
HUAECs	human umbilical arterial endothelial cells
HUVEC	human umbilical vein endothelial cells
I/R	ischemia/reperfusion
ICAM-1	intercellular adhesion molecule-1
ICL	intracellular loop
IP3	inositol triphosphate
IUPHAR	international union of pharmacology
JNKs	c-Jun N-terminal kinases
Ki	dissociation constant
KLF2	Krueppel-like factor 2
KO	knockout mice
KR	kanamycin resistance
LacZ	β-galactosidase
LyGPR	lymphocyte derived G - protein-coupled receptor
mGluR5	metabotropic glutamate receptor 5
MMP	metalloproteinase
NR	neomycin resistance
ORF	open reading frame
ovx	ovariectomised
PATJ	Pals1-associated tight junction protein
PBS	phosphate buffered saline
PCR	polymerase chain reaction
PDZ	PSD95, DlgA, ZO-1
PICK1	protein interacting with protein kinase C
PICK1	protein interacting with protein kinase C
PIP2	phosphatidylinositol-4,5-biphosphate
PKA	protein kinase A
PLCβ	phospholipase C-β
PLCγ	phospholipase C-γ
PLXND1	plexin D1
PSD95	post synaptic density protein
RAMPs	receptor activity-modifying proteins
RERG	RAS-like, estrogen-regulated, growth inhibitor
RT	room temperature
RZPD	german resource center for genome research
SAM	significance analysis of microarrays
siRNA	small interfering RNA
SMCs	smooth muscle cells

SP	single positive
SV40	simian virus
Syx	synectin-binding guanine exchange factor
TAP	tandem affinity purification
THS	trauma-haemorrhagic shock
TNNI3	and troponin I type 3
Y2H	yeast two-hybrid screening
ZO-1	zonula occludens-1 protein
αGST	α-glutathione S-transferase

LIST OF FIGURES

LIST OF TABLES

1 INTRODUCTION

1.1 G protein-coupled receptors (GPCRs)

G protein-coupled receptors (GPCRs) – also known as seven transmembrane domain receptors, 7TM receptors, and heptahelical receptors – represent one of the largest gene families. In humans, these membrane proteins control different physiological processes and also mediate most cellular responses to hormones, biogenic amines, peptides, lipids and neurotransmitters. Indeed, they are responsible for cellular metabolism, growth and inflammatory responses as well as for vision, olfaction and taste (Pierce et al., 2002).

Two main features identify a receptor as a GPCR. The first structural requirement common to all GPCRs is the presence of seven transmembrane sequences with about 25–35 consecutive amino-acid residues responsible for the protein's high hydrophobicity. These seven α-helices segments span, in a counter-clockwise manner, the membrane connected by alternating intracellular and extracellular loop (ICL and ECL) regions and with an amino terminus located on the extracellular side and a carboxy terminus on the intracellular side (Figure 1). The second feature is the ability of the receptor to bind a G protein, allowing the activation of various signalling pathways within the cell. Because of their ability to recruit and regulate the activity of intracellular heterotrimeric G proteins, they have been named GPCRs. For many GPCRs the interaction with G proteins has not yet been demonstrated, and it would therefore be more correct to name these receptors 7TM receptors, but the term GPCR is in more common use (Fredriksson et al., 2003), (Kristiansen, 2004).

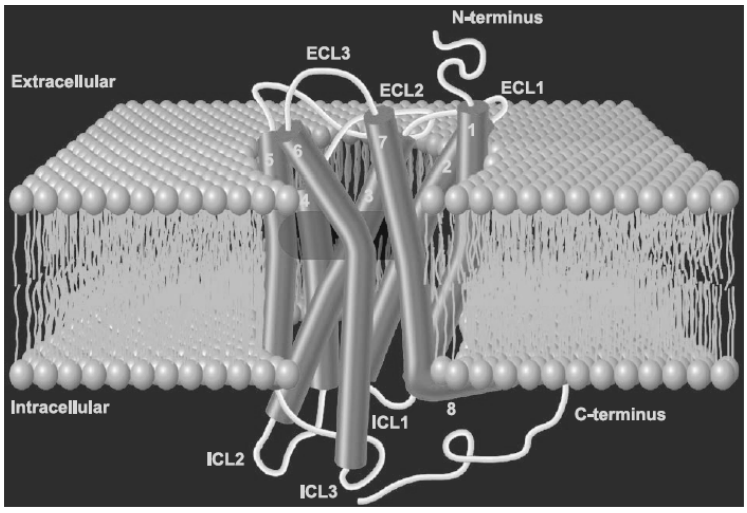

Figure 1: GPCRs structure
Seven α-helices segments span the membrane connected by intra- and extra-cellular loops (ICL and ECL). Adapted from Kristiansen *et al*. 2004 (Kristiansen, 2004).

So far, in humans, more than 1000 genes encoding GPCRs have been identified, of which over 400 are olfactory and 356 non-olfactory GPCRs, according to the International Union of Pharmacology (IUPHAR) database (http://www.iuphar-db.org/index.jsp) (Harmar et al., 2009). Among the non-olfactory receptors 134 are annotated as orphan GPCRs. These orphan receptors lack an endogenous ligand and for this reason are of great pharmacological interest as potential new drug targets (Chung et al., 2008). Indeed, GPCRs also represent therapeutic drug targets (≈50% of modern pharmaceuticals) of choice in cancer, cardiac dysfunction, diabetes, inflammation, pain, etc. (Vassilatis et al., 2003).

1.1.1 Classification of GPCRs

Significant sequence homology is found within several groups. Thus, on the basis of sequence similarity, all known GPCRs have been classified into three major families:
Family A: Receptors related to the rhodopsin and the β_2-adrenergic receptor. This group contains most of the 7TM receptor types, including the olfactory subgroup.
Family B: Receptors related to the glucagon receptor. This family comprises only about 25 members, including the receptors for the gastrointestinal peptide hormone family (secretin, glucagon, vasoactive intestinal peptide), calcitonin and parathyroid hormone.
Family C: Receptors related to the metabotropic neurotransmitter receptors. This quite small group contains, besides the metabotropic receptor $GABA_B$, the calcium-sensing receptor and some taste receptors (Pierce et al., 2002), (Gether, 2000), (Jassal et al.).

In a second classification system, based on phylogenetic analysis, 342 unique, non-olfactory, human GPCRs were classified into five families:
Family G: the glutamate receptor family,
Family R: the rhodopsin receptor family,
Family A: the adhesion receptor family,
Family F: the frizzled/taste2 receptor family,
Family S: the secretin receptor family.

Common to both classifications are three of these families, the rhodopsin (A), secretin (B) and glutamate (C) families, while families F and S are not included in the previous classification (Fredriksson et al., 2003). The GPCR investigated in the present study, the 7TMR GPR30 belongs to the class A (rhodopsin-like) receptors, sub-family peptide receptors, sub-sub-family chemokine receptor-like 2, which contains only GPR30 orthologues of different species.

1.1.2 Activation and termination of GPCR signalling

The activation of GPCRs is related to the structure of a ternary complex, which comprises the receptor, the ligand and the G protein. This complex is maintained in an equilibrium between the active and inactive states. Once the ligand binds the receptor, there is a conformational change of the receptor leading to the activation of the G protein. The G proteins (short for "guanine-nucleotide-binding proteins"), make up a family of heterotrimeric proteins consisting of three subunits called α, β and γ. They function as "molecular switches" activating the second messenger cascades. In particular, the activated G protein favours the release of GDP from the α subunit and its replacement with GTP. At this stage the G protein complex dissociates into the α subunit and a βγ dimer, both of which modulate a variety of cellular responses. Subsequently, hydrolysis of GTP to GDP leads to re-association of the G protein subunits (Figure 2) (Pierce et al., 2002).

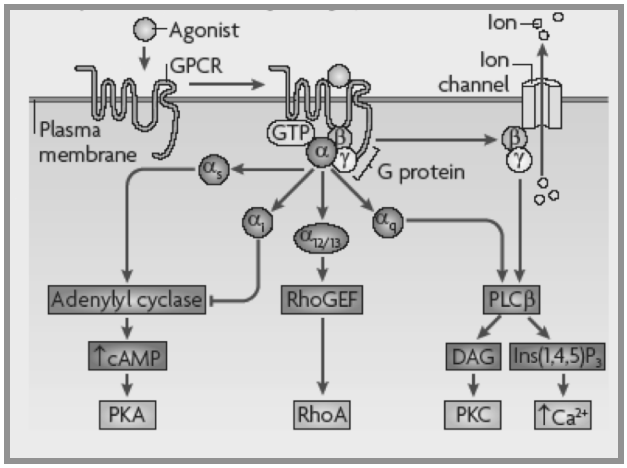

Figure 2: GPCRs signalling scheme
Once the agonist binds the receptor, the G protein complex dissociates into α subunit and a βγ dimer, both of which modulate a variety of cellular responses. Adapted from Ritter et al. 2009 (Ritter und Hall, 2009).

In humans, there are 21 Gα subunits encoded by 16 genes, 6 Gβ subunits encoded by 5 genes, and 12 Gγ subunits. Generally, the G proteins are referred to their respective Gα subunit, divided into four main classes based on similarity of their sequences: $G\alpha_s$, $G\alpha_i$, $G\alpha_q$ and $G_{\alpha 12}$. Thus the G_s heterotrimeric complex contains $G\alpha_s$, the G_i contains $G\alpha_i$, and so on. Members of the G_s (stimulatory G protein) family activate adenylyl cyclase (AC) which synthesises intracellular cyclic adenosine monophosphate (cAMP), a second messenger able to interact with and to activate protein kinase A (PKA). PKA can then phosphorylate numerous downstream targets. Relaxation of blood vessels, gene regulation and modulation of ion channels are results of the $G\alpha_s$-induced signalling cascade. In contrast, members of the G_i (inhibitory G protein) family inhibit the cAMP-dependent pathway by inhibiting AC activity; additionally, G_i act mainly by directly regulating ion channels. Stimulation of growth

and contraction of blood vessels are the results of $G\alpha_i$-induced signalling. Many GPCRs function through a G_q protein by activating phospholipase C-β (PLCβ), which catalyses the hydrolysis of phosphatidylinositol-4,5-biphosphate (PIP_2) into inositol triphosphate (IP_3) and diacylglycerol (DAG). IP_3 then promotes the mobilisation of intracellular calcium (Ca^{2+}), while DAG stimulates the activity of protein kinase C. As in the case of G_i, G_q-induced signalling is involved in the contraction of blood vessels. $G_{\alpha 12}$ is a family of proteins that can activate a guanine nucleotide exchange factor (GEF) that in turn activates a monomeric GTPase of the Rho family (regulation factors family in the transcription of DNA to RNA). Once dissociated from the Gα subunit, the Gβγ subunits can also bind to and regulate downstream effectors, such as phospholipase C-γ (PLCγ) and ion channels (Wilkie et al., 1992), (Ritter und Hall, 2009).

After ligand stimulation, most GPCRs show a rapid loss of responsiveness, also called desensitisation. Termination of a G protein-mediated signalling occurs through GPCR kinases (GRKs)-β-arrestin system. The GRKs as well as the arrestins are encoded from different genes: so far, seven different genes are known for GRKs and four genes for arrestins, of which some are exclusively expressed in specific cell-type while some are ubiquitously distributed. Only after ligand binding, the receptor, in its activated conformation, can be phosphorylated and recruits an arrestin molecule, which interacting with clathrin and clathrin adaptor protein 2 (AP2) drives GPCR internalisation into endosomes. Subsequently, GPCRs can be transported either to lysosomes, where they are degraded, or to recycling endosomes, where they can be sent back to the plasma membrane to start a new round of signalling (Krupnick und Benovic, 1998), (Jalink und Moolenaar).
Recent findings indicate that β-arrestins are also involved in the activation of distinct arrestin-mediated signalling pathways by serving as multiprotein scaffolds for a number of signalling molecules, e.g. extracellular signal-regulated kinases (ERKs), c-Jun N-terminal kinases (JNKs) (Figure 3), (DeWire et al., 2007).

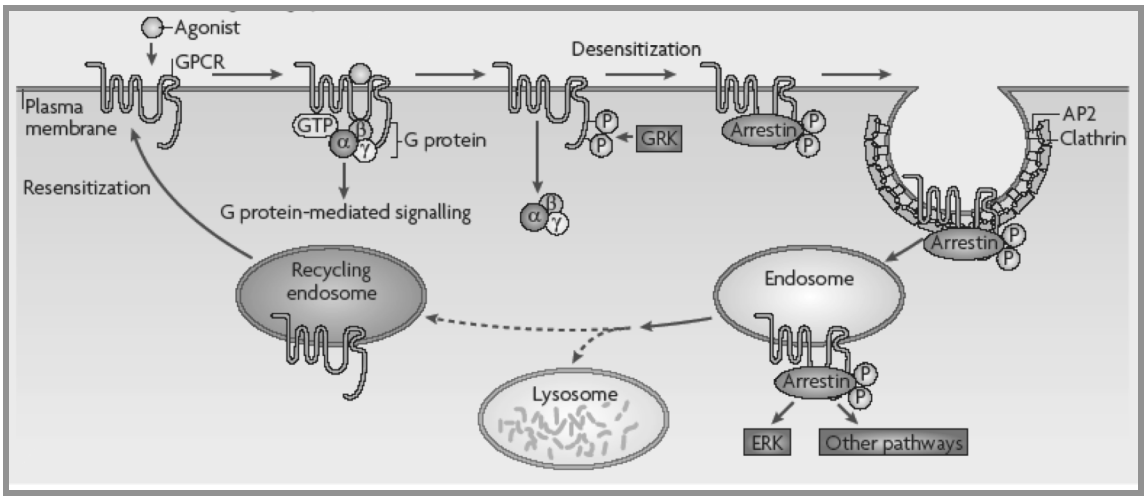

Figure 3: GPCRs desensitisation schema
Termination of a G protein-mediated signalling occurs through GPCR kinases (GRKs)-β-arrestin system. Adapted from Ritter et al. 2009 (Ritter und Hall, 2009).

1.1.3 GPCR interacting proteins

Over the last years, evidence has accumulated suggesting that GPCRs interact with, and are regulated by, several other proteins (GPCR-interacting proteins, GIP), in addition to the specific intramolecular interactions that define the activation states of the receptor, such as the established role of the interaction with heterotrimeric G proteins and the association with GRKs and β-arrestins. GPCRs can interact with another GPCR or with a wide range of GIPs: transmembrane proteins, ionic channels, ionotropic receptors, single transmembrane proteins or soluble proteins.

Indeed, it is widely accepted that many GPCRs can interact with another identical (homodimer) or different (heterodimer) GPCR unit (Milligan, 2009). The potential roles and implications of the formation of such receptor dimers might represent the rule rather than the exception for this important class of receptors. For instance, the use of co-immunoprecipitation approaches with differentially epitope-tagged receptors provided direct biochemical evidence for β2-adrenergic receptor homodimers (Hebert et al., 1996). Since then, similar co-immunoprecipitation approaches have been used to document the dimerisation of several GPCRs, including the neurotransmitter gamma-aminobutyric acid class B ($GABA_B$) (White et al., 1998), metabotropic glutamate receptor 5 (mGluR5) (Romano et al., 1996), δ-opioid (Jordan und Devi, 1999), and calcium sensing (CaSR) (Bai et al., 1998) receptors. The role of dimerisation is not yet clear: either it controls signalling specificity and efficacy, or it simply serves as chaperone to escort the receptors from the different cellular compartments (Milligan, 2009).

So far, mainly GPCRs with known ligands and functions have been studied, but recent findings show clearly that the idea of GPCRs dimerisation can also be extended to orphan

GPCRs (i.e. those without a known ligand) (Civelli et al., 2006) with consequent ligand-independent properties, which provides a novel concept for the elucidation of the function of orphan GPCRs (Levoye et al., 2006). Related to this issue, there is also the possibility that some orphan GPCRs may require the expression of special accessory proteins for their activity. This has been shown in the case of the calcitonin GPCR, which necessitate the presence of receptor activity-modifying proteins (RAMPs) for inducing its signalling pathway (Hay et al., 2006). Other examples of GIPs are PDZ domain-containing proteins which are soluble proteins interacting with the C-terminal domain of GPCRs. So far more than 50 GIPs have been identified binding through their PDZ domain (a sequence of 80–90 amino acids first identified in the three proteins PSD95, DlgA and ZO-1) the PDZ ligand (sequence expressed in the last 3–4 C-terminal residues) of GPCRs (Sheng und Sala, 2001). These proteins can be involved in different processes, depending on the cell in which the GPCR is expressed. For instance, the so-called 'protein interacting with protein kinase C' (PICK1) plays a crucial role in the axonal clustering of the metabotropic glutamate receptor mGluR7a, which localises specifically to presynaptic active zones and interacts with PICK1 (Boudin et al., 2000). Another example of interaction between GPCR and GIP is in *Drosophila* photoreceptor neurons, where the multivalent PDZ protein INAD serves as a scaffold to assemble different components of the phototransduction pathway, in a protein complex directly binding the C terminus of the GPCR rhodopsin together with a Ca^{2+} channel, phospholipase C-β and calmodulin (Chevesich et al., 1997). In conclusion, the elucidation of the nature of these interactions in different cell types is opening up the possibility to design new pharmacological drugs that can disrupt the GPCR-GIP interaction in a tissue without affecting other interactions (Bockaert et al., 2004).

1.2 The G protein-coupled receptor GPR30

The story of GPR30 started during the years 1996–97, when it was cloned by different groups using six independent approaches. Five of these clonings were performed using degenerated polymerase chain reaction (PCR) primers to amplify the transmembrane domains of new GPCRs from cDNA of Burkitt's lymphoblasts (Owman et al., 1996), B cells (Kvingedal und Smeland, 1997), human umbilical vein endothelial cells (HUVECs) stimulated with fluid shear stress (FSS) (Takada et al., 1997) and human genomic DNA (Feng und Gregor, 1997), (O'Dowd et al., 1998) or by using differential cDNA library screening between estrogen receptors (ERs)-positive MCF-7 and ERs-negative MDA-MB-231 breast cancer cell lines (Carmeci et al., 1997). During the years, other names identifying GPR30 were also used: CEPR, CMKRL2, DRY12, FEG-1, GPCR-Br, LERGU, LERGU2, LyGPR and GPER.

The GPR30 gene, well conserved in different species, is localised on human chromosome 7p22.3 and to date four transcripts, with 2 or 3 exons, are known encoding the same GPR30 protein of 375 amino acids. The protein is highly conserved in mammals, with 87% sequence identity between human and mouse.

1.2.1 GPR30: a new estrogen receptor or still an orphan receptor?

Because of the sequence homology of GPR30 with the IL-8 receptor, with other members of the chemoattractant receptor family formylpeptide-like receptor (FPRL)-1 and FPRL-2 and with the chemokine receptor CXCR1, it has been suggested that the endogenous ligand would be a chemokine or a peptide (Owman et al., 1996), (Feng und Gregor, 1997). However, none of these hypothetical ligands provoked a response in cells transfected with GPR30.

A few years later, the orphan GPR30 was found to mediate ERK-1/-2 activation in response to 17-β-estradiol (E2 or beta-estradiol) in ER-negative SKBr3 breast cancer cells by transactivation of the epidermal growth factor (EGF) receptor (Filardo et al., 2000). In another study, the same group demonstrated that, in addition, GPR30, after estrogen stimulation, could also activate the adenylate cyclase and cAMP-mediated inhibition of ERK-1/-2 (Filardo, 2002). Furthermore, they observed that estrogen was not the only substance able to act as an agonist for GPR30, but that the antagonist molecules of the estrogen receptors fulvestrant (ICI 182,780) and tamoxifen could also do this. In both studies, however, an assay demonstrating the clear binding of GPR30 with E2 was missing. It was only in 2005 that two independent groups postulated that GPR30 is a new receptor, directly binding E2 and able to mediate rapid non-genomic signalling (Thomas et al., 2005), (Revankar et al., 2005).

In the first study, Thomas *et al.* described the specific binding between GPR30 and estradiol using tritium-labelled E2 ([^{3}H]-E2) in SKBr3 cells and in GPR30-transfected human embryonic kidney (HEK)293 cells. The dissociation constant (Ki) was approximately 3 nM. The binding sites were absent in untransfected HEK293 cells and in SKBR3 cells with small interfering RNA (siRNA)-mediated knock-down of GPR30. Although dose–response curves were not produced, the authors suggested that the binding was specific, since progesterone, testosterone, and cortisol were unable to compete with [^{3}H]-E2) (Thomas et al., 2005). In the following study, the group of Prof. Prossnitz used monkey kidney fibroblasts (COS-7) transfected with ERα or GPR30, both conjugated to green fluorescent protein (GFP), and E2 linked to the fluorescent dye Alexa for the binding assays, instead of the standard cell-membrane-permeating, radioactive E2. Indeed, since E2-Alexa does not permeate the

membranes, cells were permeabilised with saponin. A linear relationship between the fluorescent signal for E2-Alexa binding and the amount of GPR30 expressed was shown by competitive binding to be ≈6 nM, but not by a specific, saturable binding assay of E2 to GPR30 (Revankar et al., 2005).

Only one year later, the first evidence against the role of GPR30 as an estrogen receptor was published. Pedram *et al*., using endothelial cells (ECs) expressing GPR30 from ERα/ERβ-deficient mice (DERKO mice), demonstrated that only the classical estrogen receptors (but not GPR30), mediated estrogen-nongenomic signalling responses. In addition, a significant binding of radioactive estradiol in SKBr3 cells, positive for GPR30, could not be shown (Pedram et al., 2006).

Subsequently, in 2008 two different reports supported these data. In the first accurate quantitative study using different cellular lines (U2OS, CHO, and COS-7) over-expressing ERα or GPR30, ERα was observed to bind [^{3}H]-E2 specifically, whereas GPR30 did not do so. The same effect was observed in cells endogenously expressing GPR30 (MDA-MB231 and HEC50). Furthermore, the signalling in response to E2 involving GPR30 showed in the earlier studies could not be reproduced (Otto et al., 2008). In line with these data, a third group provided additional evidence that MCF-7 breast cancer cells treated with the estrogen antagonist ICI 182,780 – or with ERα knock-down using siRNA – abolished estrogen-mediated gene stimulation, whereas GPR30 knock-down or treatment with the newly identified selective GPR30 agonist G1 (Bologa et al., 2006) did not influence the gene expression. In this setting, rapid extranuclear estradiol signalling was exclusively mediated by the classical ERs (Madak-Erdogan et al., 2008).
In the latest data questioning the role of GPR30 mediating non-genomic estrogen signalling, the involvement of an ERα variant, ER-α36, was introduced. Kang *et al*. demonstrated that GPR30 over-expression in cells not expressing it endogenously could induce the expression of ER-α36, by activating its promoter. Furthermore, this study provided evidence that the GPR30-selective agonist G1 could activate ER-α36, previously described to be mainly expressed at the plasma membrane of ER-negative breast cancer cells and mediating non-genomic estrogen signalling (Wang et al., 2005). Most importantly they demonstrated high-affinity, specific binding with both E2 and G1, by using a saturation and binding assay in HEK293 cells that over-expressed ER-α36. With these results, they concluded that ER-α36, but not GPR30, is responsible for the non-genomic E2 signalling (Kang et al.).

In conclusion, the question of whether GPR30 is a new estrogen receptor involved in the non-genomic signalling remains controversial, suggesting that it may still be an orphan receptor.

1.2.2 GPR30 signalling

Despite the strong controversy about GPR30 as an estrogen receptor, to date the number of publications considering GPR30 as a new estrogen receptor is almost ten times greater than in 2006 (in August 2010 *circa* 200). Already in 2007, GPR30 was renamed "G protein-coupled estrogen receptor (GPER)" in most databases (e.g. www.ensembl.org or www.ncbi.nlm.nih.gov). Thus, most studies were conducted considering estrogen to be a ligand for GPR30. As mentioned above, Filardo *et al.* proposed for the first time that GPR30 may play a role in the rapid activation of MAPKs by estrogen in breast cancer cells through the transactivation of EGFR. In particular, the Gβγ subunit promotes a non-receptor tyrosine kinase (Src)-mediated, metalloproteinase (MMP)-dependent cleavage and release of heparin-binding EGF-like growth factor (HB-EGF) from the cell surface, resulting in the activation of the ERK-1/-2 pathway. On the other hand, the Gα subunit stimulates AC, which leads to PKA-mediated suppression of EGF-induced ERK-1/-2 activity (Filardo et al., 2000), (Filardo, 2002).

Subsequently, another group provided evidence that estrogen or phytoestrogens induced the expression of the proto-oncogene c-fos in various cancer cells (breast, endometrium, thyroid cancer, ovarian) and cell lines lacking nuclear ERs. In addition, over-expression of GPR30 in BT-20 breast cancer cells could activate the up-regulation of c-fos upon estrogen stimulation, and anti-sense RNA against GPR30 blocked the up-regulation of c-fos (Maggiolini et al., 2004), (Vivacqua et al., 2006), (Vivacqua et al., 2006), (Albanito et al., 2007).
Concerning the association of GPR30 with G proteins, main transduction mechanisms have been suggested to be through G_s or through G_q. The coupling of GPR30 to $G\alpha_s$ was assumed, because stimulation of AC and subsequent cAMP production were observed (Filardo, 2002) and, moreover, direct interaction between these was demonstrated (Filardo et al., 2007). Since estrogen-mediated Ca^{2+} mobilisation mediated by PLC through GPR30 was found in an independent study, association of GPR30 with G_q was suggested (Figure 4), (Revankar et al., 2005), (Prossnitz et al., 2008).

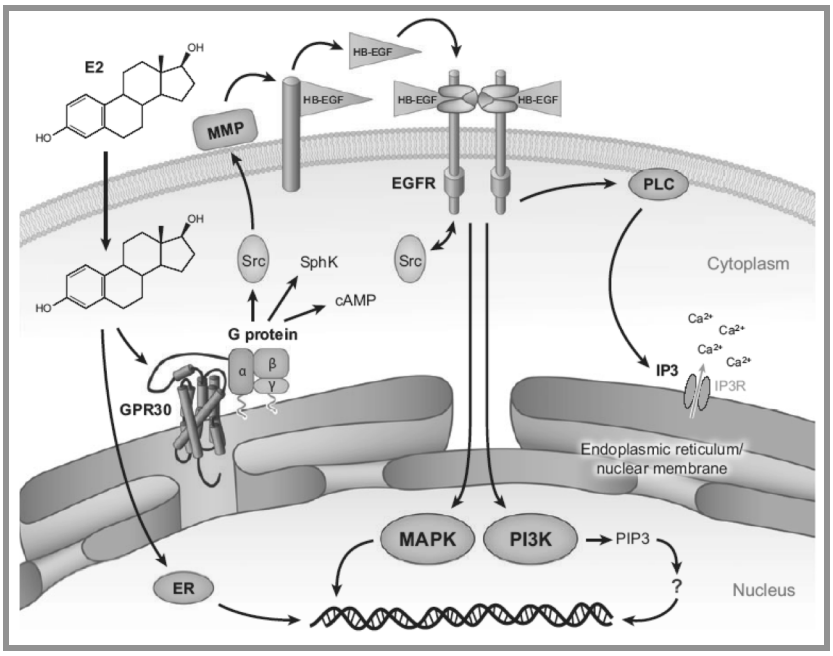

Figure 4: Model of the mechanisms of estrogen-mediated signalling via GPR30
Adapted from Prossnitz et al. 2008 (Prossnitz et al., 2008).

In contrast to these data, as reported earlier in the section on studies aimed at demonstrating whether GPR30 is an estrogen receptor, Pedram and co-workers were unable to show cAMP or ERK activation in response to E2 in GPR30-positive, ER-negative breast cancer cells (Pedram et al., 2006). Another study failed to reveal elevation of Ca^{2+} or cAMP activation in COS-7 cells transiently transfected with GPR30 or in MDA-MB231 and HEC50 expressing higher endogenous levels of GPR30 (Otto et al., 2008).

1.2.3 GPR30 cellular localisation

Apart from the fact that there is some controversy regarding GPR30's function as an estrogen receptor, there is also some dispute regarding its cellular localisation, with no less importance for the function of the receptor itself. An intracellular sublocalisation implies for instance that the ligand has to be membrane-permeating, defining a relevant biochemical characteristic of the putative ligand.

In 2005 the first report showed the expression of GPR30 at the plasma membrane of SKBr3 cells or from healthy human placental tissue after a centrifugation-series procedure (Thomas et al., 2005). Supporting these data, one year later, the localisation of GPR30 was observed at the plasma membrane by the use of an anti-GPR30 antibody in HeLa cells expressing FLAG-GPR30, even though no staining of subcellular markers was conducted (Funakoshi et al., 2006). The same conclusion was also reached by Filardo *et al*., who demonstrated the

presence of GPR30 at the cell surface by using a specific plasma membrane marker (Filardo et al., 2007).

In contradiction to these data, Revankar and colleagues could show by different approaches the expression of GPR30-GFP in the endoplasmic reticula of different cell lines (Revankar et al., 2005). Since the evidence regarding the subcellular site of GPR30 started to be contradictory, other groups tried to clarify this aspect and the group of Otto also detected the expression of GPR30 in the endoplasmic reticulum (Otto et al., 2008).

In conclusion, since the idea that other GPCRs could be located on intracellular compartments has been already contemplated (Gobeil et al., 2006), it is certainly possible that under specific conditions, intracellular GPR30 can exist in, or translocate to, the cell membrane (Prossnitz et al., 2007).

1.2.4 GPR30 *in vivo* studies

Besides the results on GPR30's function based on cell assays, several studies were performed to clarify the role of GPR30 *in vivo* by using rats, hamsters or GPR30-knockout (KO) mice. Currently, four different GPR30-KO mouse models have been realised (Isensee et al., 2009), (Martensson et al., 2009), (Otto et al., 2008), (Wang et al., 2008) and an overview of the major results is given in Table 1 (Langer et al.).

Table 1: GPR30 knockout mice overview. Adapted from Langer et al. (Langer et al.).

Parameter	Mouse model described by Wang *et al*.	Mouse model described by Martensson *et al*.	Deltagen mouse model described by Isensee *et al*.	Artemis mouse model described by Otto *et al*.
5′- and 3′-integration of the targeting vector	Analysed lege artis	3′-integration analysed lege artis	Analysed lege artis	Analysed lege artis
		5′-integration not analysed by Southern blot		
Single integration of the targeting vector	Not analysed	Not analysed lege artis	Analysed lege artis	Analysed lege artis
Targeting strategy	Replacement of exon 3 by neomycin resistance cassette	Deletion of exon 3	Replacement of amino acids 20–136 of GPR30 by a LacZ reporter/neomycin resistance cassette	Deletion of exon 3
Neomycin resistance cassette left in genome?	Yes	No	Yes	No
Genetic background	SvEv ES cells	129X1/SvJx129S1 ES cells	129/OlaHsd ES cells	C57BL/6N ES cells
	3× backcross in C57BL/6	6× backcross in C57BL/6	6× backcross in C57BL/6	C57BL/6 background
Mating scheme for generation of experimental animals	Homozygous intercrosses	Heterozygous intercrosses and use of age-matched C57BL/6 mice as control	Heterozygous intercrosses	Heterozygous intercrosses
Described phenotypes	Involvement of GPR30 in mediation of estradiol-induced thymic atrophy	Reduced body weight and skeletal growth in female mutants	No effects on body weight or glucose tolerance	No effects on body weight, visceral adiposity, glucose tolerance or fertility in mutant mice from both genders
	Increased body weight and visceral adiposity in female and male mutant mice [Ref. [23]]	Impaired glucose tolerance in 6 months old female mutants	Lower frequency of CD4+ and CD8+ T cells in peripheral blood of mutant mice	Estrogenic responses in the uterus and the mammary gland were completely maintained in female mutant mice
	No effects on body weight [Ref. [41]]	Elevated mean arterial blood pressure in 9 months old female mutants		Amount of CD4+ and CD8+ T cells in peripheral blood is unchanged in mutant mice
	Vasodilatory effects of 1 µM G1 were not present in carotid arteries of mutant mice	Increased media thickness in second-order mesenteric arteries		

The first study *in vivo* aimed to investigate the physiological function of GPR30 as a new estrogen receptor. It was conducted on rats, applying a trauma-haemorrhagic shock (THS) model (based on mechanical and controlled bleeding followed by pharmacological resuscitation). First of all, hepatic injury was evaluated at the plasma α-glutathione S-transferase (αGST) level, and treatment with E2 after THS was able to reduce it. Secondly, knock-down of GPR30 by transfection of siGPR30 attenuated the E2-dependent activation of PKA and inhibition of the pro-apoptotic B-cells lymphoma 2 gene (Bcl2). In conclusion, the hepatic injury could have been reduced in response to estrogen by way of GPR30-mediated, and not ERα-mediated, anti-apoptotic signalling (Hsieh et al., 2007).

With the first KO mouse for GPR30, an immunological study was proposed. Indeed, the estrogen-induced thymic atrophy, which normally occurs during pregnancy or prolonged

estrogen treatment, was analysed comparing GPR30-deficient mice with ERα KO (AERKO) and ERβ KO (BERKO) mice. Previous studies with ERα-, ERβ-deficient mice showed that ERα was to some extent involved in the reduction of thymus size, whereas ERβ was not relevant (Erlandsson et al., 2001). Although E2-treated female GPR30-KO mice showed alleviated (but not completely reversed) thymic atrophy and in ERα-KO mice the atrophic effect resulted rather abolished, it was possible to distinguish between the contribution of GPR30 and ERα in mediating thymic atrophy. Bearing in mind that the maturation of thymocytes to T cells (a process that occurs in the thymus) is characterised by different stages based on the expression of cell-surface markers such as CD4 and CD8, which can be expressed not at all (double negative, DN) or one at a time (single positive, SP) or doubly (double positive, DP), Wang *et al*. suggested that ERα exclusively mediates an early developmental stage of thymocytes DN after E2 treatment, whereas GPR30 was indispensable for apoptosis of a special class (TCR $\beta^{-chain-/low}$) of DP thymocytes (Wang et al., 2008). Subsequently, in the same mouse model used in another study, an increased body weight and visceral fat deposits were found in both female and male animals (Haas et al., 2009). Furthermore, in this study GPR30 was considered to be involved in the regulation of vascular tone and blood pressure in line with previous observations about an up-regulation of GPR30 in endothelial cells upon fluid shear stress (FSS) (Takada et al., 1997) and the expression of GPR30 in small vessels (Isensee et al., 2009).

In contrast to the mouse model described by Wang *et al.*, the analysis of the mouse model of Martensson *et al.*, which was restricted to female animals, showed a reduction in body weight and skeletal growth in three-months-old mice. In female mice aged six and nine months, impaired glucose tolerance and an elevation of arterial blood pressure were reported, respectively (Martensson et al., 2009).

In a third mouse model (GPR30 KO mice, generated by Artemis), questioning again the role of GPR30 involved in the E2-response, Otto *et al*. observed no significant difference in body weight or impairment in fertility. In addition, E2 responses in ovariectomised (ovx) KO mice treated with E2 were maintained in the uterus and the mammary gland. On the other hand, administration of the proposed GPR30 agonist G1 (Bologa et al., 2006) did not stimulate any estrogenic response in the uterus or in the mammary gland of wild type mice (Otto et al., 2008), (Otto et al., 2009).

Another approach used to unravel the *in vivo* function of GPR30 was the production of a KO mouse for GPR30 by Deltagene with the insertion of a LacZ/neomycin cassette into the open reading frame (ORF) of GPR30. With these mutant mice Isensee *et al.* could provide,

besides a general phenotypic analysis, a broad and detailed screening about the tissue distribution at the cell-type level. Indeed, according to the Artemis GPR30 KO model, no significant difference in body weight was noticed in a comparison of wild-type with mutant animals, even after a high-fat diet. Interestingly, the expression of GPR30, identified by colocalisation of LacZ along with cell-type-specific markers, was observed in endothelial cells of small arterial vessels of various tissues; smooth muscle cells, pericytes, and neuronal subpopulations in the brain; gastric chief cells in the stomach; and chromaffin cells in the adrenal glands. Since prominent expression of GPR30 was found in endothelial and smooth-muscle-cell subpopulations, the authors concluded by considering the involvement of GPR30 in vascular diseases, such as hypertension, arteriogenesis or vascular injury (Isensee et al., 2009).

1.3 Blood vessels in the vascular circulatory system

The function of the entire vascular system is the rapid transport of oxygen, glucose, amino acids, fatty acids, vitamins and water to appropriate tissues and to remove metabolic waste products such as CO_2, urea and creatinine. Furthermore, the circulatory system is part of the control system for hormone distribution, and it plays a vital role in the temperature regulation of the body (Risau, 1997). The function of the vascular system is of such importance that minor disorders can lead to severe disability and death. Cardiovascular diseases are the leading cause of death in industrialised countries, among which stroke is the third most common cause of death and lasting disability. Even so, therapeutic options are still limited (Jones und Peterson, 2008), (Lloyd-Jones et al., 2009).

1.3.1 The structure of the blood-vessel wall

With the exception of capillaries, all vessel types have a characteristic wall structure organised in three layers: the tunica intima, tunica media and tunica adventitia.

The tunica intima is a flat layer of endothelial cells (ECs) covering a thin layer of connective tissue, delimiting the vessel wall towards the lumen of the vessel. This endothelial layer is the main barrier for plasma proteins and may, by the mechanical sensitivity of the endothelial cells, secrete many vasoactive products. Beneath the connective tissue, the internal elastic lamina delimits the tunica intima from the tunica media, and through this information from the endothelial cells is transferred to smooth muscle cells. The tunica media consists of smooth muscle cells (SMCs), which are embedded in a matrix of elastin and collagen strands. A second layer of elastic fibres, the external elastic lamina, is located under the SMCs. The

tunica adventitia is a connective tissue layer; it serves to anchor the blood vessel and blends with the connective tissue surrounding the vessel (Figure 5) (Levick, 1995).

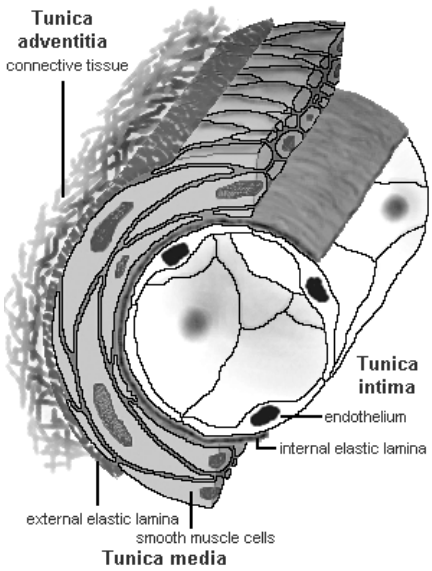

Figure 5: Structure of blood vessels
The division of the wall into three layers is the common structural pattern in all blood vessels with the exception of capillaries.
Adapted from http://www.lab.anhb.uwa.edu.au/mb140/corepages/vascular/vascular.htm.

1.3.2 Endothelial cells, a multi-functional cell layer of the blood vessel wall

The main function of endothelial cells is to form a barrier between blood and tissue for a rapid transfer of metabolites and signalling molecules. The endothelium, by the mediation of various transfer channels for different classes of substances, balances and regulates blood composition. Fat-soluble molecules such as O_2 or CO_2 diffuse through the phospholipids, and small insoluble substances such as glucose, amino acids and pharmaceuticals can penetrate with water through the intercellular gap. As a result of these different functions, the endothelial cells can modulate a multitude of blood-vessel-related processes, including regulation of blood pressure, vasodilation, vasoconstriction, regulation of the water volume in the blood stream, adhesion and transmigration of leukocytes, release of pro- and anti-thrombotic factors, growth factors and vasoactive substances (Traub und Berk, 1998). Impairment of these endothelial-cell-mediated processes plays an important role in the pathogenesis of the vessels (Ross, 1993). If, for instance, a reduction in the ambient of O_2 concentration – hypoxia – occurs, a variety of functional responses in vascular ECs, including cell proliferation, angiogenesis and cell death, are compromised; and tissue perfusion is reduced being the O_2 availability insufficient to meet tissue metabolic requirements (Rey und Semenza), (Chen et al., 2008). Another function of endothelial cells is

the regulatory response to different parameters of blood flow, as these are exposed directly to the blood stream. These comprise not only factors circulating in the blood, but also mechanical forces originating from the blood flow: pressure, tension and shear stress (Garcia-Cardena und Gimbrone, 2006).

1.3.3 Fluid shear stress, a biomechanical force acting on the vessel wall

Biomechanical forces significantly affect the structure, the growth and the functions of the blood vessel wall, resulting in a variety of intracellular molecular changes in the endothelial cells and smooth muscle cells. Biomechanical forces which have an influence in the blood vessel are: (a) the hydrostatic pressure, which is caused by blood pressure, (b) the tension, caused by the deformation of the vessel wall and (c) fluid shear stress (FSS), which results from the friction of blood against the vessel surface (Lehoux et al., 2002). Whereas pressure and tension are transferred to the whole vessel wall due to their vertical orientation, the tangentially aligned FSS is sensed mainly by the endothelium (Figure 6).

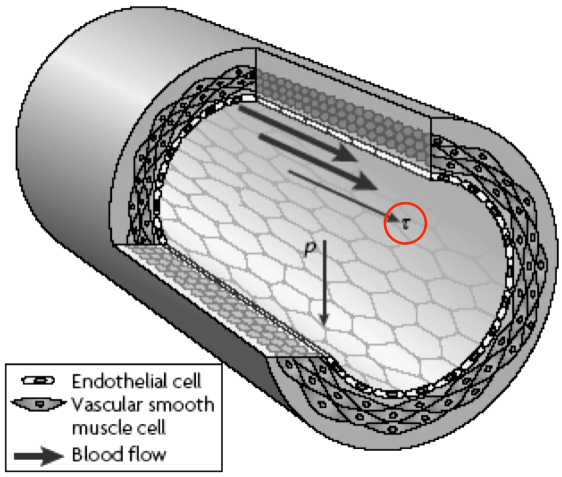

Figure 6: Mechanical forces on the vessel wall
Here are shown the blood pressure (p) and the FSS (τ). Adapted from Hahn et al. 2009 (Hahn und Schwartz, 2009).

In vessels, the flowing blood exerts a force on the endothelial cell surface acting in the direction of flow. The FSS arising can be calculated by using the Hagen–Poiseuilles law, which is valid for ideal Newtonian fluids and laminar flows in stiff tubes. FSS is proportional to blood flow velocity and inversely related to the cube of the vessel's radius. Hence, an increased blood flow velocity results directly in an increased FSS (Schaper et al., 1976).

The Hagen–Poiseuille equation:

$\tau = \frac{4\mu Q}{\pi r3}$	τ: shear stress [N/m2], [1N=105 dyn], [10 dyn/cm2] μ: blood viscosity [N ·s/m2] Q: blood flow rate [m3/s] r: vessel radius [m]

In blood vessels, the Poiseuille equation is only restrictedly applicable. The equation can be applied *in vivo* with the following assumptions: (i) the blood is considered as a Newtonian fluid, (ii) the vessel's cross-section is cylindrical, (iii) the vessel is straight with inelastic walls, and (iv) the blood flow is stable and laminar (Papaioannou und Stefanadis, 2005).

The FSS varies depending on heart minute volume, heart period and differences in vessel geometry. The FSS, which acts directly on the endothelial cells in arterial vessels, is of the order of 15–30 dyn/cm^2, much higher compared with the corresponding value in venous vessels of about 1–5 dyn/cm^2. Under physiological conditions, the mean shear stress to which the vascular endothelium is exposed is close to 10–15 dyn/cm^2 (Lehoux et al., 2002). Flow disturbances can occur in arterial irregularities – such as curvatures or bifurcations – or upstream and downstream of a stenosis. Differences in shear stress may contribute to altered endothelial gene expression (Morawietz et al., 2000).

FSS originating from the mechanical effects of blood flow on the vascular endothelium is not only considered a protective mechanism against the localisation of atherosclerotic plaques, but it is also involved in angiogenesis and arteriogenesis. The term angiogenesis describes the growth of blood vessels *de novo*, while arteriogenesis indicates the process by which pre-existing collateral arteries increase in size (Prior et al., 2004). More evidence suggests that arteriogenesis may be triggered mainly by fluid shear stress, which is induced by the altered blood flow conditions after an arterial occlusion. Arteriogenesis involves endothelial cell activation, basal membrane degradation, leukocyte invasion, proliferation of vascular cells, neointima formation (in most of the species studied), changes of the extracellular matrix, and cytokine participation. In particular, increases in FSS *in vivo* induce capillary profileration and increase in artery diameter (Hudlicka, 1994), while decreases in shear stress lead to a reduction in artery diameter and ECs apoptosis (Cho et al., 1995).

A number of *in vitro* studies using cone-and-plate devices and cultured ECs (e.g. Human Umbilical Vein Endothelial Cells, HUVECs, or Human Coronary Endothelial Cells, HCAECs) have demonstrated that ECs stimulated with FSS are affected in the production of bioactive

molecules involved in the regulation of vascular tone, such as nitric oxide (NO) (Korenaga et al., 1994), in cell growth control, such as heparin-binding epidermal growth factor (HB-EGF) (Morita et al., 1993), in blood coagulation and fibrinolysis, such as thrombin receptors (Nguyen et al., 2001), and in cell-to-cell adhesion, such as intercellular adhesion molecule-1 (ICAM-1) (Nagel et al., 1994). Moreover, it has recently been reported that mechanical stretching of cells can activate several pathways that lead to the activation of transcription factors (e.g. AP-1 and NFκB) in which various molecules such as ion channels and GPCRs – for instance, the angiotensin type I (Zou et al., 2004) and human B_2 bradykinin (Leeb-Lundberg et al., 2005) – are involved. In addition, in the past ten years several groups, in order to discover new shear-stress-responsive genes and co-regulated pathways responsive to the mechanical environment of the cell, have started to perform global gene analyses using DNA microarray techniques. In one study, looking at changes in gene expression of shear-stressed HUVECs, several previously unreported shear-stress-responsive genes were identified. For instance, argininosuccinate synthetase (involved in the synthesis of endothelial nitric oxide synthase, eNOS) or elastin peptide (which through binding to its receptor increases intracellular Ca^{2+}) were found up-regulated, and the expression of both genes lead to the release of NO. Thus, on the basis of this information it proved possible to develop new hypotheses on how shear stress regulates the synthesis of NO (McCormick et al., 2001).

1.4 Aims of the study

With the background of clear evidence about the expression of GPR30 (Isensee et al., 2009) and its involvement (Haas et al., 2009) in vascular function, the aim of the work described in this thesis was to contribute to the elucidation of the role of GPR30 signalling in blood vessels. Despite the controversy regarding whether GPR30 is an ER or still an orphan receptor, still very little is known about its relation to and its interaction with other proteins. Therefore, the aims of the present study were:

(1) To identify and confirm hitherto new human interaction partners for GPR30:

- establishing a western blotting protocol for GPR30;
- verifying potential candidates from a yeast two-hybrid screening (Y2H) with CoIP;
- investigating the cellular localisation of GPR30 and the confirmed interaction partner(s) by over-expression.

(2) To establish a human cellular system to evaluate the potential role of GPR30 in a vascular model:

- by measurement of the expression of GPR30 in the hypoxia/reperfusion model and the FSS stimulation model;
- by characterisation of the model system by gene expression and cellular morphology;
- by determination of the cell type where GPR30 is regulated.

(3) To evaluate the downstream effects of the interaction between GPR30 and/or the newly identified interaction partners in the vascular model at the transcript level:

- over-expressing GPR30 and/or interaction partners in the model system chosen;
- analysing the genome-wide gene expression of the different experimental groups (e.g. ± FSS);
- identifying differentially expressed genes and pathway analysis.

2 MATERIALS AND METHODS

METHODS

2.1 Cloning

Standard protocols for various techniques in molecular biology were followed, according to *Molecular Cloning* (3rd edition, Sambrook & Russell, Cold Spring Harbor Laboratory Press, 2001). Overview tables of all constructs and primers are given in Sections 2.10 and 2.11. Detailed cloning strategies for constructs generated within the scope of this thesis are described in Section 2.1.8

2.1.1 Polymerase chain reaction (PCR)

PCR reactions for cloning approaches were performed with Pfx50 DNA polymerase (Invitrogen), since this enzyme possesses proofreading exonuclease activity. If 3'-A overhangs were necessary (e.g. for TOPO cloning), Platinum Taq DNA polymerase (Invitrogen) was used. Analytical PCR reactions were conducted with standard Taq DNA Polymerase.

2.1.2 Agarose gel electrophoresis

DNA molecules were separated by gel electrophoresis in gels containing 0.8–1.4% agarose. Standard electrophoresis grade agarose (Invitrogen) was used for analytical gels. If gel extraction of the DNA fragment was required for cloning purposes, gels were prepared with SeaKem GTC agarose (Cambrex). The electrophoresis was performed in a custom system (Bächler Feintech) at 50 V for 20–40 min. The buffer system was TBE (45 mM Tris-borate, 1 mM EDTA, pH 8.3) in case of analytical gels and TAE (40 mM Tris-acetate, 1 mM EDTA, pH 8.0) for cloning approaches. Ethidium bromide (50 µg/l) was included in the buffer and gel to visualise DNA bands by UV light (Syngene).

2.1.3 PCR Purification and gel extraction

PCR products were purified by QIAquick PCR Purification Kit (QIAGEN) and eluted in 50 µl double-distilled water (ddH_2O). Restricted DNA fragments were separated from linearised vectors by gel electrophoresis, cut from the gel, extracted using the QIAquick Gel Extraction Kit (QIAGEN), and eluted in 50 µl ddH_2O.

2.1.4 Ligation

DNA inserts and linearised vectors were ligated with T4 DNA ligase (Biolabs) according to the manufacturer's protocol. Ligations were incubated for 1 hour at 16 C or overnight (o/n) at room temperature (RT).

2.1.5 *E. coli* strains

Electrocompetent DH5α (Invitrogen) and chemically competent Top10 were used for the propagation of standard vectors and routine subcloning. Bacteria were grown in standard LB medium (QBIOgene) or LB agar (MP Biomedicals) at 37 C unless noted.

2.1.6 Transformation of electro- and chemically competent bacteria

Electrocompetent DH5α cells (100 µl) were thawed on ice and mixed with 10 µl ligation reaction. The reaction was transferred into pre-chilled 0.1 cm electroporation cell (BioRad) and pulsed in an electroporator (BioRad). The cells were resuspended in 1 ml SOC medium. For transformation of chemically competent cells, 100 µl cell suspension was mixed with ligation reaction. The reaction was chilled on ice for 30 min, heat-shocked for 1 minute at 42 C, and placed on ice for an additional 5 min. Subsequently, 0.5 ml SOC medium was added. Either the cells were electro- or chemically competent, were regenerated at 37 C for 1 h while shaking and finally plated onto selection agar plates which were incubated at 37 C o/n.

2.1.7 Plasmid isolation

For small-scale plasmid isolations (max. 10 µg), 3 ml LB medium including antibiotics was inoculated with one colony and cultured o/n at 37 C under shaking (225 rpm). Cells growing in o/n culture were pelleted and plasmids were isolated by using the QIAprep Spin Miniprep Kit (QIAGEN) according to the manufacturer's protocol and eluted in 50 µl ddH_2O. If larger amounts (max. 500 µg) of plasmid DNA were desired, 100–200 µl of the o/n cultures was used to inoculate 200 ml LB medium. The next day, plasmids were isolated with the QIAGEN Plasmid Maxi Kit (QIAGEN) according to the instruction manual. Plasmids were eluted in 500 µl ddH_2O and stored at –20 C.

2.1.8 GPR30 constructs

GPR30/pcDNA3-EGFP

Two OmicsLinkTM clones encoding GPR30 with C-terminal His-tag (EX-M0792-M01) or GFP-tag (EX-M0792-M03) were obtained from the German Resource Center for Genome Research (RZPD). The constructs are based on the vectors pReceiver-M01 or pReceiver-M02, respectively. Sequencing of the constructs revealed a frame shift mutation in the His-tagged clone and several point mutations in the GFP-tagged one. However, no mutations were found in the sequences encoding the N- or C-terminal domain in EX-M0792-M03. Therefore, the clone was used to construct bait vectors for yeast two-hybrid screening (Y2H). Furthermore, a construct encoding GPR30 tagged with EGFP based on pcDNA3 (i.e. pcDNA3-GPR30-EGFP) was kindly provided by Prof. Eric Prosnitz (University of New Mexico, Albuquerque, USA).

pcDNA3.1(+)/GPR30

For this construct, GPR30/pcDNA3-EGFP was used as a template to amplify GPR30 by PCR and to subclone the product into pcDNA3.1(+) for native expression without tag. The forward primer P13 included a *Hind*III site and the reverse primer P14 included a *Not*I site, respectively. In addition, the reverse primer had a two-bp mismatch to introduce a stop codon. The PCR was performed using Pfx50 DNA polymerase (annealing temperature 45 °C). The 1185-bp product was purified (QIAquick PCR purification), cut using *Hind*III and *Not*I according to the instruction manual, again purified by gel extraction, and finally ligated with linearised pcDNA3.1(+) by using T4 DNA ligase at 16 °C for 1 h. Electrocompetent DH5α was transformed by the ligation reaction and plated onto selection agar plates containing 100 µg/ml ampicillin. Plasmids were isolated from positive clones and controlled by restriction-endonuclease digestion and sequencing.

pTL1-HA2/GPR30

This construct was easily obtained by cutting GPR30 from pcDNA3.1(+)/GPR30, using *Hind*III and *Not*I, purification by gel extraction and ligation in pTL1-HA2, to put in frame with the HA (haemagglutinin) tag.

2.2 Mammalian cell culture

2.2.1 Cell lines and primary cells

Cell lines HeLa, HEK293, SKBR3 and EAhy926 were cultured in DMEM (Dulbecco's Modified Eagle Medium, Biochrom, FG 0435) containing 10% FBS including antibiotics (penicillin/ streptomycin, Biochrom A 2213).

HMEC-1 (Human Microvascular Endothelial Cells) were cultured in MCDB 131 medium (GIBCO, 10372) containing 7.5% FBS and 200 mM L-glutamine.
HUVECs (Human Umbilical Vein Endothelial Cells), HUAECs (Human Umbilical Arterial Endothelial Cells) and HAoECs (Human Aortic Endothelial Cells) were cultured in Endothelial Cell Basal Medium (Promocell, C-22220) with Supplement Pack (2% FCS, 0.4% ECGS/H, 0.1 ng/ml epidermal growth factor, 1 µg/ml hydrocortisone, 1 ng/ml basic fibroblast factor, Promocell, C-39210). All cells were cultured in a humidified incubator with 5% CO_2 at 37 °C.

2.2.2 Transfections

Mammalian cell lines were transfected with either FuGENE 6 reagent (Roche Applied Science) or polyethylenimine (PEI, 50% solution in H_2O, Sigma P3143). For transfection with FuGENE 6 reagent, the cells were seeded 24 h before transfection at a density of 10,000-20,000 cells/cm^2. For transfections in 10-cm plates (55 cm^2 surface area, 10 ml medium), 18 µl FuGENE 6 reagent was diluted in 582 µl serum-free medium (OptiMEM, GIBCO) and incubated for 5 min at RT. Then 6 µg plasmid DNA was added, vortexed for a second, and incubated for at least 15 min at RT. Finally the transfection complex was added to the cell-culture vessel in a dropwise manner while swirling. The expression of transfected constructs was assayed 24 or 48 hours later.
For co-immunoprecipitations (CoIP) and HMEC-1 over-expression for the microarray experiment, PEI transfections were performed in 10-cm plates. About $3x10^6$ HEK293 cells (for CoIP) or $2x10^6$ of HMEC-1 cells (for microarray) were seeded per plate and grown over night. Before starting the transfection, the standard medium was replaced with 10 ml DMEM containing 2% FBS. Then 475 µl serum-free OptiMEM was mixed with 25 µl PEI (1 mg/ml, pH 7.0) and 10 µg DNA (DNA concentration = 0.5–2 µg/µl) and incubated for 10 min at RT. The transfection mixture was added in a dropwise manner while swirling. The expression of transfected constructs was assayed 24 h later.

2.3 Fluid shear stress *in vitro* model

Cells were subjected to laminar shear stress at different physiological levels (1, 15, and 30 dyn/cm^2) in a cone-and-plate viscometer in a humidified environment with 5% CO_2 at 37 °C over a plate seeded with a confluent monolayer of endothelial cells (Bartling et al., 2000). Cells were rinsed twice with warmed PBS and afterwards PBS was replaced by warmed culturing medium containing 5% dextran (Roth, 9228.2). As shown in Figure 7, the viscometer consists of a cone with an angle of 0.58 rotating on top of a cell-culture dish. The cone is driven by a computer-controlled stepper motor. A control dish accompanied each cell-culture dish from the same human endothelial cell preparation, which was incubated without application of shear stress. For each set of experiments, four identical flow devices were used simultaneously.

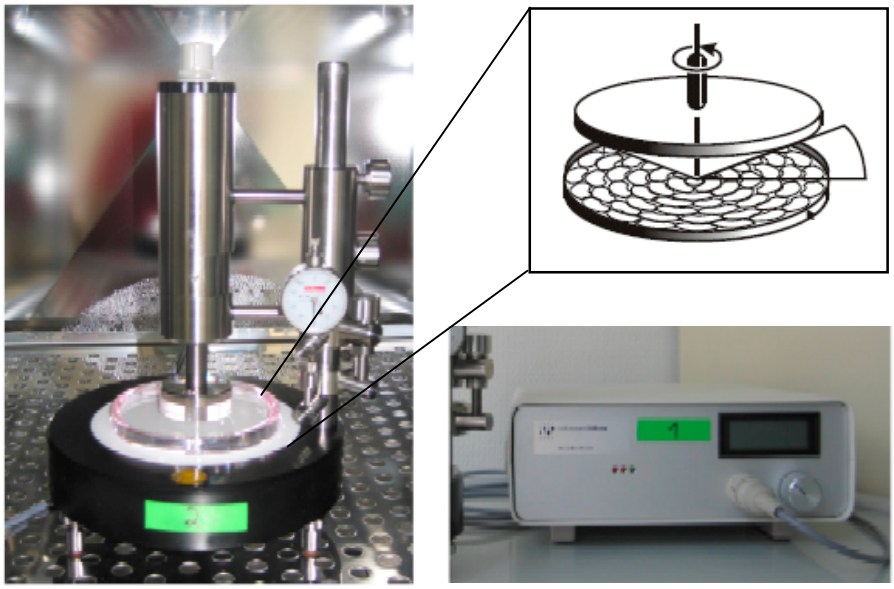

Figure 7: Cone and plate apparatus (photograph, scheme and controller).

2.4 Hypoxia/re-oxygenation *in vitro* model

Cells were seeded out in 10-cm plates 24 h beforehand. Hypoxia was generated in a dedicated, humidified gas-tight incubator (INVIVO2 400, Ruskinn Technologies, Bridgend, UK) and flushed with gas of the following composition: 5% CO2, 85% N2, and 10% H2. During oxygen glucose deprivation (OGD; 1, 2, 3, 6, 12, 24 h) oxygen tensions in the media were below 1 mmHg (polarographic probe, Licox GSM). Cells were rinsed twice with warmed PBS and placed in OGD chamber. In the chamber, PBS was replaced by warmed balanced salt solution (BSS0; containing 143.8 mM Na^+, 5.5 mM K^+, 1.8 mM Ca^{2+}, 1.8 mM Mg^{2+}, 125.3

mM Cl^-, 26.2 mM $HCO3^-$, 1.0 mM PO_4^{3-} and 0.8 mM SO_4^{2-}, pH 7.4) which was put into the chamber 6-12 hours prior to the performance of the experiment. The experiment was terminated by taking the culture plates out of the OGD chamber and replacing BSS_0 by warmed cell culturing medium. Subsequently, culture plates were returned to normoxic cell culture incubator for re-oxygenation (1, 2, 3, 6 h). In control experiments the medium was replaced by BSS_{20} (BSS_0 containing 4.5 gm/l glucose) after being washed with PBS, and cells were incubated in a normoxic atmosphere containing 5% CO_2, for the same duration as for the experiment, followed by return of the cell culturing medium.

2.5 Immunocytochemistry

The cells were cultured and transfected in chamber slides (BD Biosciences) or 6 well plates and fixed with 4% paraformaldyde in PBS (Riedel-de Haen) for 10 min at RT. The fixed cells were rinsed twice for 2 min in washing buffer (PBS, 0.05% Tween 20, pH 7.2) and incubated in serum blocking buffer (2% serum, 1% BSA, 0.1% fish skin gelatine, 0.1% Triton X-100, 0.05% Tween 20) for 30 min at RT or o/n at 4 °C. The serum used was derived from the same species as the secondary antibody (normally goat). The fixed cells were incubated with the primary antibody diluted in PBS with 1% BSA (100 µl per chamber) for 1 hour at RT or o/n at 4 °C. The cells were rinsed several times in washing buffer and then incubated with the secondary antibody (Alexa Fluor 568- or Alexa Fluor 488 conjugated, Molecular Probes) diluted 1:500 in PBS for 30 min at RT. Cell nuclei were counterstained with DAPI (0.2 ng/µl). Slides were coverslipped with aqueous Antifade fluorescent mounting medium (Vector Labs) or Fluoromount-G (Southern Biotech) and sealed with nail polish.

2.6 Western blotting and co-immunoprecipitation

2.6.1 Standard SDS-PAGE protocol

For SDS-PAGE, the samples were mixed with 6x loading buffer (300 mM Tris pH 6.8, 12% SDS, 0.6% bromophenol blue, 60% glycerol, 12% fresh β-mercaptoethanol), denatured by heating briefly to 100 °C or at 37 °C for 15 min (GPR30 only), loaded onto a polyacrylamide gel composed of a 4% stacking gel and a 10–15% separating gel, and separated by gel electrophoresis (BioRad) in Laemmli buffer (25 mM Tris, 192 mM glycine, 0.1% SDS, pH 8.3) at 90 V until the sample focussed in the stacking gel and then at 120 V until the dye ran off the gel. The separated proteins were transferred onto a PVDF membrane (Hybond-P, Amersham) using a semi-dry blotter (Bio Rad). PVDF membranes were equilibrated in methanol for 30 sec. The gel, the PVDF membrane, and extra thick Whatman 3MM papers were pre-soaked in Towbin buffer (25 mM Tris, 192 mM glycine, 200 ml/l methanol) for 1 min

before use. The transfer was conducted at 100 mA per gel for 1 h at RT. The membrane was blocked in TBST (125 mM Tris-HCl, 625 mM NaCl, 0.05% Tween 20, pH 8.0) containing 5% low-fat milk powder for 1 h and incubated with the primary antibody dissolved in blocking buffer for 1 h at RT or at 4 °C over night while shaking. The membrane was washed 6x in TBST for 5 min and incubated with the secondary antibody diluted in TBST (sheep anti-mouse peroxidase conjugated, Amersham, 1:7500; goat anti-rabbit peroxidase conjugated, Calbiochem, 1:7500) for 1 h at RT. The immune complexes were detected with an ECL detection system according to the manufacturer's protocol (Amersham).

2.6.2 Western blotting to detect GPR30 in HeLa cell lysates

Total cell lysates were prepared from cells grown on 10-cm plates. Cells were lysed 48 h after transfection in either 300 µl urea-SDS lysis buffer (100 mM Tris-HCl pH 8.0, 2% SDS, 3.2 M urea) supplemented with 64 mM DTT, 0.5 mM phenylmethylsulphonyl fluoride, and 1X complete protease inhibitor mixture (Roche) or urea-Triton lysis buffer (40 mM Tris-HCl pH 8.0, 4% Triton, 8.0 M urea) supplemented with 50 mM DTT, 0.5 mM phenylmethyl-sulphonyl fluoride and 1X complete protease inhibitor mixture (Roche). After 5 min incubation on ice, cell lysates were sonicated for 20 sec (4 times for 5 sec each) on ice and mixed with loading buffer. Finally, the cell lysates were denatured at 37 °C for 15 min and separated by SDS-PAGE in a 10% polyacrylamide gel (see Section 2.6.1). The blocked membranes were incubated with the different anti-GPR30 antibodies diluted 1:500 at 4 °C o/n.

2.6.3 Co-immunoprecipitation of GPR30

The day before transfection, 3 x 10^6 HEK293 cells were seeded in a 10-cm dishes. The cells were transfected with HA-GPR30 (pTL1-HA2/GPR30), myc-PATJ (pRK5myc/PATJ), GFP, or empty vector pcDNA3.1(+) using the PEI transfection procedure with 10 µg plasmid DNA in total (see Section 2.2.2). The transfection efficiency was controlled by inspection of the GFP transfection and in general was about 70–80%. 48 h after transfection, cells were washed twice with cold PBS and harvested directly from the dish with a cell scraper (Nalge Nunc International) in 5 ml PBS on ice. The cells were collected in 15-ml Falcon tubes by centrifugation (500 g for 5 min) and stored at –80 °C. After 4 days the cells were lysed in 500 µl RIPA-buffer (50 mM Tris-HCl pH 7.5, 150 mM NaCl, 1% Nonidet P-40, 0.1% SDS, 1 mM EDTA, 1 mM EGTA) freshly supplemented with 0.5% sodium deoxycholate and 1x protease inhibitors (complete Mini, Roche). The tube was rotated for 1 h at 4 °C and then centrifuged at 8000 g for 10 min. The supernatant was transferred into a new tube; 40-µl aliquots were stored for total lysate (input) western blots. The remaining 440 µl supernatant was incubated with 2 µg of primary antibody (mouse monoclonal anti-myc, Santa Cruz) for

4 h at 4 °C on a roller shaker, centrifuged at 16,000 g for 10 min, and transferred into a new tube. In parallel, 50 µl of a protein G–Sepharose bead slurry was prepared by mixing 25 µl protein G–Sepharose beads (GE Healthcare, solution in 20% ethanol) with 25 µl lysis buffer. The beads were washed with lysis buffer (3x 1 ml lysis buffer, 1000 rpm for 1 min), added to the lysate, and incubated at 4 °C over night. Subsequently, the beads were washed with lysis buffer (3x 1 ml, 1000 rpm for 1 min) and resuspended in 40 µl 2x Laemmli sample buffer. The samples were denatured at 37 °C for 10 min. Finally, the beads were removed by centrifugation (1000 g, 1 min) and the supernatant was analysed by SDS-PAGE (see Section 2.6.1), (Rondou et al., 2008).

2.7 Protein–protein interaction bioinformatic tools

STRING is a database of known and predicted protein interactions.
The interactions include direct (physical) and indirect (functional) associations; they are derived from four sources:

Genomic context | High-throughput experiments | (Conserved) co-expression | Previous knowledge

STRING quantitatively integrates interaction data from these sources for a large number of organisms, and transfers information between these organisms where applicable. The database currently covers 2,590,259 proteins from 630 organisms.

PIPs is a database of predicted human protein–protein interactions. The predictions have been made using a naïve Bayesian classifier to calculate a “score of interaction”. There are 37606 interactions with a score ≥1, indicating that the interaction is more likely to occur than not to occur. The probability of interaction between two proteins is calculated by combining different features, including:

Gene Co-expression | Orthology | Domain Co-occurrence

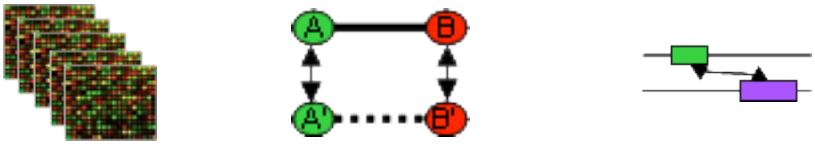

Co-localisation | Post Translational Modification | Network Analysis (Transitive)

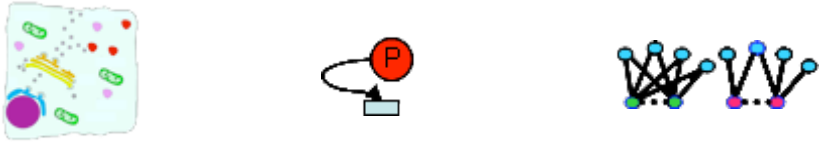

2.8 Real-time PCR

2.8.1 Total RNA isolation

Total RNA from cells cultivated in 10-cm plates was extracted by using Trizol ultrapure reagent (Invitrogen), according to the manufacturer's instructions. The concentration of total RNA was measured and its integrity was assessed by using an RNA 6000 Nano LabChips Kit and Agilent 2100 Bioanalyzer (Agilent Technologies, Palo Alto, CA, USA) according to the manufacturer's instructions.

2.8.2 DNase treatment

If amplification products are detected from the PCR reaction in the absence of reverse transcriptase (no RT control), it may be necessary to eliminate residual genomic DNA from the RNA sample.

For 1 µg of total RNA, 1 U of DNAse I (Invitrogen, Cat. No. 18047-019) was used in 10 µl DEPC-treated water. After incubating at RT for 15 min, the reaction was terminated by adding 1 µl 25 mM EDTA and heating for 10 min at 65 °C. This mixture was used directly for reverse transcription.

2.8.3 cDNA synthesis

Approximately 1 µg total RNA was reverse-transcribed by using 50 U of Multi-Scribe RT of the High Capacity cDNA Reverse Transcription Kit (Applied Biosystems, Cat. No. 4368814) with random primers in 20-µl reactions. Reactions were carried out for 10 min at RT and for 2 h at 37 °C. Finally, cDNAs were diluted to 1 ng/µl and stored at –20 °C.

2.8.4 Real-time PCR

Real-time PCR (qRT-PCR) reactions were performed in triplicate using SYBR-Green I master mix (Applied Biosystems) and 10 ng cDNA as template in 25-µl reactions. No template and no reverse transcriptase controls were included, and products were analysed by gel electrophoresis. As housekeeping gene the human hypoxanthine-guanine phosphoribosyl transferase (HPRT1) was assayed. Normalised expression levels of target genes were calculated by dividing the corresponding relative quantity by expression level of HPRT1. Gene-specific primers were designed by using the Primer 3 software (Rozen und Skaletsky, 2000); sequences are given in Section 2.11.

2.8.5 Statistical analysis

Statistical significance was assessed by using a two-sided *t* test assuming unequal variance of the biological replicates. The significance level was fixed at 5%, and null hypothesis were rejected of the *p* value was below 0.05.

2.9 Microarray RNA analysis

2.9.1 Experimental design

For RNA extraction, 2 x 10^6 HMEC-1 cells were seeded and, after 24 hours, transfected with one of four different vectors. Twenty-four hours after transfection, fluid shear stress stimulation (30 dyn/cm^2) was applied. Identical transfected cells plates, but without any application of shear stress, were used as the control group.

RNA isolation for gene-expression analysis was performed for eight different groups:

Table 2: Gene chip hybridisation experiment study design

	24h control (0 dyn/cm^2)	24h FSS (30 dyn/cm^2)
pTL1-HA2	6	6
pTL1-HA2/GPR30	6	6
pRK5myc/PATJ	6	6
pTL1-HA2/GPR30 pRK5myc/PATJ	6	6

2.9.2 Isolation of total RNA

HMEC-1 cells were scraped in Trizol immediately after fluid shear stress stimulation and stored at –80 °C, during the time of performing the 6 biological replicas (7 weeks). Total RNA from the 48 samples was obtained according to the manufacturer's protocol. The RNA was stored at –80 °C in RNase-free water.

2.9.3 Chip hybridisation, reverse transcription and fluorescent labelling

Four chip (HumanHT-12 v3 Expression BeadChip, Cat. No. BD-103-0203) hybridisations were performed with RNA from all the samples mentioned above. The high-value content on the HumanHT-12 Expression BeadChips provides genome-wide transcriptional coverage of well-characterised genes, gene candidates, and splice variants, with a significant portion targeting well-established sequences supported by peer-reviewed literature. Each array on the HumanHT-12 Expression BeadChip targets more than 25,000 annotated genes with more than 48,000 probes (27,455 coding transcripts, well-established annotation; 7870 coding transcripts, provisional annotation; 446 non-coding transcripts, well-established

annotation; 196 non-coding transcripts, provisional annotation; and 12,837 experimentally confirmed mRNA sequences that align to EST clusters).

Illumina Gene Expression protocols feature a first- and a second-strand reverse transcription step, followed by a single *in vitro* transcription (IVT) amplification that incorporates biotin-labelled nucleotides. Subsequent steps include array hybridisation, washing, blocking, and finally staining with streptavadin-Cy3. Direct hybridisation gene expression assays are run on the iScan system or BeadArray Reader. Fluorescence emission by Cy3 is quantitatively detected for downstream analysis. GenomeStudio software provides results in standard file formats that can readily be processed with most commercial expression-analysis software programs (performed by Aydah Sabah, Max Planck Institute for Molecular Genetics, Berlin).

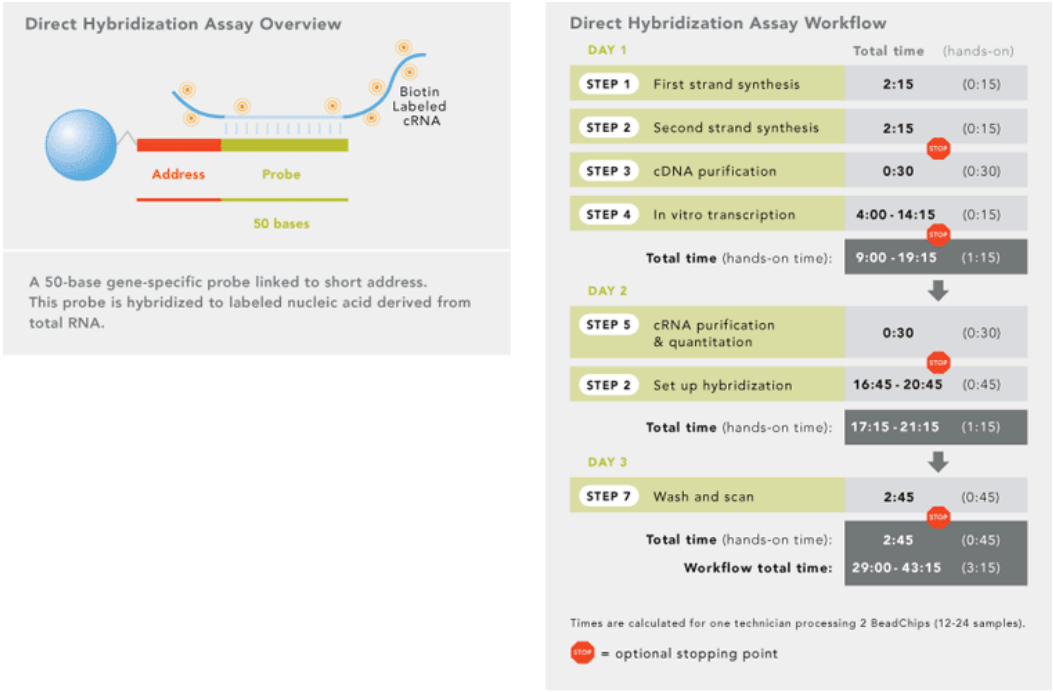

Figure 8: Schematic representation of Illumina chip hybridisation

2.9.4 Normalisation

Normalisation is the process of adjusting raw microarray data to remove systematic variation of non-biological origin. BeadStudio software offers three algorithms for normalising data generated from Illumina Gene Expression BeadChips and panel sets.

Three major assumptions are made when one is normalising microarray data:

(1) The effect of any systematic error will be uniform over the spatial distribution of bead types;

(2) The majority of genes will not be differentially expressed;

(3) The normalisation will remove systematic variation while leaving biological variation intact.

For the normalisation the rank invariant method was adopted. This is an appropriate selection in which the investigator can assume that a reasonable percentage of the genes in an experiment is not differentially expressed. For rank invariant normalisation, a subset of probes whose rank does not change across the experiment are identified and serve to define the normalisation parameters.

2.9.5 Detection of differentially expressed genes

For the identification of differentially expressed genes in the comparison of two sets of conditions with microarrays, Significance Analysis of Microarrays (SAM) was used. The SAM statistic identifies significant changes in gene expression by performing a set of gene-specific *t* tests. For each gene, a score is calculated on the basis of expression change relative to the standard deviation of repeated measurements for that gene. Genes with scores greater than a threshold delta were defined as significantly deregulated. Manual adjustment of this threshold delta allows the identification of smaller or larger gene cohorts. In addition, on the basis of random permutations of all measurements, a 'false discovery' rate was estimated.

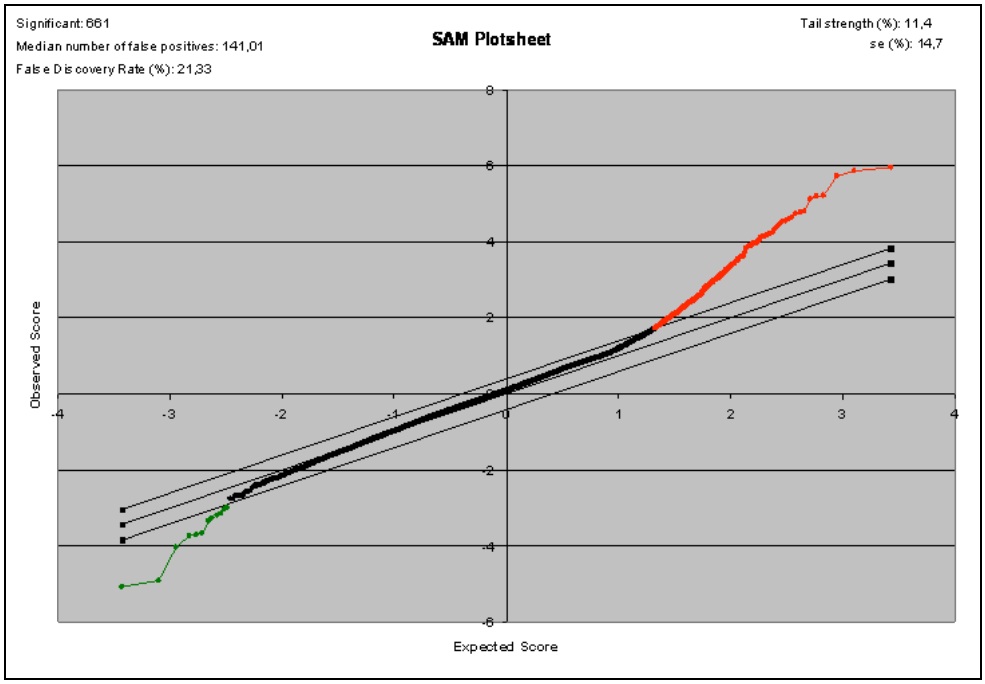

Figure 9: SAM plot example

2.9.6 Functional annotation and pathway analysis

In order to understand molecular and biological relations of candidate genes, significantly deregulated genes were functionally annotated using the web-based Database for Annotation, Visualisation, and Integrated Discovery (DAVID), (Dennis et al., 2003).

Significantly deregulated genes were further analysed by using Ingenuity Pathways Analysis, IPA 3.0, which identifies physical, transcriptional, and enzymatic interaction networks. Ingenuity Pathways Analysis is a web-based software application containing most literature knowledge of biological interactions between gene products (http://www.ingenuity.com/products/pathways_analysis.html). In this study, the gene expression profile is presented by the networks generated by Ingenuity: the significantly deregulated genes are displayed in list form together with the corresponding Illumina gene identification number and '*n*-fold change' expression values.

Networks are scored on the basis of the number of Network Eligible Molecules that they contain. The higher the score, the lower the probability of finding the observed number of Network Eligible Molecules in a given network by random chance.

Ingenuity Pathways Analysis calculates a significance score for each network. The score is generated using a *p*-value calculation, and is displayed as the negative decadic logarithm of that *p* value.

This score indicates the likelihood that the assembly of a set of focus genes in a network could be explained by random chance alone. A score of 2 indicates that there is a 1 in 100 chance that the focus genes are together in a network because of random chance. Therefore, networks with scores of 2 or higher have at least a 99% confidence of not being generated by random chance alone: p score $= -\log_{10}$ (p value)

MATERIALS

2.10 Vectors and constructs

Table 3: Vectors and constructs

No.	Construct	Selection	Description
Empty vectors			
17	pcDNA3.1(+)	AR, NR	Empty vector (Invitrogen)
49	pTL1-HA2*	AR,	Empty vector for N-term HA-tag fusion
10	pEGFP-N1	KR	Empty vector for N-term EGFP fusion
GPR30 constructs			
13	GPR30-EGFP/pcDNA3**	AR, NR	Expression of GPR30 with C-term EGFP tag
18	pcDNA3.1(+)/GPR30	AR, NR	Expression of full-length GPR30
45	pTL1-HA2/GPR30	AR	Expression of GPR30 with N-term HA-tag
PATJ constructs			
44	pRK5myc/PATJ***	AR	Expression of PATJ with N-term myc-tag

* provided by Dr. Markus Ralser, Max-Planck Institut für Molekulare Genetik, Berlin.

** provided by Prof. Eric Prossnitz, University of New Mexico, Albuquerque, USA.

*** provided by Prof. Ben Margolis, University of Michigan Medical School, Ann Arbor, Michigan, USA.

Abbreviations: AR, ampicillin resistance; KR, kanamycin resistance; NR, neomycin resistance.

2.11 Primers

All primers were obtained from MWG Biotech in a quantity of 0.01 µmol (HPSF purification) and were resuspended in H_2O to give a stock concentration of 100 pmol/µl (100 mM). Equal amounts of forward and reverse primer were combined and diluted with ddH_2O to 5 µM each.

Table 4: Primers

No.	Sequence (5' → 3')	Comment
P69	CGACCACTTTGTCAAGCTCA	qRT-PCR, human GAPD
P70	TTACTCCTTGGAGGCCATGT	qRT-PCR, human GAPD
P73	TTGTTGTAGGATATGCCCTTGA	qRT-PCR, human HPRT1
P74	GGCTTTGTATTTTGCTTTTCCA	qRT-PCR, human HPRT1
P120	TTGAGGTGTTCAACCTGCAC	qRT-PCR, human GPR30, ORF
P121	GAGGAAGAAGACGCTGCTGT	qRT-PCR, human GPR30, ORF
P128	TTCCAGGCTCCTCTGTCAGT	qRT-PCR, human PATJ
P129	CTGCTGCCCCTTCTTCATAG	qRT-PCR, human PATJ
P186	CCCCTGCACTATGGAGTCTG	qRT-PCR, human eNOS
P187	AGTGCCTGGACCCACCAG	qRT-PCR, human eNOS
P188	CGCTGAGCTCCTCTGCTACT	qRT-PCR, human ICAM-1
P189	GATGACTTTTGAGGGGGACA	qRT-PCR, human ICAM-1
P203	GGCCACGTCATGTCTCTAAA	qRT-PCR, human GPR30, 3´UTR
P204	CTGTGTGAGGAGTGCAAGGT	qRT-PCR, human GPR30, 3´UTR
P213	CCCAAGCTTGCCACCATGGAT GTGACTTCC	Cloning of pcDNA3(+)/GPR30, HindIII
P214	TAGTTTAGCGGCCGCACGTTAG CACCTGCATTACCTACACGGCACTGCTG	Cloning of pcDNA3(+)/GPR30, NotI
KLF-2-f3	CTTTCGCCAGCCCGTGCCGCG	qRT-PCR, human KLF-2
KLF-2-r3	AAGTCCAGCACGCTGTTGAGG	qRT-PCR, human KLF-2

2.12 Antibodies

Table 5: Primary and secondary antibodies

Antibody	Company	Cat#	Dilution
Primary antibodies			
rabbit polyclonal anti-GPR30 N-ter domain	Acris	SP4209P	1:500
rabbit polyclonal anti-GPR30 1st extracellular domain	MBL	LS-AA1184	1:500
rabbit polyclonal anti-GPR30 3rd extracellular domain	MBL	LS-A4271	1:500
rabbit polyclonal anti-GPR30 C-ter domain antiserum	MBL	LS-A4272	1:500
rabbit polyclonal anti-GPR30 C-ter domain antiserum	provided by E. Prossnitz		1:1000
goat polyclonal anti-GPR30 internal domain	Santa Cruz	sc-48524	1:500
mouse monoclonal anti-GFP	Roche	11814460001	1:750
rabbit polyclonal anti-Myc	Sigma	C3956	1:2000
mouse monoclonal anti-Myc, clone 9E10	Santa Cruz	sc-40	1:1000
mouse monoclonal anti-HA, clone F-7	Santa Cruz	sc-7392	1:1000
mouse monoclonal anti-HA, clone 16B12	Covance	MMS-101R	1:1000
Secondary antibodies for immunofluorescence			
Alexa Fluor 488 goat anti-rabbit IgG (H+L)	Mol. Probes	A-11008	1:500
Alexa Fluor 568 goat anti-rabbit IgG (H+L)	Mol. Probes	A-11011	1:500
Alexa Fluor 488 goat anti-mouse IgG (H+L)	Mol. Probes	A-11001	1:500
Alexa Fluor 568 goat anti-mouse IgG (H+L)	Mol. Probes	A-11004	1:500
Secondary antibodies for western blotting			
sheep anti-mouse peroxidase conjugated	Amersham	NXA931	1:5000
goat anti-rabbit peroxidase conjugated	Calbiochem	DC03L	1:5000

3 RESULTS

3.1 Detection of GPR30 protein by western blotting

Since GPR30 is a heptahelical transmembrane receptor with strong lipophilic properties, its solubilisation, e.g. for western blotting, represents a challenging task. Although GPR30 could be solubilised and therefore detected by several investigators (Thomas et al., 2005), (Vivacqua et al., 2006), (Filardo et al., 2007), these protocols never gave successful results in the laboratory where the present project was carried out. Therefore, many protocols were re-evaluated and optimised using different antibodies. First, GPR30 fused to EGFP (Enhanced Green Fluorescent Protein) was detected using an anti-GFP antibody as well as a specific anti-GPR30 antibody. Finally, endogenous GPR30 could be detected with the same specific anti-GPR30 antibody.

3.1.1 Detection of GPR30-EGFP using an urea-SDS protocol and GFP antibody

All the experiments were performed in the HEK (Human Embryonic Kidney) 293 cell line, since it is one of the most commonly used cell lines on account of its high transfection efficiency and, more importantly, because it does not express GPR30. Therefore, HEK293 cells were transfected with a vector expressing EGFP as a positive control (pEGFP-C1) or a vector expressing GPR30 fused to EGFP (GPR30/pEGFP-C1) in order to visualise the successful transfection. Mock cells (cells that receive the same reagent treatment but without fluorescent label) were used as a negative control. Since no specific anti-GPR30 antibody was initially available to detect and evaluate GPR30 expression, an antibody against EGFP was used to detect the GPR30-EGFP fusion protein in western blotting.

To detect endogenous as well as over-expressed GPR30 by western blotting, the first step was the solubilisation of GPR30. Many different protocols for the solubilisation of GPCRs were evaluated: one used RIPA buffer (Vivacqua et al., 2006), one crude membrane preparations or cell fractionation (Nagamatsu et al., 1992), (Moore et al., 2000). The first successful result was obtained using a urea–SDS-based protocol (an important step was the incubation of lysates at 37 C for 15 min, to avoid GPR30 aggregation), (Edinger et al., 2003) and a commercially available anti-GFP antibody. As shown in Figure 10, lane 3, a specific band corresponding to GPR30-EGFP with a molecular weight of 71 kDa was detected. In lane 6, in which a urea-Triton lysis buffer was used, it was not possible to detect a specific band for GPR30-EGFP, demonstrating that only the combination of urea and SDS – and not

urea in combination with Triton – was successful in solubilising the extremely hydrophobic GPR30 protein. In lanes 2 and 5, where pEGFP-C1 was transfected as a positive control, two bands are detected for EGFP (29 kDa and >29 kDa) indicating a mature and a pre-processed form of the protein (Waller et al., 2000); the smaller of these corresponded to the expected molecular weight of GFP, whereas the larger is consistent with the size of a mono-ubiquitylated GFP molecule, (Riess et al., 2005).

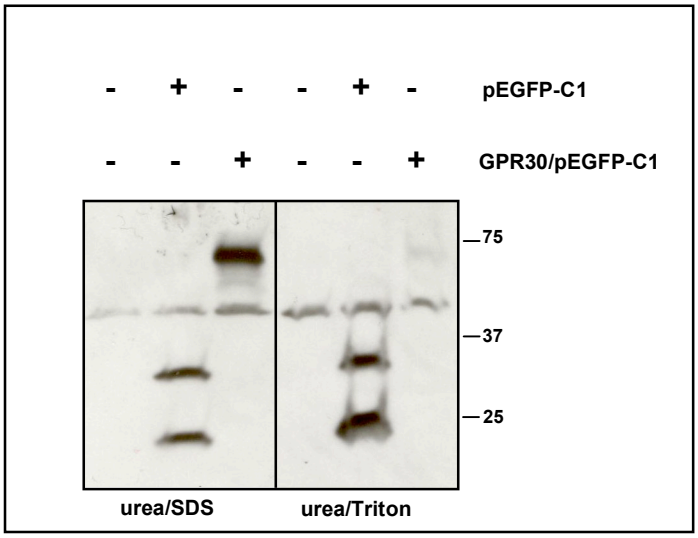

Figure 10: Detection of GPR30-EGFP in HEK293 cells using an urea-SDS lysis buffer.
Note that in lanes 2 and 5 EGFP expression (bands <37 kDa) was detected using two different buffers (SDS and Triton), while in lane 3 GPR30-EGFP (71 kDa) could only be detected using a urea-SDS buffer, but not under urea–Triton conditions (lane 6).

3.1.2 Detection of GPR30 by western blotting using a specific anti-GPR30 antibody

After successful expression and solubilisation of GPR30 in HEK293 cells, the next goal was to optimise a western blotting protocol for GPR30 detection. Therefore, several commercially available antibodies against different epitopes (N terminus, C terminus, different extra- or intra-cellular domains) and an antiserum detecting the C terminus (kindly provided by Prof. Eric Prossnitz, University of New Mexico, Albuquerque, USA) of GPR30 were tested. In Figure 11 an *in silico* prediction of the secondary structure of GPR30 (generated with the SOSUI free online tool) is shown and the binding sites of the six antibodies tested are depicted.

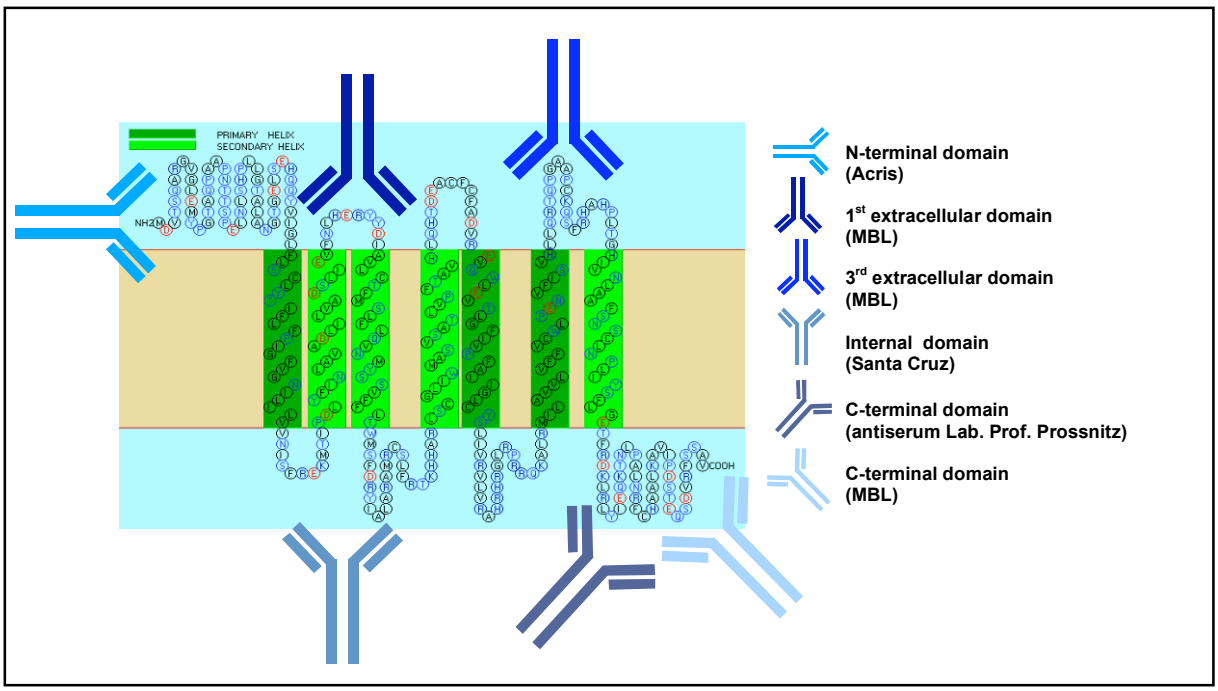

Figure 11: In silico prediction of the domain of GPR30 using the program SOSUI
Expected binding sites of the six different GPR30 antibodies are depicted.

In order to test these antibodies, HEK293 cells were transfected with an empty vector (pcDNA3.1(+)), as a negative control, with a vector expressing EGFP, as a transfection control (pEGFP-C1), and a vector expressing GPR30 fused to EGFP (GPR30/pEGFP-C1) or full-length GPR30 (pcDNA3.1(+)/GPR30). Cells were then lysed using the urea–SDS-buffer protocol described above, and a new RIPA-buffer-based protocol (Filardo et al., 2007). The blots were probed with an antibody directed against EGFP to check for successful over-expression and lysis, and with the six different antibodies against GPR30. Two of the six antibodies tested produced a specific signal at the expected size (an example is shown in Figure 12). In combination with the urea–SDS-based lysis protocol, the antibody against the 3rd extracellular domain (MBL) and the polyclonal antibody against the C-terminal domain (Prof. E. Prossnitz laboratory) detected both full-length and EGFP-fused GPR30 (Figure 12). In contrast, when the antibody against an internal domain of GPR30 (Santa Cruz) was used along with various lysis conditions, no specific band for GPR30 was observed (Figure 12, panel A, left and right sides). As a positive control, the anti-GFP was used to check, first, the solubilisation properties of the lysis buffers used (lane 4, panels D, left and right) and, second, to detect the expression of GPR30-EGFP (lane 2, panels B, C and D).

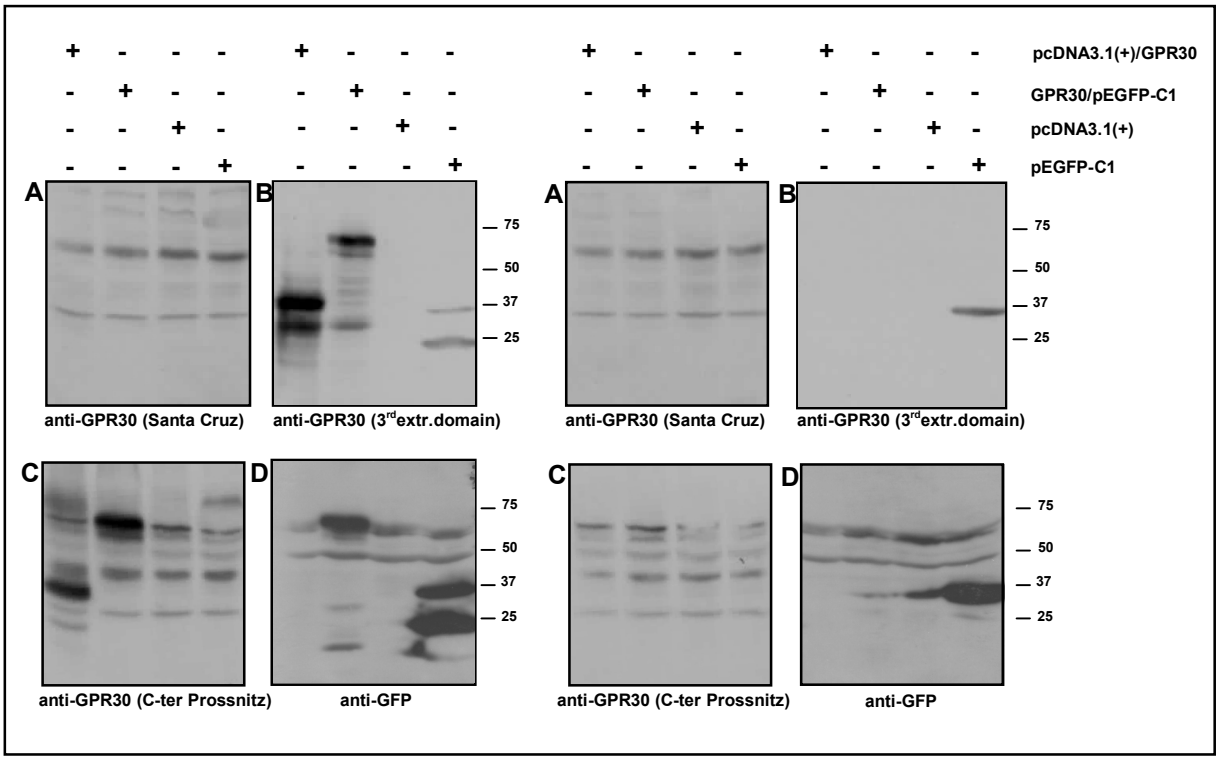

Figure 12: Detection of GPR30 in HEK293 cells by using different anti-GPR30 and anti-GFP antibodies
Cells were lysed by using either a urea/SDS buffer (left panels) or a RIPA buffer (right panels). GPR30 could be detected specifically using a urea/SDS buffer and anti-GPR30 antibodies against the 3rd extracellular domain (left panel B) as well as against the C terminus (left panel C). As a positive control, pEGFP could be detected in the corresponding samples (left panel D, lane 2, and both panels D, lane 4).

3.1.3 Detection of endogenously expressed GPR30

Subsequently, the western-blotting protocol was successfully applied to detect GPR30 in a cell line expressing it endogenously, in order to prove the absence of endogenous GPR30 in GPR30-LacZ mutant mice (PhD of Jörg Isensee). Therefore, SkBr3 breast cancer cells that were ER-negative (estrogen receptor α and β) (Vladusic et al., 2000) but GPR30-positive were transfected with an expression vector for an N-terminally HA-tagged GPR30 (pTL1-HA2/GPR30). Transfected cells were used as a positive control to compare GPR30 over-expression with the endogenous expression of GPR30 in SkBr3 cells.

In Figure 13 (left panel), using the anti-GPR30 against the 3rd extracellular domain antibody (MBL), specific bands are shown for endogenous GPR30 in non-transfected SkBr3 cells (lane 2) as well as in the transfected SkBr3 cells over-expressing HA-GPR30 (lane 1). Using an anti-HA antibody (right panel) a band with a molecular weight of 42 kDa corresponding to over-expressed HA-GPR30 is observed, but only in transfected cells (lane 3).

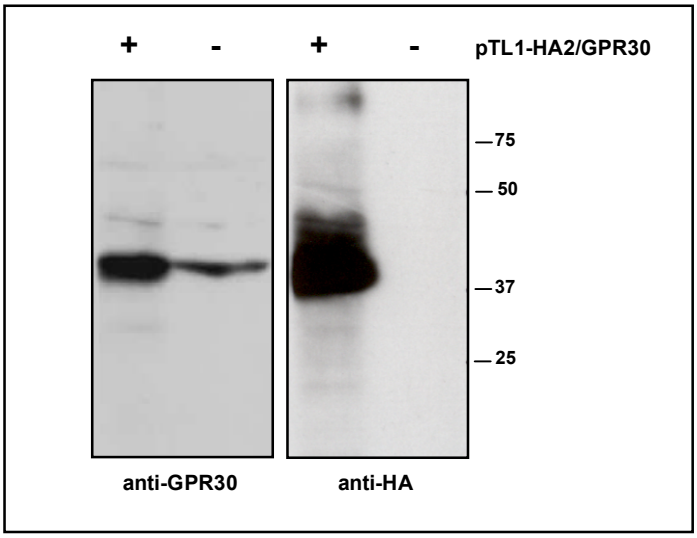

Figure 13: Detection of endogenous GPR30 using a specific anti-GPR30 antibody
The detection of endogenous GPR30 was achieved using a specific anti-GPR30 antibody against an epitope present in the 3rd extracellular domain (lane 2) in SkBr3 cells. In lanes 1 and 3 the over-expression of HA-GPR30 as a positive control is shown. Anti-GPR30 (left panel) or anti-HA (right panel) antibodies were used.

This optimised protocol was evaluated in wild-type and in GPR30-deficient mouse tissue samples, but without success. These findings underline the difficulty of detecting murine GPR30 protein in tissues, probably due to low expression levels, to the lipophilic properties as a 7TMR, and most importantly, to the lack of mouse antibodies.

3.2 Detection of GPR30 protein by immunocytochemistry

In order to look at the cellular expression of GPR30 and to test whether the two antibodies (3rd extracellular domain antibody obtained from the MBL and C-terminal domain antiserum obtained from the laboratory of Prof. E. Prossnitz) detecting the protein by western blotting were also suitable for immunocytochemistry, HeLa cells were transfected with a vector expressing GPR30 fused to EGFP (GPR30/pEGFP-C1), fixed and then probed with the two antibodies. As shown in Figure 14, the cells showed a cellular localisation of GPR30-EGFP (left panels) at the level of endoplasmic reticulum, according to the results of others (Revankar et al., 2005), (Otto et al., 2008). When the cells were stained with the two anti-GPR30 antibodies (3rd extracellular domain and C-terminal domain; upper and lower middle panels, respectively) again a specific signal was detected. In the right-hand panels, the merged pictures showed co-localisation of the EGFP signal and both antibodies.

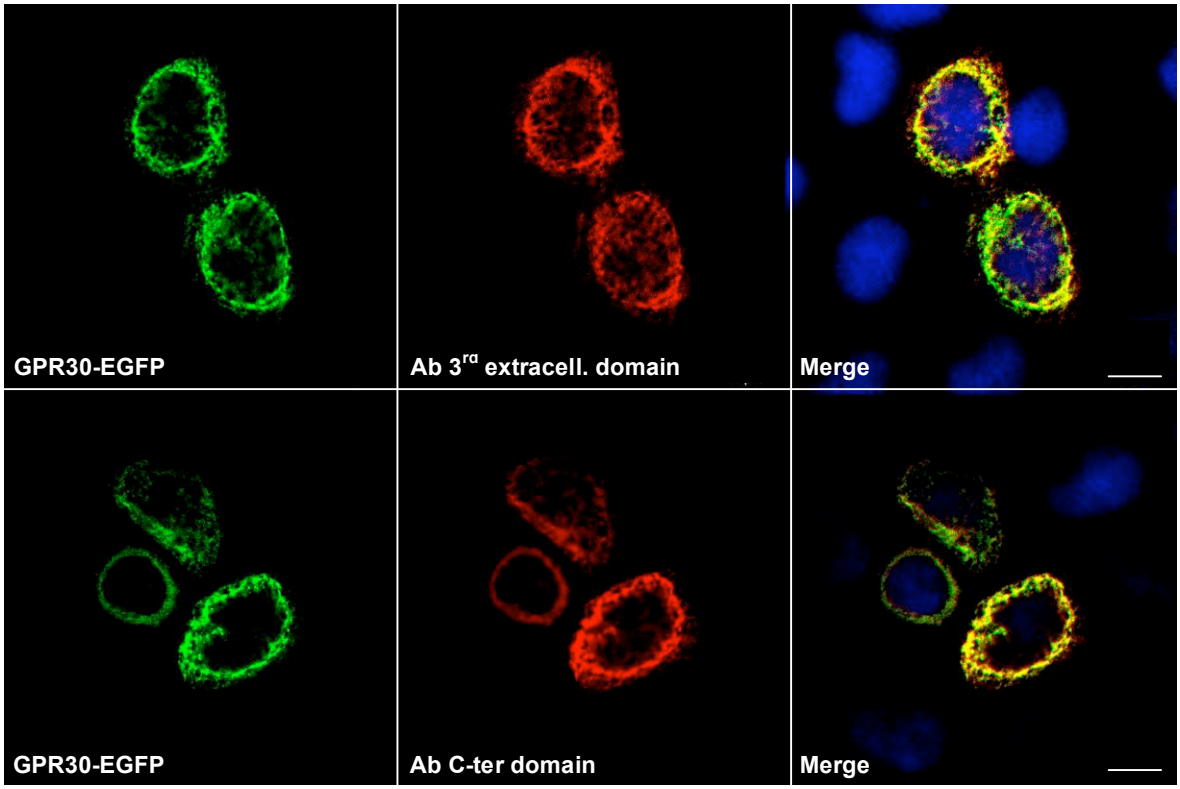

Figure 14: Detection of GPR30 by immunocytochemistry
HeLa cells transiently transfected with GPR30-EGFP and stained with antibodies detecting the 3rd extracellular domain (upper panel) or C-terminal domain (lower panel) of GPR30. The EGFP signal (green) and the antibody signal (red) co-localised for both antibodies (yellow signal in the merged images). Scale bar: 10 µm.

3.3 GPR30 interacts specifically with PATJ in mammalian cells

To understand better the potential involvement of GPR30 in cell signalling, the next step was to identify intracellular proteins able to interact with GPR30. Therefore, Y2H screenings were performed in a preliminary study (PhD project of Jörg Isensee) using the N- or the C-terminal domain of the human GPR30 as baits.

Briefly, the N- and C-terminal domains were chosen, since most interactions with other proteins are expected to occur within these regions. Bait vectors were generated encoding amino acids 1–54 for the N-terminal construct and amino acids 330–375 for the C-terminal construct, respectively. A human heart cDNA library was subcloned into a prey vector and co-transformed with either bait vector. Interaction of bait and prey proteins leads to the formation of an active transcription factor complex that induces the expression of the two reporter genes HIS3 and LacZ in LV40 yeast cells. For both bait vectors, more than 200 colonies were obtained in two independent screens, of which 20 (N-terminal bait) and 30 clones (C-terminal bait) were randomly selected. Informative results of the sequencing analysis were obtained for only 19 clones from the N- and 22 clones from the C-terminal

screen, respectively. BLAST (Basic Local Alignment Search Tool) analysis of these sequences against the human genome revealed that most clones mapped to five genes and two encoded genomic sequences without homology to known genes. Further controls were performed to check these candidate genes, but finally only two were validated and considered for further analysis. Both came from the C-terminal screen: one mapped to the Pals1-associated tight junction protein (PATJ) and the other to FUN14 domain-containing 2 (FUNDC2) protein.

To confirm the interaction between GPR30 and the newly identified interacting proteins in a mammalian system, co-immunoprecipitation (CoIP) studies were performed. First, the cDNA encoding full-length GPR30 was cloned into the pTL1-HA2 vector in-frame with an HA tag fused at its N-terminus. The cDNA encoding N-terminally myc-tagged PATJ was kindly provided by Dr. Margolis (University of Michigan) and the cDNA for FUNDC2 was obtained from the German Resource Center for Genome Research (RZPD, IOH40818-pdEYFP-C1amp) and cloned into the N-terminally myc-tagged expressing vector pEXP475 (FUNDC2 cloning was performed by Jörg Isensee). Second, several CoIP protocols (Devost und Zingg, 2003), (Okuma und Reisine, 1992), (Harvey et al., 2001), were evaluated (data not shown) before solubilisation and co-immunoprecipitation of GPR30 was successful. Therefore, to validate the interaction between GPR30 and PATJ or FUNDC2, HEK293 cells were transfected with HA-GPR30 and either myc-PATJ or myc-FUNDC2 expression plasmids. Forty-eight hours after the transfection, cells were lysed by using a RIPA-buffer based protocol (Rondou et al., 2008) and myc-PATJ or myc-FUNDC2 were immunoprecipitated by using a monoclonal anti-myc antibody. As shown in Figure 15, GPR30 was detected in total cell lysates (INPUT, lanes 1 and 3 in the bottom left panel and lanes 2 and 4 in the bottom right panel). Note that in addition to the specific 42-kDa band, a second band was observed. This band may represent a degraded form of GPR30 and has also been observed by other investigators (Rondou et al., 2008). PATJ and FUNDC2 were also detected in total cell lysates (Figure 15, INPUT lanes 2 and 3 in the left panel and lanes 3 and 4 in the right panel).

For immunoprecipitation purposes an anti-myc antibody was used. Myc-PATJ and myc-FUNDC2 were found to bind to protein G Sepharose beads and could be detected with the anti-myc antibody (Figure 15, IP: anti-myc, lanes 2 and 3 in the left panel and lanes 3 and 4 in the right panel). Note that GPR30 could only be detected when co-expressed with PATJ (Figure 15, IP: anti-HA, lane 3 in the left panel). The interaction of GPR30 with FUNDC2 could not be verified in HEK293 cells, as shown by the absence of a band using an anti-HA antibody (Figure 15, IP: anti-HA, lane 4 in the right panel).

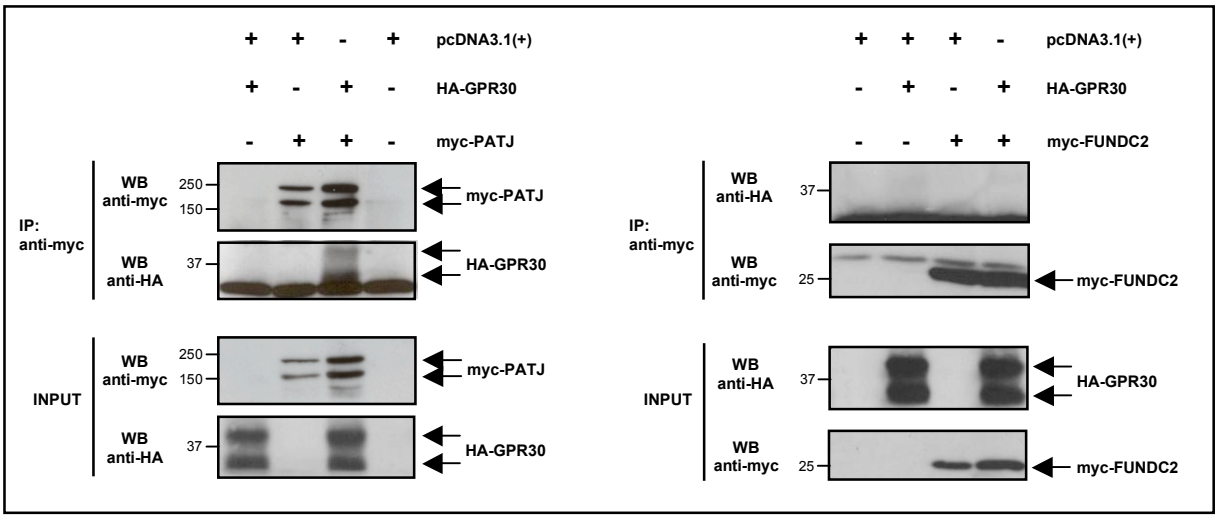

Figure 15: Detection of the interaction of GPR30 with PATJ
HEK293 cells transiently co-expressing N-terminally HA-tagged GPR30 (HA-GPR30) with N-terminally either myc-tagged PATJ (myc-PATJ) or myc-tagged FUNDC2 (myc-FUNDC2). A specific band for GPR30 is shown only in the CoIP lysates over-expressing HA-GPR30 and myc-PATJ (lane 3, left panel). Note the absence of a specific band for GPR30 co-immunoprecipitated when co-expressed with myc-FUNDC2 (lane 4, right panel).

Since no specific interaction between GPR30 and FUNDC2 was found, the focus in subsequent studies was only on the interaction of PATJ with GPR30.

3.4 GPR30 partially co-localises with PATJ

The next step was to investigate the localisation of the interaction between GPR30 and PATJ at the cellular level. Since the function of PATJ was predominantly investigated in epithelial cell types (Roh et al., 2003; Roh et al., 2002; Roh et al., 2002), (Lemmers et al., 2002) and GPR30 was found to be expressed in the epithelial cancer cell line SkBr3, epithelial HeLa cells were used for further studies. HeLa cells were transfected simultaneously with GPR30-EGFP and myc-PATJ. After 48 hours the cells were fixed and then probed with an anti-myc antibody to visualise myc-PATJ. DAPI (4′.6-Diamidin-2-phenylindol, blue signal) staining was performed in order to visualise cell nuclei. In Figure 16 the merge of both signals representing the corresponding expression patterns indicates a partial co-localisation of GPR30 with PATJ, probably at the level of the endoplasmic reticulum, as already described for GPR30 (Revankar et al., 2005), (Otto et al., 2008).

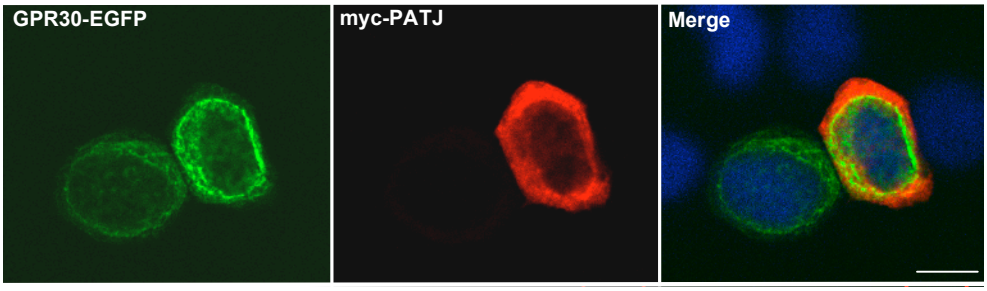

Figure 16: Co-localisation of GPR30 and PATJ
HeLa cells were co-transfected with PATJ-Myc (red) and GPR30-EGFP (green). Note the partial co-localisation of PATJ and GPR30 in the rightmost panel. Scale bar: 10 µm.

3.5 GPR30 becomes up-regulated in endothelial cells upon fluid shear stress (FSS)

The blood vessels in the body are responsible for the transport of oxygen, blood and plasma throughout the body and they are characterised by different cell types. In particular the inner layer of the blood vessels is made up of endothelial cells directly in contact with the flowing blood. Blood vessel occlusion can lead for instance to an increase of fluid shear stress (FSS) caused by the strong difference between the high pre-occlusive and the very low post-occlusive pressure regions (Schaper, 2009). In addition, during a vessel constriction tissue are exposed to prolonged hypoxic conditions and this phenomenon leads to cellular remodelling (Rey und Semenza).

In 1997, in one of the first cloning approaches, GPR30 was found to be up-regulated in Human Umbilical Vein Endothelial Cells (HUVECs) exposed to fluid shear stress. Isensee *et al.* have shown that GPR30 is expressed in small arterial vessels of numerous tissues (e.g. kidney, heart, peritoneum, genital tract), in particular in an endothelial cell subpopulation (Isensee et al., 2009), and in a previous publication from another group the expression of GPR30 mRNA was reported for human internal mammary arteries and saphenous veins (Haas et al., 2009). Moreover, GPR41 (orthologue of GPR30) was found to be up-regulated in a rat cardiac cell line (H9c2, cardiomyocyte-like cells derived from embryonic myocardium) after 2 hours of post-ischemic re-oxygenation (Kimura et al., 2001).

For these reasons, the second part of this thesis focusses on the relation between GPR30 and either the ischemia/reperfusion (I/R) or the FSS model. The first model evaluated was an *in vitro* approach of I/R namely hypoxia/re-oxygenation using primary endothelial cells (HUVECs) and their derived cell line (EAhy926). The cells were exposed to oxygen glucose

deprivation (OGD) in an hypoxic chamber (0.5% oxygen) for different time points (in collaboration with Dr. Dorette Freyer Department of Experimental Neurology, Charité, Berlin), (Ruscher et al., 2002). With this model only a minimal (and statistically not significant) change in the expression of GPR30 was detected, probably due to the use of a different cell type, i.e. endothelial cells instead of cardiomyocytes. Therefore this model was not followed up within the scope of this thesis.

Subsequently, the FSS model was considered as a second approach. Takada *et al*. showed, using a semi-quantitative RT-PCR (reverse transcription PCR), that GPR30 expression was 5-fold higher under a FSS of 1.5 dyn/cm^2, reaching an 8-fold up-regulation at 15 dyn/cm^2 for 24 hours, compared with unstimulated cells. Stimulation of the cells for shorter periods (8 hours) but under the same FSS conditions induced a lower up-regulation (Takada et al., 1997). Thus, HUVECs were used to verify these findings before the analysis was extended to other endothelial cells. First, the morphological changes were evaluated by microscopical analysis and, as shown in Figure 17, the cells were found to be aligned in the flow direction only when a shear stress of 30 dyn/cm^2 was applied. Secondly, a significant up-regulation comprising a 4.57-fold increase in GPR30 expression (p = 0.016) was detected by qRT-PCR (quantitative real-time PCR) in cells stimulated for 24 hours with 30 dyn/cm^2 shear stress. The effect of FSS conditions on gene expression regulation was validated by measuring the transcript level of Intercellular Adhesion Molecule-1 (ICAM-1) as a positive control (8.62-fold change at 30 dyn/cm^2, p = 0.019) (Nagel et al., 1994).

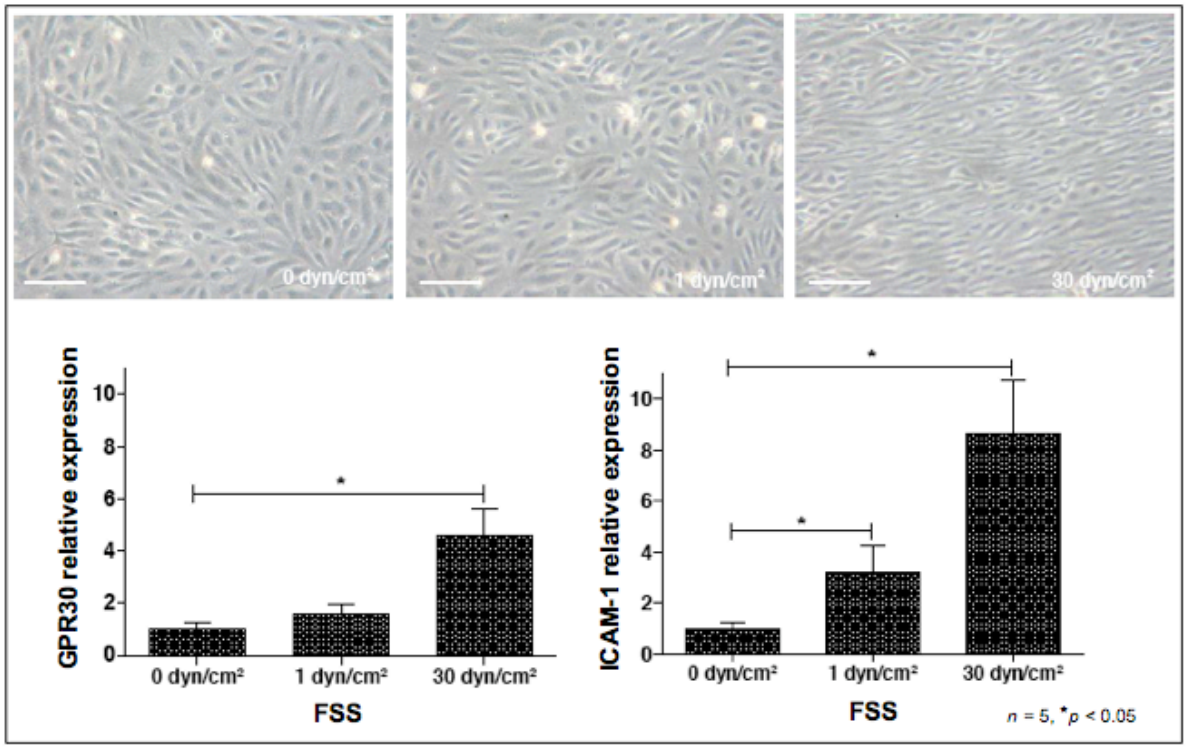

Figure 17: GPR30 is up-regualted in HUVECs upon FSS
HUVECs morphological changes upon increasing fluid shear stress (FSS 0, 1 and 30 dyn/cm^2), in the upper panel. Note the elongation of the cells under high FSS (30 dyn/cm^2). Scale bar: 50 µm. The figure shows relative gene expression levels of GPR30 (lower panel, left) and ICAM-1 (lower panel, right) by real-time PCR in HUVECs exposed to different FSS conditions. GPR30 was found to be significantly up-regulated (4.57-fold at 30 dyn/cm^2) as well as the positive control ICAM-1 (8.62-fold at 30 dyn/cm^2). Gene expression of GPR30 and ICAM-1 was measured relative to HPRT levels. * $p < 0.05$ ($n = 5$, t test).

To assess whether the effect of FSS on the expression of GPR30 was a phenomenon related only to HUVECs, other human endothelial cells were subjected to it and analysed. Therefore, primary cells Human Umbilical Arterial Endothelial Cells (HUAECs) and Human Aortic Endothelial Cells (HAoECs) were used, and in all cases GPR30 was found to be expressed and to behave in the same way under conditions of FSS.

In Figure 18, morphological changes of HUAECs with FSS are shown. Only when stimulated with FSS at 30 dyn/cm^2 were the cells found to respond to shear stress. In these cells, GPR30 and ICAM-1 were found to be up-regulated, with changes of 1.99-fold and of 3.67-fold respectively, but – possibly owing to the lack of a large number of samples (only three replicates) – these factors were statistically not significant ($p = 0.06$ for GPR30 and 0.16 for ICAM-1).

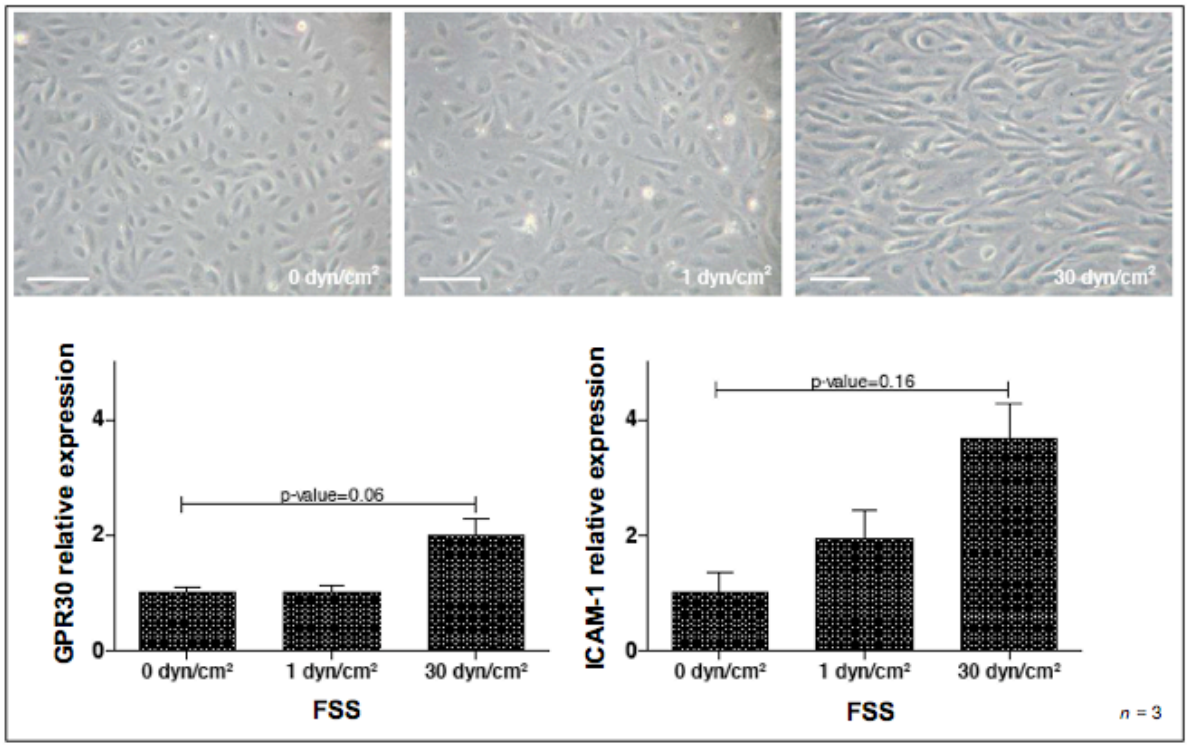

Figure 18: GPR30 is up-regualted in HUAECs upon FSS
HUAECs morphological changes upon increasing fluid shear stress (FSS 0, 1 and 30 dyn/cm^2), in the upper panel. Scale bar: 50 µm. The figure shows relative mRNA expression levels of GPR30 (lower panel, left) and ICAM-1 (lower panel, right) in HUAECs. Note that GPR30 was found to be up-regulated upon FSS (30 dyn/cm^2), but not significantly, as was also the case for ICAM-1 (p = 0.06 and 0.16, respectively). Gene expression of GPR30 and ICAM-1 was measured relative to HPRT levels.

Human Aortic Endothelial Cells (HAoECs) were also investigated. When subjected to FSS for 24 hours, they showed the same morphological changes as HUVECs and HUAECs (data not shown). Here, gene expression levels of GPR30 also appeared up-regulated at 30 dyn/cm^2 of shear stress, with a change of 6.43-fold and p = 0.019. Up-regulation of ICAM-1 (4.01-fold change, p = 0.045), used as a positive control, demonstrated again the effect of FSS. Although up-regulation of GPR30 and ICAM-1 was statistically significant at 30 dyn/cm² of FSS, a rather high standard deviation was observed among the four biological replicates analysed. The heterogeneity among samples may be related to the different origins of these cells (vein and arterial *vs.* aortic).

Since GPR30 is expressed in small arterial vessels, a Human Microvascular Endothelial Cell (HMEC-1, microvascular cells immortalised by SV40 transformation, (Ades et al., 1992)) line was investigated, in order to verify the expression of both GPR30 and PATJ and their response to FSS and possibly to make use of this in future experimental approaches. When subjected to FSS, HMEC-1 cells showed changes in morphology, cellular alignment and

elongation in the direction of flow that were similar to the changes already seen in the other endothelial cells tested (Figure 19).

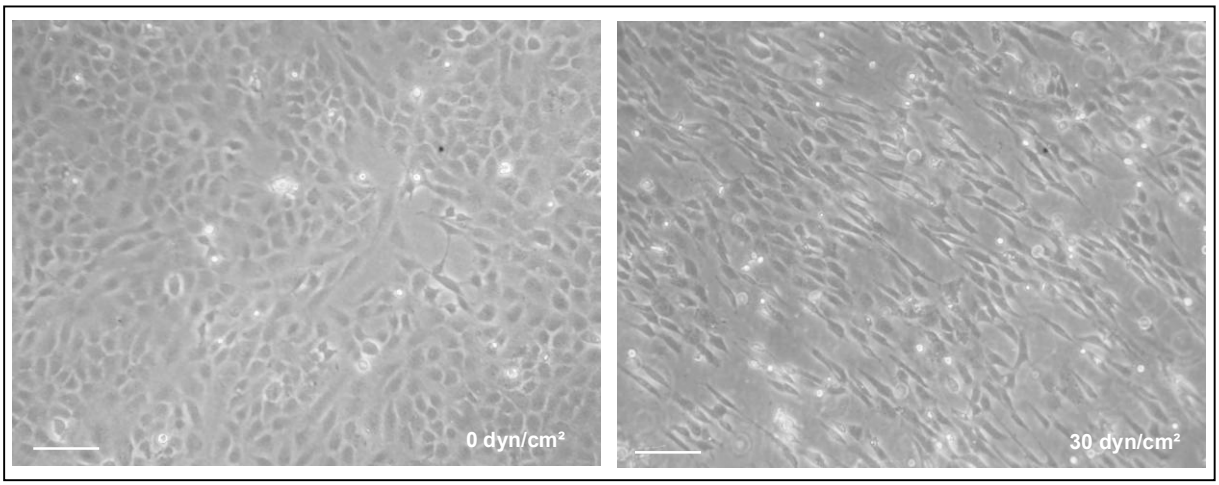

Figure 19: Morphological changes of HMEC-1 cells upon FSS
Note the elongation of the cells at 30 dyn/cm². Scale bar: 50 µm.

More importantly, using RT-PCR, HMEC-1 cells were found to express GPR30 as well as PATJ, which would allow in future approaches to e.g. knock down or over-express either of the genes or gene products and to perform microarray analysis. Cells transfected with an empty vector (as a control for further experiments) expressed GPR30 and PATJ at basal levels (0 dyn/cm²) and up-regulation of GPR30 (2.05-fold change, $n = 2$) upon FSS was found as well as up-regulation of PATJ (3.51-fold change, $n = 2$). Furthermore, the expression of ICAM-1, used as a positive control to validate the effects of shear stress, was limited (1.65-fold change, $n = 2$), probably owing to a different expression level of this cell type, but expression of Krueppel-like factor 2 (KLF-2), another FSS responsive gene (Dekker et al., 2002), was found clearly up-regulated at 30 dyn/cm² (5.34-fold change, $n = 2$), (in collaboration with Dr. Kerstin Lehmann, laboratory of Prof. Ivo Buschmann, Charité, Berlin).

3.6 Gene-expression profiling in human microvascular endothelial cells

To evaluate the effects of GPR30 and of its interaction with PATJ in endothelial cells under FSS conditions at gene expression level, a suitable cellular system was established. First, it was necessary to decide upon the best cell type and approach (knock-down or over-expression) to use. Thus, HUVECs were evaluated for RNA interference (knock-down of GPR30 transcript or lamin A/C, used as positive control), and also for transfection (over-expression of pEGFP-1). For neither approach was it possible to obtain any substantive result. Indeed, the RNA interference was effective only for lamin A/C and the transfection

efficiency of these cells was very low (Appendices 6.1.1 and 6.1.2). Secondly, the endothelial cell line HMEC-1 was chosen to test the same methods. In this case too, the silencing did not lead to the expected reduction at transcript level of GPR30, but the transfection efficiency was much higher compared to the efficiency in HUVECs (Appendices 6.1.3 and 6.1.4). Therefore, HMEC-1 cells were chosen as a cellular system for over-expression and the RNA interference approach had to be discarded.

Once a reliable and reproducible cellular system for (a) biomechanical stimulation (FSS) using the HMEC-1 cells and (b) GPR30 and PATJ over-expression had been established, a microarray experiment was performed to investigate the overall gene expression pattern in these cells to gain insight into GPR30 and/or PATJ molecular effects. Therefore, HMEC-1 cells were transfected with GPR30-HA and/or PATJ-myc and were subjected to 30 dyn/cm² of FSS for 24 hours in six biological replicates. As shown in the Materials and Methods section (Table 2) the experimental design was as follows and included eight experimental groups:

	Experimental groups	
	- FSS	+ FSS
Empty vector	1	2
GPR30	3	4
PATJ	5	6
GPR30 + PATJ	7	8

After cell transfection total RNA was isolated and, before proceeding with the microarray assay, successful over-expression of GPR30 and PATJ was tested and confirmed: a 1500-fold up-regulation of both GPR30 and PATJ was found by real-time PCR. The up-regulation of KLF-2 as a positive control was also determined by real-time PCR to validate the effects of FSS (4.9-fold change, $p = 0.003$). In addition, the successful application of FSS was assessed and could be confirmed on the basis of morphological changes in the eight experimental groups and six replicates.

The microarray assay was performed by using the Illumina platform (Materials and Methods, Section 2.9.3) which targets more than 25,000 annotated genes with more than 48,000 probes for human genes. The normalisation to adjust the raw data was done by the rank invariant method (Materials and Methods, Section 2.9.4).

3.6.1 Effects of FSS on HMEC-1 cells

To identify differentially expressed genes, significance analysis of microarrays (SAM) (Materials and Methods, Section 2.9.5) was applied and a 'false discovery' rate (FDR) less than 5% was considered.

When the gene's expression in cells transfected with an empty vector and under FSS (24 hours) conditions (group 2) was compared with the gene's expression in cells transfected with an empty vector but without any shear stress stimulation (group 1), 217 genes were found to be up-regulated and 6 down-regulated (Appendix 6.2). A selection of 30 significantly up-regulated genes known to be responding to shear stress or vascular remodelling, e.g. VEGF C, KLF2, JAG1 (Thi et al., 2007), (Dekker et al., 2002), (McCormick et al., 2001) is shown in Table 6.

Table 6: Selection of thirty genes regulated upon FSS in HMEC-1 cells

Changes are indicated as ratios (x-fold changes) in the column Ratio and q values at a 'false discovery' rate (FDR) of < 5%.

ILLUMINA_ID	Gene ID	Gene Name	Ratio	q-value(%)
ILMN_1787186	NOV	NEPHROBLASTOMA OVEREXPRESSED GENE	4.12	0.00
ILMN_1802205	RHOB	RAS HOMOLOG GENE FAMILY, MEMBER B	3.81	0.00
ILMN_1735930	KLF2	KRUPPEL-LIKE FACTOR 2 (LUNG)	2.83	0.00
ILMN_2137789	KLF4	KRUPPEL-LIKE FACTOR 4 (GUT)	2.59	0.00
ILMN_1679929	KLF13	KRUPPEL-LIKE FACTOR 13	2.52	0.00
ILMN_1701461	TIMP3	TIMP METALLOPEPTIDASE INHIBITOR 3 (SORSBY FUNDUS DYSTROPHY, PSEUDOINFLAMMATORY)	2.52	0.00
ILMN_1760778	ENG	ENDOGLIN (OSLER-RENDU-WEBER SYNDROME 1)	2.47	0.00
ILMN_1775501	IL1B	INTERLEUKIN 1, BETA	2.03	0.00
ILMN_1703531	EDG3	ENDOTHELIAL DIFFERENTIATION, SPHINGOLIPID G-PROTEIN-COUPLED RECEPTOR, 3	1.99	0.00
ILMN_2050183	MYLK2	MYOSIN LIGHT CHAIN KINASE 2, SKELETAL MUSCLE	2.51	0.91
ILMN_1652185	IL4R	INTERLEUKIN 4 RECEPTOR	2.25	0.91
ILMN_1762106	MMP2	MATRIX METALLOPEPTIDASE 2 (GELATINASE A, 72KDA GELATINASE, 72KDA TYPE IV COLLAGENASE)	2.24	0.91
ILMN_1701204	VEGFC	VASCULAR ENDOTHELIAL GROWTH FACTOR C	1.86	0.91
ILMN_2359287	ITGA6	INTEGRIN, ALPHA 6	1.86	0.91
ILMN_1661194	CLDN14	CLAUDIN 14	3.40	2.36
ILMN_1711566	TIMP1	TIMP METALLOPEPTIDASE INHIBITOR 1	1.83	2.52
ILMN_1658709	LAMB1	LAMININ, BETA 1	1.46	2.52
ILMN_1654563	EFNB1	EPHRIN-B1	1.87	2.65
ILMN_1713499	WISP1	WNT1 INDUCIBLE SIGNALING PATHWAY PROTEIN 1	1.91	2.89
ILMN_1731736	RIN3	RAS AND RAB INTERACTOR 3	1.56	3.37
ILMN_1743966	BCL9L	B-CELL CLL/LYMPHOMA 9-LIKE	2.13	3.54
ILMN_1719236	CDH5	CADHERIN 5, TYPE 2, VE-CADHERIN (VASCULAR EPITHELIUM)	1.78	3.54
ILMN_1796755	ITGB5	INTEGRIN, BETA 5	1.75	3.54
ILMN_2214910	EPHB4	EPH RECEPTOR B4	1.66	3.54
ILMN_2318638	TGIF1	TGFB-INDUCED FACTOR (TALE FAMILY HOMEOBOX)	1.46	3.54
ILMN_1691376	JAG1	JAGGED 1 (ALAGILLE SYNDROME)	1.87	4.47
ILMN_1758542	BMP1	BONE MORPHOGENETIC PROTEIN 1	1.83	4.47
ILMN_1735052	ULK1	UNC-51-LIKE KINASE 1 (C. ELEGANS)	1.65	4.47
ILMN_2374340	PLAUR	PLASMINOGEN ACTIVATOR, UROKINASE RECEPTOR	1.39	4.47
ILMN_2212878	ESM1	ENDOTHELIAL CELL-SPECIFIC MOLECULE 1	9.92	4.71

Global gene expression profiles raise the difficulty of handling, ordering, filtering and/or sorting large amounts of data to focus e.g. on a particular cellular function with a view to questioning an initial hypothesis. Therefore, after the identification of differentially expressed genes, several bioinformatic software tools were used to organise the data obtained. Genes deregulated were grouped using the DAVID (Database for Annotation, Visualisation and Integrated Discovery), an enrichment analysis for Gene Ontology (GO)-categories (Materials and Methods, Section 2.9.6).

DAVID was applied to identify gene ontology categories with an over-representation of genes. The summary for the biological function annotation revealed that most genes were assigned to the GO-categories: 'organ and tissue development', 'vasculature development', 'blood vessel morphogenesis' and 'angiogenesis'. For example, genes involved in 'organ and tissue development' were Krueppel-like factor 4 (KLF4) and cadherin 5 (CDH5). In the category 'angiogenesis' some of the genes involved were interleukin 1-beta (IL1B), ras homologue gene family member 2 (RHOB) and vascular endothelial growth factor C (VEGF-C).

To further analyse the genes regulated upon FSS, these were grouped into networks by knowledge-based analysis of physical, transcriptional, or enzymatic interactions using the Ingenuity Pathway Analysis (IPA) software tool (Materials and Methods, 2.7.7). Deregulated genes could be clustered into 23 functional networks using this tool and top networks are shown in Figure 20.

Top Networks

ID	Associated Network Functions	Score
1	Cardiovascular System Development and Function, Organismal Development, Cellular Movement	44
2	Cellular Movement, Skeletal and Muscular System Development and Function, Cell-To-Cell Signaling and Interaction	34
3	Cell-To-Cell Signaling and Interaction, Embryonic Development, Tissue Development	33
4	Cell Death, Inflammatory Response, Molecular Transport	31
5	Cellular Compromise, Protein Degradation, Protein Synthesis	23

Figure 20: Top networks from the IPA analysis for the deregulated genes of the analysis HMEC-1 without FSS versus HMEC-1 with FSS

Top networks are, for example, Network 1 which comprises "Cardiovascular system development and function", "Organism development", "Cellular development" (score = 44, focus molecules = 24, e.g. Krueppel-like factor 2, KLF2 and Actin gamma 2, ACTG2), Network 2 with genes involved in "Cellular movement", "Skeletal and muscular system development and function", "Cell-to-cell signalling and interaction" (score = 34, focus molecules = 20, e.g. Laminin beta 1, LAMB1 and Nephroblastoma over-expressed gene, NOV) or Network 4 related to "Cell death", "Inflammatory response", "Molecular transport" (score = 31, focus molecules = 20, e.g. CDH5, IL1B). Networks 1 and 4, designed by IPA, are represented in Figure 21.

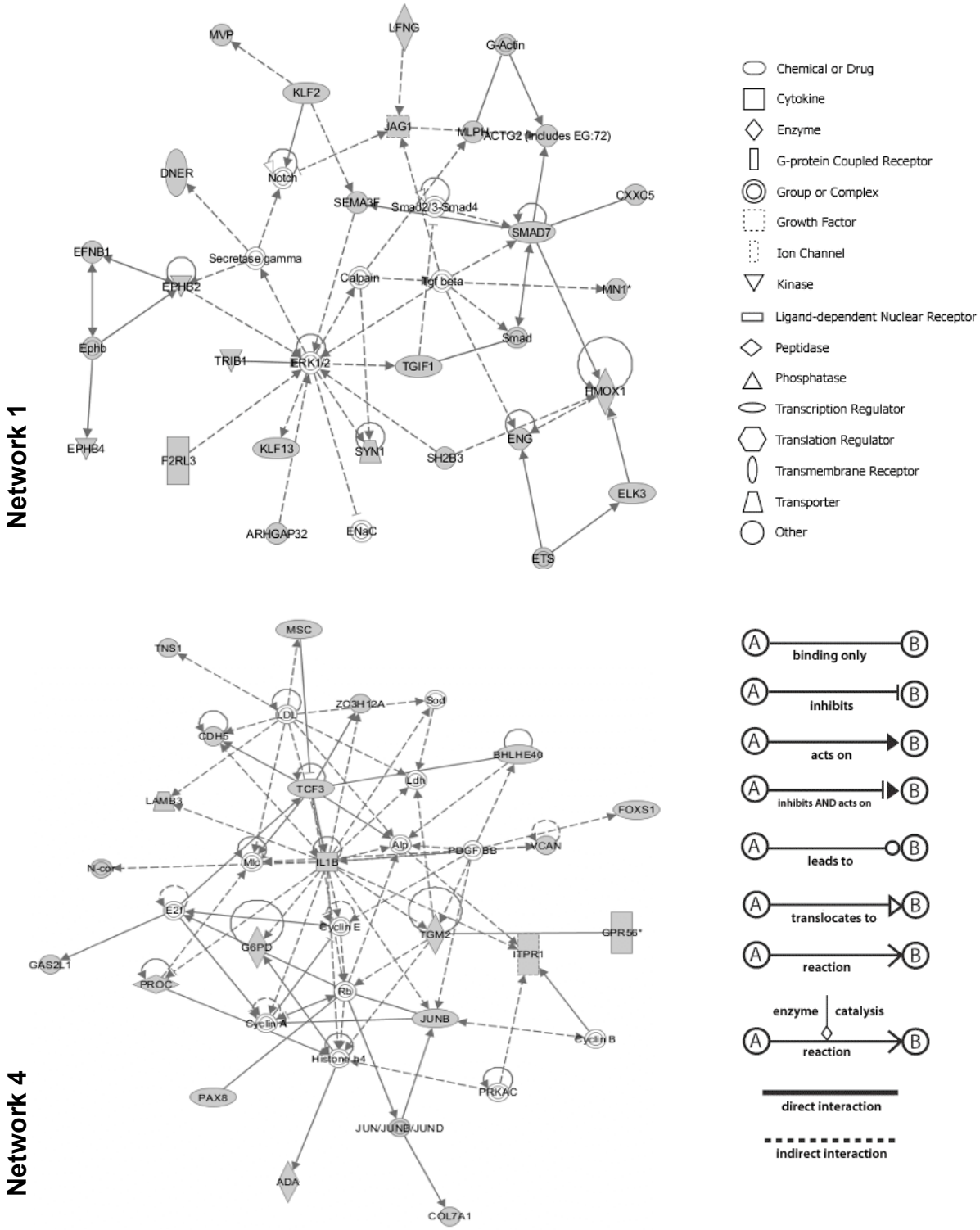

Figure 21: IPA of deregulated genes in HMEC-1 cells upon FSS
Genes were grouped into 23 different functional networks, of which two are represented here (upper panel, network 1; lower panel, network 4). The legend at the right side explains the meaning of the symbols in the networks. Grey-filled symbols indicate focus molecules (from the deregulated gene list) while white-filled symbols are molecules involved in the networks but not present in the deregulated gene lists.

3.6.2 Effects of GPR30 over-expression in HMEC-1 cells

To identify gene regulation effects that are related to the over-expression of GPR30 but are independent of FSS, the GPR30-overexpressing cells (group 3) were analysed in comparison with the cells transfected with the empty vector (group 1). Surprisingly, no genes were found to be deregulated at an FDR below 5%. Subsequently, all groups of cells over-expressing GPR30 (groups 3, 4, 7 and 8) were compared with all groups not expressing GPR30 (groups 1, 2, 5 and 6). By this approach, only a very small number of genes were found to be deregulated, with very low ratios of change. As expected, a strong up-regulation of GPR30 (136-fold) was found and six additional up-regulated genes were identified (SAM < 5%), shown in Table 7.

Table 7: List of genes deregulated in HMEC-1 cells over-expressing GPR30.
Note the high induction of the expression of GPR30 and the rather limited number and only slightly deregulated genes.

ILLUMINA_ID	Gene ID	Gene Name	Ratio	q-value(%)
ILMN_1665435	GPER/GPR30	G PROTEIN-COUPLED RECEPTOR 30	136.11	0.00
ILMN_1806165	HSPA6	HEAT SHOCK 70KDA PROTEIN 6 (HSP70B')	5.10	0.00
ILMN_1838319	LOC730249	IMMUNORESPONSIVE 1 HOMOLOG (mouse)	1.62	0.00
ILMN_1790136	C20orf20	MRG-BINDING PROTEIN (MRGBP)	1.54	0.00
ILMN_2393968	SYNJ1	SYNAPTOJANIN 1	1.50	0.00
ILMN_1801122	LOC401317	HYPOTHETICAL LOC401317	1.42	0.00
ILMN_1779225	C7orf33	CHROMOSOME 7 OPEN READING FRAME 33	1.34	0.00

The low number of identified genes could not be further analysed neither with DAVID nor with IPA software tool.

3.6.3 Effects of GPR30 over-expression in HMEC-1 cells upon FSS

This analysis was performed in order to see whether the effect of fluid shear stress was influencing the gene expression of HMEC-1 cells over-expressing GPR30 in a different manner compared with cells stimulated only by FSS or only over-expressing GPR30. Therefore, HMEC-1 cells over-expressing GPR30 and subjected to FSS (group 4) were compared with cells over-expressing GPR30 but unstimulated (group 3). In this group 201 deregulated genes were identified, in particular 198 genes as up-regulated and 3 as down-regulated (Appendix 6.3). In this group, 159 genes present (shown in grey in Appendix 6.3) are different from the list of genes deregulated in cells stimulated with FSS alone (Appendix 6.2). A selection of genes, present only in this group and different from the list shown in Table 6, is shown in Table 8.

Table 8: Selection of genes deregulated only in HMEC-1 cells over-expressing GPR30 after stimulation with FSS

ILLUMINA_ID	Gene ID	Gene Name	Ratio	q-value(%)
ILMN_1692177	TSC22D1	TSC22 domain family, member 1	3.55	0.00
ILMN_2276952	TSC22D3	TSC22 domain family, member 3; GRAM domain containing 4	2.03	0.00
ILMN_1747314	MYO5B	similar to acetyl-Coenzyme A acyltransferase 2 (mitochondrial 3-oxoacyl-Coenzyme A thiolase); similar to KIAA1119 protein; myosin VB	1.16	0.00
ILMN_1715863	MLKL	mixed lineage kinase domain-like	2.36	1.05
ILMN_1758067	RGS4	regulator of G-protein signalling 4	2.20	1.05
ILMN_1757825	ZNF230	zinc finger protein 230	2.03	1.05
ILMN_1839422	JRK	jerky homolog (mouse)	1.98	1.05
ILMN_1692967	AXIN1	axin 1	1.84	1.05
ILMN_1746359	RERG	RAS-like, estrogen-regulated, growth inhibitor	1.73	1.05
ILMN_2316278	MAGED4B	melanoma antigen family D, 4B; melanoma antigen family D, 4	1.45	1.05
ILMN_1769201	ELF3	E74-like factor 3 (ets domain transcription factor, epithelial-specific)	4.58	2.52
ILMN_1810864	PMP22	peripheral myelin protein 22	3.60	2.52
ILMN_1802646	EPHB6	EPH receptor B6	2.98	2.52
ILMN_1805466	SOX9	SRY (sex determining region Y)-box 9	2.13	2.52
ILMN_2113490	NTN4	netrin 4	2.12	2.52
ILMN_1695773	STK24	serine/threonine kinase 24 (STE20 homolog, yeast)	2.07	2.52
ILMN_2361181	C1QTNF6	C1q and tumour necrosis factor related protein 6	1.89	2.52
ILMN_1785768	PDE4A	phosphodiesterase 4A, cAMP-specific (phosphodiesterase E2 dunce homolog, Drosophila)	1.65	2.52
ILMN_1706644	BDNF	brain-derived neurotrophic factor	1.42	2.52
ILMN_1738707	S100A13	S100 calcium binding protein A13	1.42	2.52
ILMN_1807050	SHC4	SHC (Src homology 2 domain containing) family, member 4	1.34	2.52
ILMN_1675819	FAM101A	family with sequence similarity 101, member A	1.27	2.52
ILMN_1758597	NAGS	N-acetylglutamate synthase	1.21	2.52
ILMN_1652525	FAM125B	family with sequence similarity 125, member B	1.20	2.52
ILMN_1670959	CEACAM5	carcinoembryonic antigen-related cell adhesion molecule 5	1.14	2.52

After the identification by SAM, the relevant deregulated genes were functionally annotated using DAVID and IPA.

For the biological function annotation with DAVID, most genes were assigned to the same GO-categories found for deregulated genes of samples subjected only to FSS, e.g. ‘organ and tissue development‘, ‘vasculature development’ and ‘blood vessel morphogenesis’. For example, genes involved in ‘blood vessel morphogenesis’ are plexin D1 (PLXND1) and troponin I type 3 (TNNI3).

To continue the analysis, the genes deregulated in cells over-expressing GPR30 and upon FSS, were grouped into 17 networks by IPA. The top networks identified by this second tool were different, as shown in Figure 22, from those designed for cells subjected to FSS, probably owing to the over-expression of GPR30 in these samples.

Top Networks

ID	Associated Network Functions	Score
1	Neurological Disease, Reproductive System Development and Function, Tissue Development	45
2	Cellular Development, Cellular Growth and Proliferation, Cellular Movement	34
3	Carbohydrate Metabolism, Lipid Metabolism, Molecular Transport	31
4	Neurological Disease, Drug Metabolism, Endocrine System Development and Function	21
5	Cellular Function and Maintenance, Gene Expression, Amino Acid Metabolism	19

Figure 22: Top networks from the IPA analysis for the deregulated genes of the analysis HMEC-1/GPR30 without FSS versus HMEC-1/GPR30 with FSS

Of note are, for example, Network 1 which comprises “Neurological disease”, “Reproductive System Development and Function”, “Tissue development” (score=45, focus molecules=23, e.g. AXIN1 and SRY (sex-determining region Y)9, SOX9) and in particular Network 4, related to “Neurological disease”, “Drug metabolism”, “Endocrine system development and function”, (score = 21, focus molecules = 13, e.g. RAS-like, estrogen-regulated, growth inhibitor, RERG and S100 calcium binding protein A13, S100A13). In Figure 23 Networks 1 and 4 are shown.

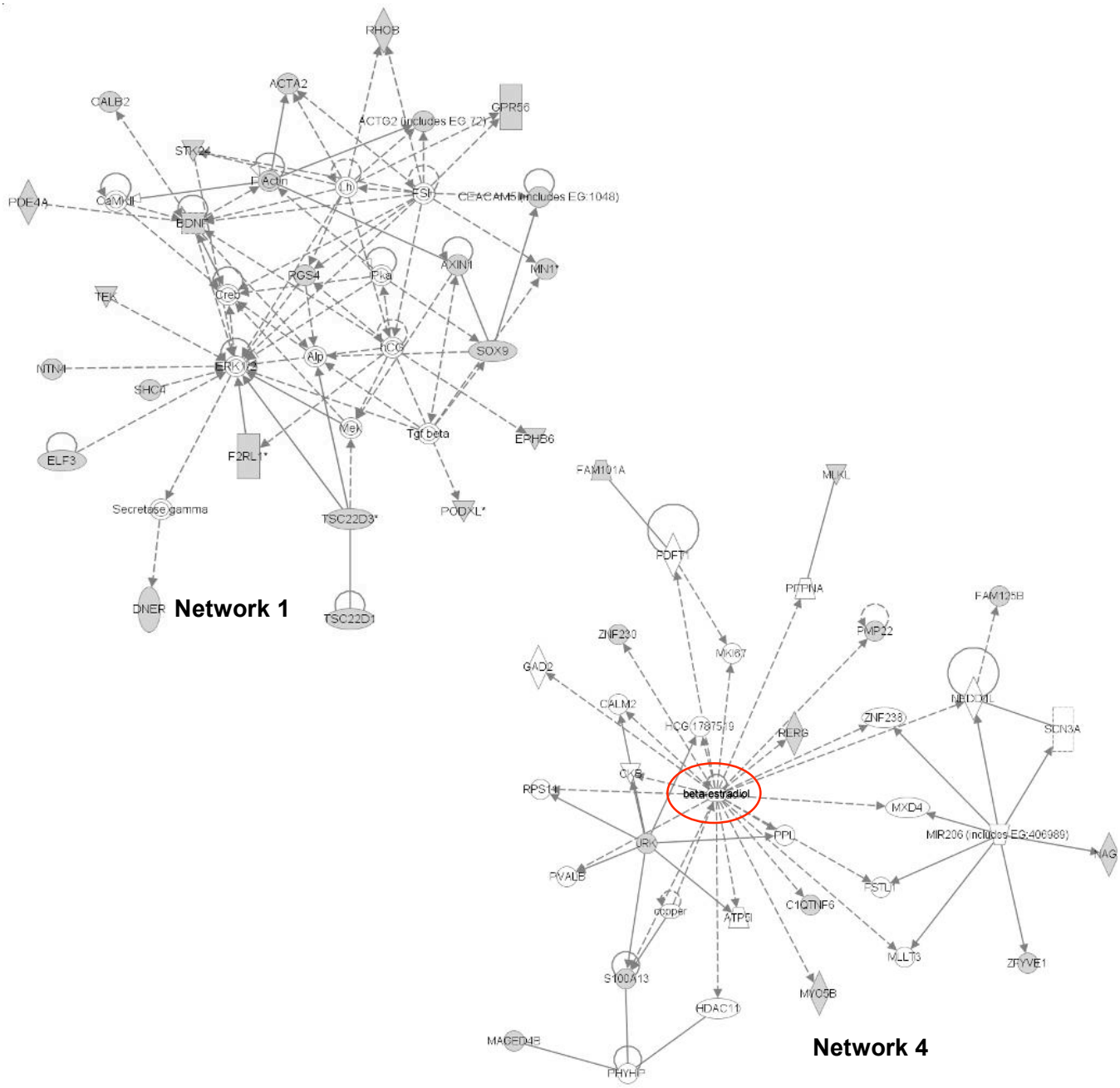

Figure 23: Ingenuity pathway analysis of deregulated genes in HMEC-1 cells over-expressing GPR30 upon FSS
Genes were grouped into 17 different functional networks, of which two are represented here (left panel, network 1; right panel, network 4). In network 4, beta-estradiol is highlighted in a red circle.

3.6.4 Effects of PATJ over-expression in HMEC-1 cells

Since PATJ was found to interact with GPR30, and it was previously shown that the Amot/PATJ/Syx complex controls the migration of endothelial cells and zebrafish angiogenesis (Ernkvist et al., 2009), the gene expression of HMEC-1 cells over-expressing PATJ (group 5) was also analysed. The SAM (FDR < 5%) was performed comparing this

group with cells transfected with empty vector (group 1); neither group was subjected to FSS. As expected, we found a strong up-regulation of PATJ, also called INADL (Inactivation No Afterpotential Drosophila-Like), (633-fold for one Illumina probe or 45-fold for a second Illumina probe, both identifying the same INADL gene). From this analysis the 28 up-regulated genes identified are shown in Table 9.

Table 9: List of genes deregulated in HMEC-1 cells over-expressing PATJ.

ILLUMINA_ID	Gene ID	Gene Name	Ratio	q-value(%)
ILMN_1773312	INADL/PATJ	InaD-like (Drosophila)	633.16	0.00
ILMN_1747318	INADL/PATJ	InaD-like (Drosophila)	44.83	0.00
ILMN_1691048	SLC22A18AS	solute carrier family 22 (organic cation transporter), member 18 antisense	1.63	0.00
ILMN_1745570	KLK7	kallikrein-related peptidase 7	1.50	0.00
ILMN_1786559	FLJ46020	FLJ46020 protein	1.49	0.00
ILMN_1658883	ARAF	v-raf murine sarcoma 3611 viral oncogene homolog	1.23	0.00
ILMN_2048647	NBEA	neurobeachin	2.25	3.49
ILMN_1698753	PRDM13	PR domain containing 13	1.97	3.49
ILMN_2278590	MEST	mesoderm specific transcript homolog (mouse)	1.87	3.49
ILMN_2262957	WIPF1	WAS/WASL interacting protein family, member 1	1.77	3.49
ILMN_2100046	IL22	interleukin 22	1.63	3.49
ILMN_1798837	PTPN20B	protein tyrosine phosphatase, non-receptor type 20B; protein tyrosine phosphatase, non-receptor type 20A	1.62	3.49
ILMN_1682176	CLEC3B	C-type lectin domain family 3, member B	1.46	3.49
ILMN_1806189	C16orf3	chromosome 16 open reading frame 3	1.45	3.49
ILMN_1699170	LOC51149	chromosome 5 open reading frame 45	1.40	3.49
ILMN_1652946	LOC387804	chromosome 11 open reading frame 90	1.40	3.49
ILMN_2413508	CD97	CD97 molecule	1.39	3.49
ILMN_1765373	LOC644686	hypothetical protein LOC644686	1.39	3.49
ILMN_1679600	ACOT8	acyl-CoA thioesterase 8	1.36	3.49
ILMN_1771348	ACN9	ACN9 homologue (S. cerevisiae)	1.35	3.49
ILMN_1789338	SORBS3	sorbin and SH3 domain containing 3	1.34	3.49
ILMN_2186108	DGCR6	DiGeorge syndrome critical region gene 6	1.34	3.49
ILMN_1766793	C9orf23	chromosome 9 open reading frame 23	1.32	3.49
ILMN_1780591	FAT3	FAT tumour suppressor homolog 3 (Drosophila)	1.31	3.49
ILMN_1664773	C11orf49	chromosome 11 open reading frame 49	1.30	3.49
ILMN_1704065	LOC400768	hypothetical gene supported by BC051808	1.28	3.49
ILMN_2144574	CTBS	chitobiase, di-N-acetyl-	1.26	3.49
ILMN_1708041	PLEKHF1	pleckstrin homology domain containing, family F (with FYVE domain) member 1	1.25	3.49

Owing to the small number of deregulated genes it was not possible to perform an enrichment analysis using the DAVID software tool. Instead, the analysis with IPA was possible, although the networks associated with this list of genes were only two: network 1, “Gene expression”, “Cellular growth and proliferation”, “Tissue morphology” (score = 27, focus molecules = 11) and network 2, “Cell cycle”, “Cellular development”, “Cardiovascular system development and function” (score = 21, focus molecules = 9), (Figure 24).

Top Networks

ID	Associated Network Functions	Score
1	Gene Expression, Cellular Growth and Proliferation, Tissue Morphology	27
2	Cell Cycle, Cellular Development, Cardiovascular System Development and Function	21

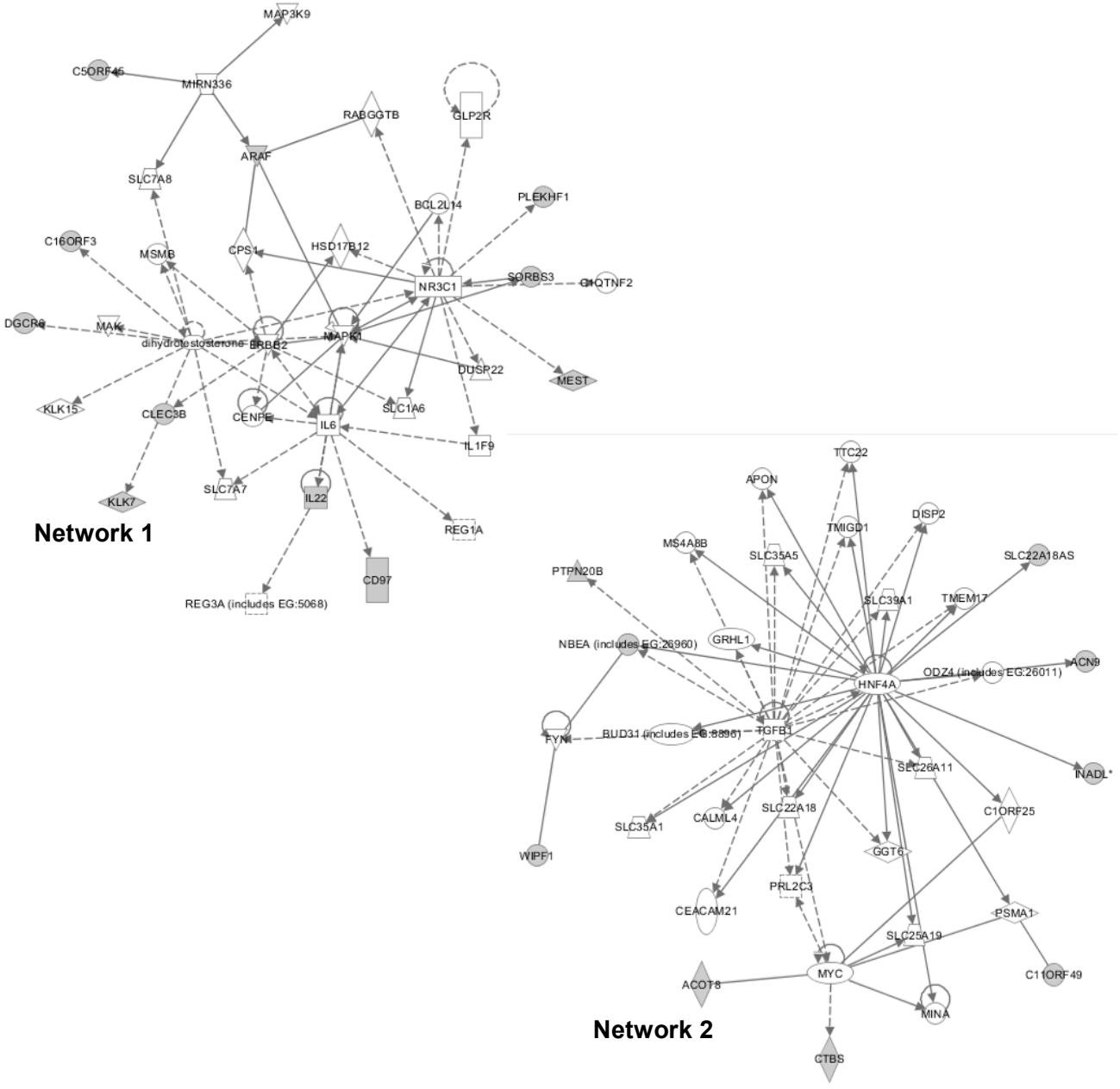

Figure 24: Top networks from the IPA for the deregulated genes of the analysis HMEC-1/PATJ versus HMEC-1/empty vector
The two networks 1 and 2 are shown in the lower panel.

3.6.5 Effects of PATJ over-expression in HMEC-1 cells upon FSS

Once genes differentially regulated in HMEC-1 cells over-expressing PATJ had been identified, the next step was to look at the influence of the fluid shear stress applied to the same group of transfected cells. Therefore, cells over-expressing PATJ and subjected to FSS (group 6) were compared with the cells that over-expressed PATJ but were not stimulated (group 5). With an FDR of <5%, 69 genes were found to be up-regulated (Appendix 6.4). In Table 10 the 20 genes with the highest relative changes are shown.

Table 10: Selection of genes deregulated in HMEC-1 cells over-expressing PATJ after stimulation with FSS

ILLUMINA ID	Gene ID	Gene Name	Ratio	q-value(%)
ILMN_1766264	PI16	peptidase inhibitor 16	6.11	0.00
ILMN_1787186	NOV	nephroblastoma overexpressed gene	4.97	0.00
ILMN_1802205	RHOB	ras homolog gene family, member B	3.29	0.00
ILMN_2189027	LIPG	lipase, endothelial	3.21	0.00
ILMN_2307861	COL6A3	collagen, type VI, alpha 3	3.11	0.00
ILMN_1799575	IL19	interleukin 19	3.11	0.00
ILMN_1738742	PLAT	plasminogen activator, tissue	3.03	0.00
ILMN_2137789	KLF4	Kruppel-like factor 4 (gut)	3.01	0.00
ILMN_1665035	KRT14	keratin 14	2.97	0.00
ILMN_1844408	PLXNA2	plexin A2	2.94	0.00
ILMN_1763837	ANPEP	alanyl (membrane) aminopeptidase	2.80	0.00
ILMN_2314169	PTHLH	parathyroid hormone-like hormone	2.79	0.00
ILMN_2150851	SERPINB2	serpin peptidase inhibitor, clade B (ovalbumin), member 2	2.75	0.00
ILMN_1659856	C1orf90	family with sequence similarity 167, member B	2.71	0.00
ILMN_1696048	C13orf33	chromosome 13 open reading frame 33	2.69	0.00
ILMN_2043306	EPB41L5	erythrocyte membrane protein band 4.1 like 5	2.59	0.00
ILMN_1765446	EMP3	epithelial membrane protein 3	2.51	0.00
ILMN_1709674	GFPT2	glutamine-fructose-6-phosphate transaminase 2	2.45	0.00
ILMN_2413158	PODXL	podocalyxin-like	2.44	0.00
ILMN_1735930	KLF2	Kruppel-like factor 2 (lung)	2.44	0.00

Using DAVID for the whole list, the genes were gathered in the similar gene ontology categories designed for all the other lists of genes, when the cells were stimulated with FSS. IPA was used to create networks for cells over-expressing PATJ upon fluid shear stress. The five top networks are presented in Figure 25.

Top Networks

ID	Associated Network Functions	Score
1	Immunological Disease, Neurological Disease, Cardiovascular System Development and Function	45
2	Cell Morphology, Skeletal and Muscular System Development and Function, Respiratory Disease	29
3	Cellular Development, Cell Cycle, Cellular Compromise	16
4	Genetic Disorder, Skeletal and Muscular Disorders, Connective Tissue Development and Function	12
5	Gene Expression, Cancer, Dermatological Diseases and Conditions	2

Figure 25: Top networks from the IPA for the deregulated genes of the analysis HMEC-1/PATJ without FSS versus HMEC-1/PATJ with FSS

The number of networks found, by IPA analysis for the genes over-expressing PATJ and upon FSS, was 11 and, although grouping some functional pathways already pointed out for the previous lists of genes, here presented new associated network functions, i.e. network 2 for “Cell morphology”, “Skeletal and muscular system development and function”, “Respiratory disease” (score = 29, focus molecules = 14) and network 4 for “Genetic disorder, “Skeletal and muscular disorders”, “Connective tissue development and function” (score = 12, focus molecules = 7). Networks 2 and 4 are represented in Figure 26.

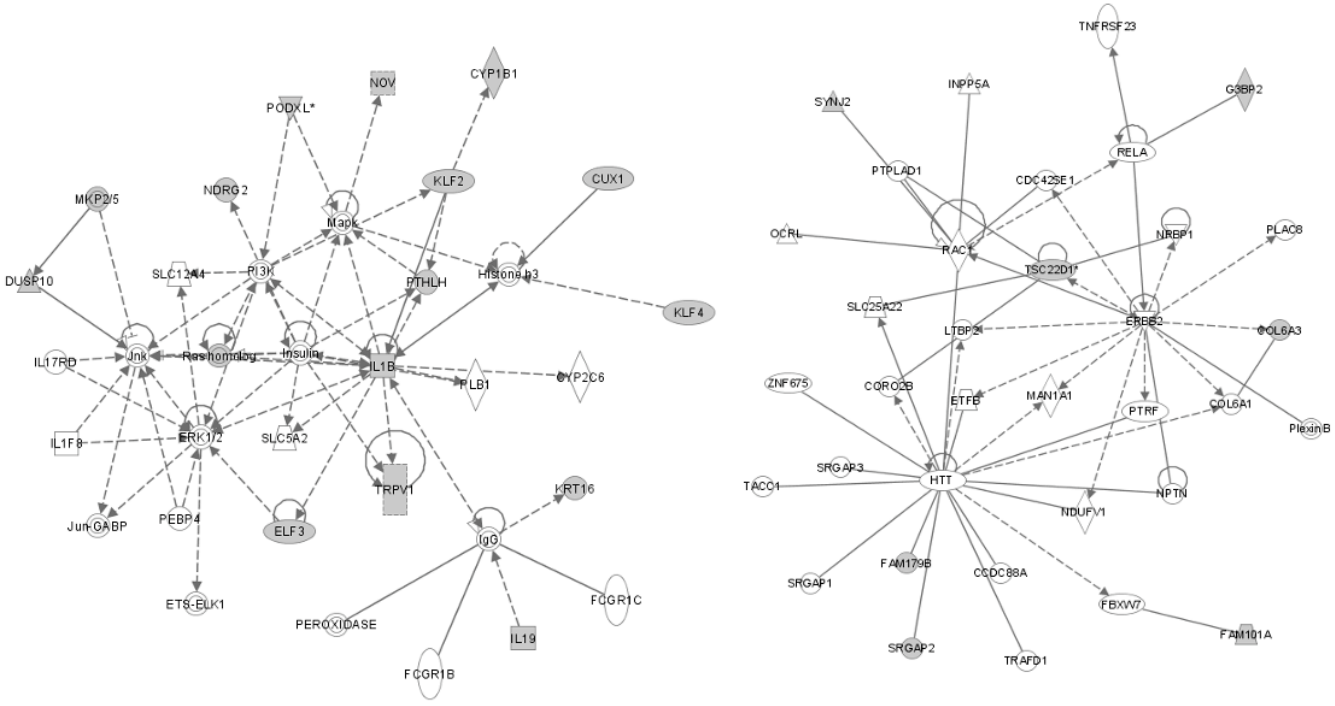

Network 2 **Network 4**

Figure 26: Top networks from the IPA for the deregulated genes of the analysis HMEC-1/PATJ without FSS versus HMEC-1/PATJ with FSS

3.6.6 Effects of GPR30 and PATJ over-expression in HMEC-1 cells

The last aim was to analyse the gene-expression pattern in cells over-expressing GPR30 and PATJ in order to find out more about this new interaction. First, the groups without shear stress stimulation were examined; for this purpose, HMEC-1 over-expressing GPR30 and PATJ (group 7) were compared with HMEC-1 over-expressing the empty vector (group 1).

Table 11: List of genes deregulated in HMEC-1 cells over-expressing GPR30 and PATJ

ILLUMINA ID	Gene ID	Gene Name	Ratio	q-value(%)
ILMN_1773312	INADL/PATJ	InaD-like (Drosophila)	560.84	0.00
ILMN_1665435	GPER/GPR30	G protein-coupled estrogen receptor 1	116.56	0.00
ILMN_1789502	GPC4	glypican 4	1.68	0.00
ILMN_1695711	FAM105A	family with sequence similarity 105, member A	1.94	0.00
ILMN_1740041	LOC645197	hypothetical LOC645197	1.63	0.00
ILMN_1720496	GUCY1A2	guanylate cyclase 1, soluble, alpha 2	1.43	0.00

In this case, only 4 genes, besides PATJ and GPR30, were found to be deregulated. Similarly to the other groups with too few genes, it was not possible to perform any further bioinformatic analysis using either DAVID or IPA.

3.6.7 Effects of GPR30 and PATJ over-expression in HMEC-1 cells upon FSS

The last group of deregulated genes obtained with the microarray experiment and presented in this thesis is the result of the comparison of cells over-expressing GPR30 and PATJ with FSS stimulation (group 8) versus cells over-expressing GPR30 and PATJ but without FSS (group 7). With SAM analysis (FDR < 5%) 246 genes were found to be up-regulated and 4 to be down-regulated (Appendix 6.5). In this group, 148 genes are different from those in the list of genes deregulated in cells stimulated with FSS alone (Appendix 6.2). Table 12 shows a selection of 20 genes differentially regulated and present only in this group.

Table 12: Selection of genes deregulated in HMEC-1 cells over-expressing GPR30 and PATJ after stimulation with FSS

ILLUMINA ID	Gene ID	Gene Name	Ratio	q-value(%)
ILMN_1736760	KRT16	KERATIN 16 (FOCAL NON-EPIDERMOLYTIC PALMOPLANTAR KERATODERMA)	10.95	0.00
ILMN_1766264	PI16	PEPTIDASE INHIBITOR 16	5.27	0.00
ILMN_1799575	IL19	INTERLEUKIN 19	3.30	0.00
ILMN_1762529	SLC12A8	HYPOTHETICAL PROTEIN FLJ23188	2.90	0.00
ILMN_2327860	MAL	MAL, T-CELL DIFFERENTIATION PROTEIN	2.54	0.00
ILMN_1693338	CYP1B1	CYTOCHROME P450, FAMILY 1, SUBFAMILY B, POLYPEPTIDE 1	2.53	0.00
ILMN_2387214	PALM	PARALEMMIN	2.35	0.00
ILMN_1711786	NFE2	NUCLEAR FACTOR (ERYTHROID-DERIVED 2), 45KDA	2.28	0.00
ILMN_1688780	S100A4	S100 CALCIUM BINDING PROTEIN A4 (CALCIUM PROTEIN, CALVASCULIN, METASTASIN, MURINE PLACENTAL HOMOLOG)	2.26	0.00
ILMN_1769201	ELF3	E74-LIKE FACTOR 3 (ETS DOMAIN TRANSCRIPTION FACTOR, EPITHELIAL-SPECIFIC)	2.20	0.00
ILMN_2148527	H19	H19, IMPRINTED MATERNALLY EXPRESSED UNTRANSLATED MRNA	2.17	0.00
ILMN_1758067	RGS4	REGULATOR OF G-PROTEIN SIGNALLING 4	2.13	0.00
ILMN_1701424	LAMC2	LAMININ, GAMMA 2	2.11	0.00
ILMN_2308903	WFDC3	WAP FOUR-DISULFIDE CORE DOMAIN 3	2.00	0.00
ILMN_2113490	NTN4	NETRIN 4	1.97	0.00
ILMN_1726597	C6orf32	CHROMOSOME 6 OPEN READING FRAME 32	1.95	0.00
ILMN_2150851	SERPINB2	SERPIN PEPTIDASE INHIBITOR, CLADE B (OVALBUMIN), MEMBER 2	1.95	0.00
ILMN_1774685	IL24	INTERLEUKIN 24	1.94	0.00
ILMN_2356578	TH	TYROSINE HYDROXYLASE	1.94	0.00
ILMN_1761968	PPP1R14A	PROTEIN PHOSPHATASE 1, REGULATORY (INHIBITOR) SUBUNIT 14A	1.89	0.00

In this case too, it was reasonable to use the bioinformatic software tools DAVID and IPA.
In DAVID analysis, the summary for the biological function annotation revealed that most genes were again assigned to the same GO-categories found for the other groups described above.

To obtain new hints, the Ingenuity Pathway Analysis software tool was also considered. It proved possible to cluster the deregulated genes into 19 functional networks using this tool, and the top five networks are presented in Figure 27.

Top Networks

ID	Associated Network Functions	Score
1	Cellular Movement, DNA Replication, Recombination, and Repair, Cellular Growth and Proliferation	57
2	Small Molecule Biochemistry, Lipid Metabolism, Drug Metabolism	39
3	Cellular Movement, Cell Morphology, Cellular Development	38
4	Embryonic Development, Tissue Morphology, Cell Cycle	36
5	Genetic Disorder, Hepatic System Disease, Amino Acid Metabolism	29

Figure 27: Top networks HMEC-1 cells over-expressing GPR30 and PATJ with FSS stimulation

These networks showed most of the network functions that had already appeared for the other gene sets. Nevertheless, the association between networks in each analysis was

different. For example, network 1 for “Cellular movement”, “DNA replication, recombination and repair”, “Cellular growth and proliferation” (score = 57, focus molecules = 29) and network 8 for “Cancer”, “Cell cycle”, “Reproductive system, development and function” (score = 19, focus molecules = 13) presented a different number of genes if compared with the same networks but with a different list of genes, as shown in the next picture (Figure 28).

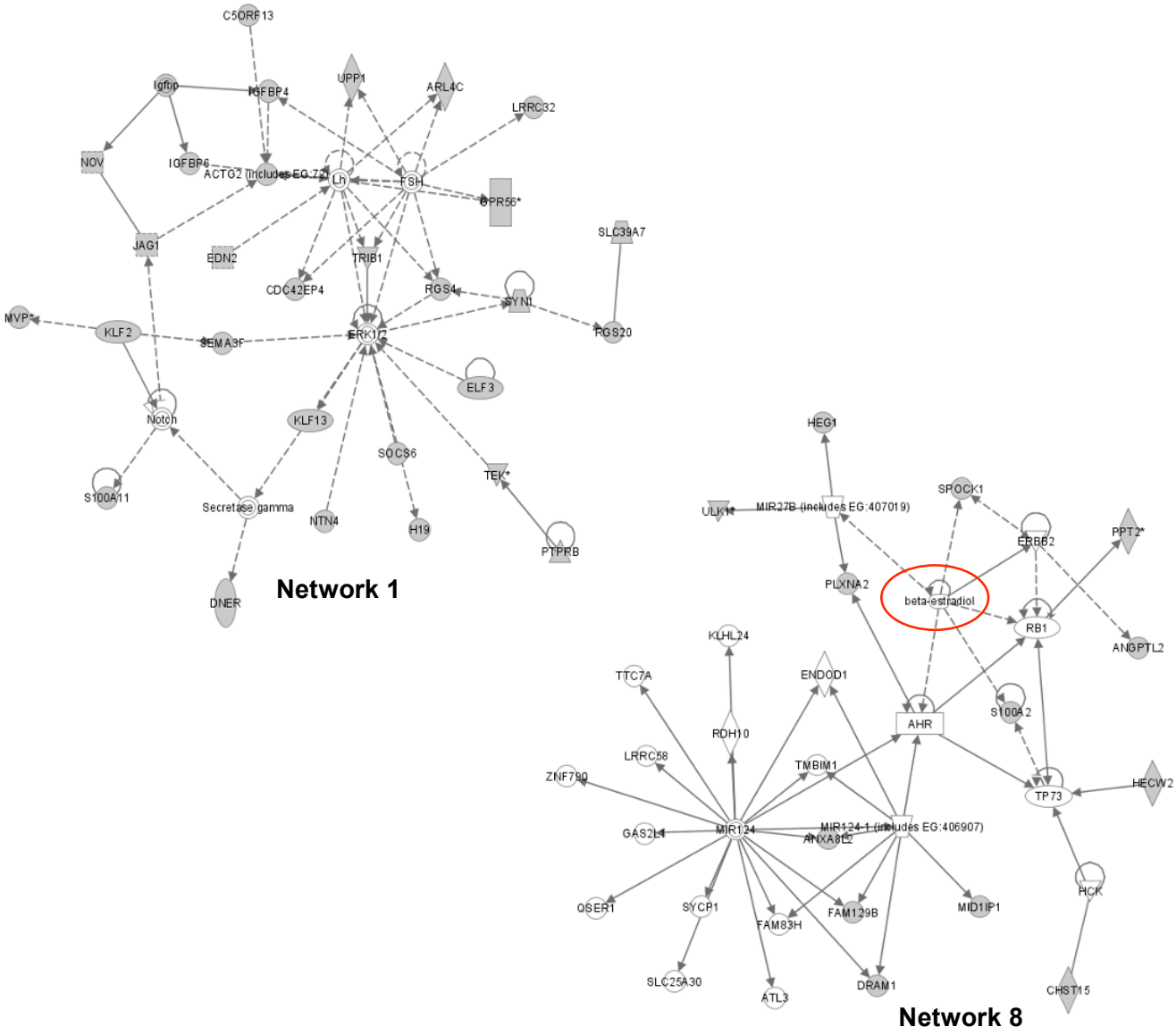

Figure 28: Top networks from the IPA for the deregulated genes of the analysis HMEC-1/GPR30/PATJ without FSS versus HMEC-1/GPR30/PATJ with FSS
In network 8, beta-estradiol is highlighted in a red circle.

4 DISCUSSION

More than 800 G protein-coupled receptors (GPCRs) are transcribed in the human genome (Kroeze et al., 2003) and are involved in a wide range of physiological processes and, therefore, are exploited as drug targets in a multitude of therapeutic areas (Pierce et al., 2002).

After binding a specific ligand, activated GPCRs can initiate cellular signalling, but for many of them no endogenous ligand has yet been found, and, therefore, these are currently designated as orphan receptors (Oh et al., 2006). The orphan G protein-coupled receptor 30, GPR30, was claimed in 2005 by two independent groups to bind directly to 17-β-estradiol (E2 or beta-estradiol) and to mediate rapid non-genomic signalling (Revankar et al., 2005), (Thomas et al., 2005). In contrast, various reports indicate that E2 fails to bind GPR30 in a saturable or specific manner and in consequence exerts only a modest signal-transduction effect (Thomas et al., 2005) compared with the dramatically stronger actions of physiological E2 at classical estrogen receptor (ER)α, (Otto et al., 2008). Thus, the function of GPR30 as an ER remains under discussion.

In a recent study performed in the laboratory of Prof. Ruiz-Noppinger, where the work for this thesis was carried out, the cellular and tissue distribution of GPR30 in mouse was investigated in a very broad screen. For this purpose, a mutant mouse was generated by inserting a LacZ/neomycin resistance cassette into the exon 3 encoding the ORF of the GPR30 gene. The strength of this mouse model was the presence of a LacZ reporter in the GPR30 locus that allowed the identification of cells expressing GPR30 protein *in vivo*. Predominantly GPR30 was expressed in endothelial cells of small arteries in several tissues (Isensee et al., 2009).

Independently of the controversy about whether GPR30 is an ER or is still an orphan receptor, in 1997 one of the cloning approaches for GPR30 used human umbilical vein endothelial cells (HUVECs) exposed to fluid shear stress (FSS), the driving force of arteriogenesis. In this study it was shown that the GPR30 mRNA level is increased markedly in response to FSS after 24 hours (Takada et al., 1997). In another study it was found that the expression of GPR41 (orthologue of GPR30 in the rat) in H9c2 cells (a rat-heart-derived cell line) is induced during post-ischaemic re-oxygenation with a peak at 2 hours after re-oxygenation (Kimura et al., 2001). Ischaemia is present during development or can be caused, for instance, by blockage of an artery leading to a temporarily decreased supply of oxygen and nutrients from the blood, and it induces angiogenesis.

With the background of a clear evidence about the expression of GPR30 (Isensee et al., 2009) and its involvement (Haas et al., 2009) in the vascular tissue, the overall goal of this project was to elucidate the role of GPR30 signalling in blood vessels. Despite the controversy about whether GPR30 is an ER or is still an orphan receptor, nothing is known at present about its relation to and its interaction with other proteins. Therefore, also according to several reports suggesting that GPCRs interact with and are regulated by several other proteins, beyond the established role of heterotrimeric G proteins, the first aim of this project was to identify new interaction partners and to gain information about the signalling complex of human GPR30 at the molecular level (I). The second aim was to establish a human cell model to evaluate the potential role of GPR30 in a vascular model (II) and finally the third aim was to evaluate the downstream effects of the interaction between GPR30 and newly identified interaction partners in the vascular model at the transcript level (III).

4.1 Detection of GPR30 by western blotting and co-immunoprecipitation

GPCRs are characterised by seven transmembrane domains. Therefore, solubilisation of GPR30 with its strong lipophilic properties represented a challenging task, but it was a prerequisite for the detection of GPR30 by western blotting and CoIP.
This step was important for two reasons:

1) to detect both endogenous and over-expressed GPR30 by western blotting (i.e. to confirm the absence of GPR30 protein in the GPR30/LacZ mouse mutant);

2) to confirm the interaction between GPR30 and potential interaction partners in mammalian cell lines by CoIP.

For these two purposes, the choice of solubilisation conditions was very important. To detect GPR30 at the protein level by western blotting it was necessary to use a lysis buffer with strong denaturing characteristics, to solubilise a large proportion of the expressed protein for quantitative measurements. For a CoIP the detergent to be used in such lysis buffer had to be strong enough to extract GPR30 from the native membrane, but not so strong as to denature the receptor and disrupt protein–protein interactions that might be of physiological interest.

Therefore, several protocols for western blotting were considered, including some specific for detecting human GPR30 (Thomas et al., 2005), (Vivacqua et al., 2006), (Filardo et al., 2007). In parallel, other protocols designed to solubilise proteins, without considering the possible

strong denaturing conditions (and therefore not useful for CoIP), were evaluated (Nagamatsu et al., 1992), (Moore et al., 2000), (Edinger et al., 2003). The choice of the right antibody is another critical step in any western blotting; therefore, in a search for a specific antibody against GPR30, first trials were performed using an anti-GFP (Green Fluorescent Protein) antibody able to recognise the fusion protein of GPR30 tagged with EGFP (Enhanced Green Fluorescent Protein). A second reason to choose an anti-GFP in the beginning was to have the possibility to check for transfected cells, in order to visualise GPR30-EGFP in such cells under the microscope before attempting to extract proteins for western blotting.

One of the first published protocols evaluated, showing a specific band for GPR30 in western blotting, was the protocol from the publication of Vivacqua *et al.* in 2006 where the lysis buffer used was a simple RIPA-buffer, with a detergent that was not too strong and was therefore possibly suitable also for CoIP (Vivacqua et al., 2006). Following this protocol, in the laboratory where this work was carried out, no band for GPR30-EGFP was detected, but since an anti-GFP antibody − instead of a commercial anti-GPR30 antibody − was used to detect GPR30, it was reasonable to hypothesise that the cause of the negative result could have come from the use of a different antibody. Therefore, other western blotting protocols, where the goal was the solubilisation of other GPCRs using different antibodies, hence suitable using an anti-GFP antibody, were screened. Among various protocols, two in particular were considered, and only one of these led to a first successful result. In this protocol the lysis buffer contained a combination of two compounds, urea and SDS, both powerful denaturants that disrupt the non-covalent bonds within proteins and therefore not suitable for the CoIP (Edinger et al., 2003) (Results 3.1.1). In this experiment, using pEGFP-C1 as a positive control, two bands were detected instead of the single band expected. The presence of the two bands could indicate a mature and a pre-processed form of the protein (Waller et al., 2000); the smaller of these corresponded to the expected molecular weight of GFP whereas the larger was consistent with the size of a mono-ubiquitylated GFP molecule, suggesting that a proportion of over-expressed GFP in the cells might be turned over by normal cellular mechanisms of protein degradation (Riess et al., 2005).

Subsequently, many other protocols for GPR30 western blotting were assessed, by using human GPR30 antibodies. In total six different antibodies were screened. None of these protocols led to positive results, but two of these antibodies (3rd extracellular domain antibody and C-terminal domain antiserum, from the laboratory of Prof. E. Prossnitz), and only in combination with the previously adjusted urea–SDS-based protocol, detected GPR30 (full-length and fused with EGFP) by western blotting (Results, Section 3.1.2). Although two antibodies could detect over-expressed GPR30, once again this was with the urea–SDS lysis

buffer and was therefore not useful for CoIP experiments, since the strong denaturing conditions set out in the protocol would not allow the detection of potential interacting proteins. Nevertheless, this protocol in combination with one of those anti-GPR30 antibodies could be helpful for other approaches, e.g. to demonstrate the absence of GPR30 in GPR30-LacZ mutant mice. Therefore, the next step was to detect the endogenously expressed GPR30 with the urea–SDS lysis buffer and an anti-GPR30 antibody (i.e. against the 3rd extracellular domain antibody). Indeed, under these conditions it proved possible to detect a specific band for endogenous human GPR30 (Results, Section 3.1.3) in SkBr3 breast cancer cells that were negative for ER (estrogen receptor α and β) but positive for GPR30 (Vladusic et al., 2000).

The last goal was to transfer this protocol established to detect human endogenous GPR30 cells to the mouse system. Therefore, the protocols optimised were evaluated in wild-type (wt) and in GPR30-deficient mouse tissue samples but without success. These findings underline the difficulty of detecting murine GPR30 protein in tissues, which is probably due to low expression levels, the lipophilic properties as a 7TMR and, most importantly, the lack of mouse antibodies. Indeed, the antibodies so far mentioned were produced to recognise specifically human GPR30 and not epitopes of the mouse receptor. Therefore, the only way to tackle the question about the expression of GPR30 in mice was to investigate the expression of a LacZ reporter in GPR30-lacZ mice and characterise the cell types identified by co-localisation of LacZ along with cell-type-specific markers. This approach is especially useful if low expression levels are assumed, because the LacZ assay allows remarkable signal amplification (Isensee et al., 2009).

Concerning the CoIP, several protocols were evaluated, (Filardo et al., 2007), (Devost und Zingg, 2003), (Okuma und Reisine, 1992), (Harvey et al., 2001), but in none of the cases was it possible to solubilise GPR30. For example, with the Ripa-buffer-based protocol used by Filardo *et al*. in 2007 where the interaction between GPR30 and a G protein was shown, in particular with the $G\alpha_s$ subunit, it was not possible in the laboratory where the work for this thesis was carried out to detect a specific band for GPR30, although every step of their CoIP protocol was followed. One explanation could be the use in their protocol of an anti-GPR30 antiserum produced in their laboratory, therefore commercially not available (monospecific GPR30 antibody, 2F2, generated in BALB/C mice that were immunised with synthetic peptide CAVIPDSTEQSDVRFSSAV from the C terminus of human GPR30). Only after visiting the Laboratory of Prof. Guy Haegemann (Eukaryotic Gene Expression and Signal Transduction (LEGEST), Department of Molecular Biology, Ghent University, Gent, Belgium), a protocol for the confirmation of the interaction between GPR30 and the new hypothetical

proteins was finally found (Rondou et al., 2008). There, with few new experimental features (e.g. freezing/thawing before cell lysis, or the use of an antibody not employed before) it was very easy to solubilise and co-immunoprecipitate HA-tagged GPR30, using an anti-HA antibody (Results 3.3). In conclusion, for the successful CoIP protocol the choice of the lysis buffer together with the choice of the antibody was of crucial importance. Indeed, some antibodies require samples to be processed or treated in a specific manner, since many antibodies can recognise only proteins that reveal their epitopes in a particular state; for example, if the samples have been reduced and denatured the proteins can show epitopes otherwise obscured by secondary and tertiary folding.

4.2 GPR30 interacts specifically with PATJ in mammalian cells

Protein–protein interactions (PPI) represent a pivotal aspect of protein function. Almost every cellular process relies on transient or permanent physical binding of two or more proteins in order to accomplish the respective task. Prediction of protein interactions using bioinformatic tools and online software could be a first step to gain insight into this topic. Currently, publicly available PPI databases contain few entries from mammals, such as would be required for building a high-quality, manually curated database of protein–protein interactions.

To check for new hypothetical interaction partners for GPR30, some of these bioinformatic tools were evaluated, i.e. the human Protein–protein Interaction Prediction (PIPs, http://www.compbio.dundee.ac.uk/www-pips/) (McDowall et al., 2009), the Biomolecular Object Network Databank (BOND, http://bond.unleashedinformatics.com/) (Alfarano et al., 2005) or the Search Tool for the Retrieval of Interacting Genes/Proteins (STRING, http://string-db.org/) (Snel et al., 2000). These databases use different sources: while the interactions in PIPs are calculated by combining information from expression, orthology, post-translational modifications, sub-cellular location of each protein and topology of the predicted interaction network, STRING and BOND base their prediction on experimental repositories, computational prediction methods and public text collections.
Using PIPs, GPR30 does not have predicted interactions with a score of 1.0 or above, which indicates that the interaction is more likely to occur than not to occur (the higher the value, the greater the confidence that the predicted protein interacts with the main protein). With a score above 0.5, six proteins were identified (GPR63, OR5V1, OR3A3, TAAR8, OR1G1, EDNRA). With BOND the only interaction found was with E2, based on a literature record, and with STRING several interaction partners were detected, among them the two ERs, ESR1 and ESR2, as shown in Figure 29.

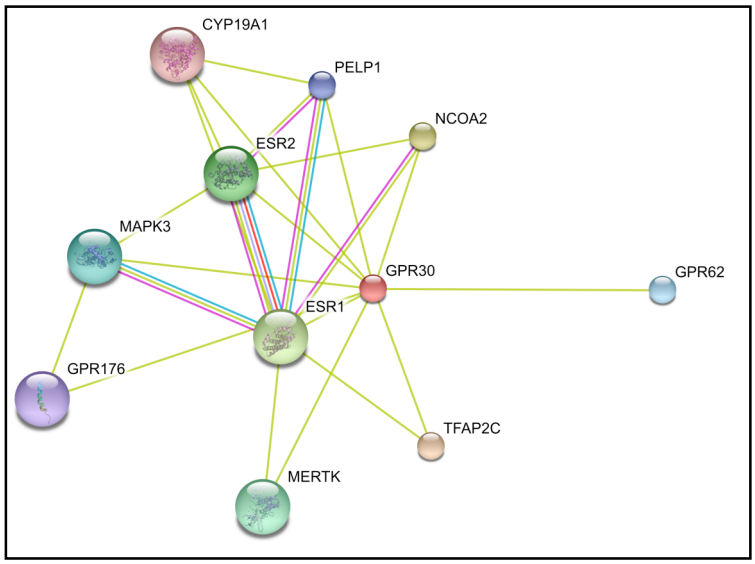

Figure 29: GPR30 and potential interaction partners using the bioinformatics tool STRING for the prediction of protein–protein binding

Bioinformatic approaches can be a first step for the determination of protein interaction partners, but they can yield false results. For that reason these tools can be considered only as a suggestion, and other methods available to probe protein–protein interactions have to be used, i.e. yeast two-hybrid screening (Y2H) or tandem affinity purification (TAP). One of the most frequently used is the Y2H analysis, which, using a genetically engineered strain of yeast, screens for physical interactions between two proteins.

Therefore, Y2H screenings were performed in a preliminary study (PhD project of Jörg Isensee) using the N- or the C-terminal domain of GPR30 as baits and a human heart cDNA library as prey. The N- and C-domains were selected, since they are most likely to adopt the native conformation when isolated from the receptor. C-tails have frequently been used as baits in Y2H screening, allowing the identification of numerous interaction partners (Bockaert et al., 2003). In contrast, intracellular loops such as the I3 loop (third intracellular loop) that mainly contacts the G protein are unlikely to adopt the native conformation. In line with the observation that the N-terminal domain of GPR30 is not well conserved between species, no putative interaction partners were identified in the N-terminal screen. Using the C-tail as bait, two candidates were found: PALS1-associated tight junction protein (PATJ), and FUN14 domain-containing 2 (FUNDC2). It is of note that these two newly identified proteins were not predicted by STRING, underlining the importance of an experimental approach.

To confirm the interaction between GPR30 and the newly identified interacting proteins, co-immunoprecipitation studies were performed. With this technique, only the interaction between GPR30 and PATJ was confirmed, while an interaction with the second potential

partner, FUNDC2, could not be verified, indicating a false positive interaction in the Y2H screening (Results 3.3). One explanation could be that although yeast is a well established model organism, not all interactions in higher eukaryotes have equivalent counterparts in unicellular systems (Huang und Bader, 2009).

PATJ, a component of the evolutionarily conserved multi-protein complex CRB-PALS1-PATJ (Crumbs–PALS1, protein associated with Lin seven 1, and also known as Stardust–PATJ), is essential in the determination of epithelial polarity, (Shin et al., 2007). In an earlier study it was shown that a reduction of PATJ expression by RNA interference (RNAi) in Madin–Darby canine kidney II (MDCKII) cells leads to delayed tight-junction formation as well as to defects in cell polarisation. The authors therefore concluded that PATJ regulates tight junction formation and epithelial polarity (Shin et al., 2005).
Several splicing variants have been reported for PATJ that encode up to 10 PDZ domains and an N-terminal L27 domain (Roh et al., 2002), (Lemmers et al., 2002). Through its PDZ domains, PATJ interacts with tight junction proteins such as claudins and zonula occludens 3 (ZO-3) (Lemmers et al., 2002). The L27 domain of PATJ binds a complex containing the protein associated with Lin seven 1 (PALS1), human lin-7 homologue (LIN-7) and crumbs protein homolog 3 (CRB3) (Roh et al., 2002), (Lemmers et al., 2002). The CRB3-PALS1-PATJ complex is a key component required for cell polarisation and localises to tight junctions at the apical site of the cell (Straight et al., 2006). In recent work, the association of PATJ in a protein complex with the membrane-associated scaffold protein Angiomotin (Amot) and the RhoA GTPase exchange factor protein Syx was demonstrated. The Amot/PATJ/Syx complex is involved in the migration of endothelial cells during zebrafish angiogenesis, adding a new hint in understanding vessel formation and suggesting how a guidance signal might be translated into directional migration (Ernkvist et al., 2009).

The potential interaction site of PATJ with the C-terminal domain of GPR30 found by Y2H screening was within the last three C-terminal PDZ domains (amino acids 1381–1801). Numerous GPCR-binding proteins have been identified, and PDZ-domain-containing proteins might constitute the largest class of proteins that is involved in organising GPCR signalling complexes, (Bockaert et al., 2004). PDZ domains (PDZ is a common motif, ~90 amino acids in length) are found in 126 proteins in the human genome. These proteins have many functions, from regulating the trafficking and targeting of proteins to assembling signalling complexes and networks designed for efficient and specific signal transduction (Nourry et al., 2003).

PDZ domains bind PDZ ligands expressed at the C termini of GPCRs (Bockaert et al., 2004). PDZ ligands usually include three or four amino acids at the C terminus, although residues upstream may influence the specificity (Sheng und Sala, 2001). The PDZ-binding sites have been divided into three classes: class I (-E-S/T-x-V/I), class II (-φ-x-φ), and class III (-ψ-x-φ), where ψ and φ are acidic and hydrophobic residues, respectively (Sheng und Sala, 2001). The C-terminal sequence of GPR30 (S-S-A-V) is highly conserved and similar to class I PDZ ligands. Indeed, Vaccaro *et al.* determined the consensus ligand for seven isolated PDZ domains of human PATJ by screening a random peptide library displayed on the phage lambda and found that each PDZ domain had a unique peptide binding preference (Vaccaro et al., 2001). Remarkably, the consensus ligand of the eighth PDZ domain was -S-x-V-, indicating that the C-tail of GPR30 probably interacts with this domain. Experiments with a deletion mutant of PATJ lacking this hypothetical interacting PDZ domain would help to answer this question.

In conclusion, the C-terminal tail of GPR30 probably represents a PDZ ligand that specifically binds a PDZ domain of PATJ, and the interaction may tether GPR30 to a signalling complex in endothelial cells during the formation of new vessels.

4.3 GPR30 expression in primary endothelial cells upon fluid shear stress (FSS)

Blood vessels are responsible for the transport of oxygen, blood and plasma throughout the body and are composed of various different cell types: endothelial cells, smooth muscle cells and fibroblasts. Endothelial cells make up the inner layer of the blood vessels and are in direct contact with flowing blood. Blood vessels may also become affected by disorders such as thrombosis, restenosis, and atherosclerosis, which greatly affect the general health of adults (Risau, 1997). For instance, arterial occlusion can lead to increase of fluid shear stress (FSS) caused by the strong difference between the high pre-occlusive and the very low post-occlusive pressure regions (Schaper, 2009). In addition, an artery's constriction causes less oxygenated blood to flowing to various parts of the body and therefore, since tissue are exposed to prolonged hypoxic conditions, this phenomenon leads to cellular remodelling (Rey und Semenza).

The expression of GPR30 in vessels of different tissues has been clearly demonstrated. Isensee *et al.* showed that GPR30 is expressed in small arterial vessels of several tissues (e.g. kidney, heart, peritoneum, genital tract), in particular in an endothelial cell subpopulation (Isensee et al., 2009). In a previous publication from another group the expression of GPR30 mRNA was reported for human internal mammary arteries and saphenous veins (Haas et al.,

2007). Moreover, one decade earlier, GPR30 was cloned using human umbilical vein endothelial cells (HUVECs) exposed to fluid shear stress (FSS) (Takada et al., 1997).

Therefore the idea to establish an *in vitro* human cell model to assess the role of GPR30 in vessels potentially related to pathological conditions and the two models of ischemia/reperfusion (I/R) or FSS were evaluated.

Since GPR30 was found to be up-regulated in a rat cardiac cell line after 2 hours of post-ischemic re-oxygenation (Kimura et al., 2001), the first model evaluated was an *in vitro* approach of hypoxia/reoxygenation (I/R) using primary endothelial cells (HUVECs) and their derived cell line (EAhy926). The cells were exposed to oxygen glucose deprivation (OGD) in an hypoxic chamber (0.5% oxygen) for different time points. With this model only a minimal (and statistically not significant) change in the expression of GPR30 was detected, probably due to the use of a different cell types, i.e. endothelial cells instead of cardiac cells. Nevertheless, in the last year several groups have adduced evidence supporting the involvement of GPR30 in ischaemia/reperfusion. In particular, it was demonstrated that GPR30 can protect the heart against I/R injury (Deschamps und Murphy, 2009), (Weil et al.), (Patel et al.) and can play a role in neuronal survival after ischemia (Lebesgue et al., 2009).

Subsequently, the data found by Takada *et al.*, where GPR30 was up-regulated in HUVECs subjected to FSS (Takada et al., 1997), were confirmed by using a different, more accurate, approach, namely by quantitative real-time PCR (qRT-PCR) instead of semi-quantitative reverse-transcription PCR (RT-PCR) and using as positive control the expression of ICAM-1, a gene known to respond to FSS (Nagel et al., 1994), (Results, Section 3.5). Secondly, other primary endothelial cells isolated from different vessels (HUAECs, HAoECs) and the HMECs were investigated under the same conditions of FSS, and there GPR30 was found to be up-regulated as well. The fact that the data were statistically not significant (HUAECs, HMECs) or the statistical analysis presented high standard deviations (HAoECs), could be explained by the relatively small number of replicates and the different origins of these cells (venous, arterial, aortic and primary cells compared with a cell line). A general comment is that GPR30 mRNA levels were very low in the stationary controls for all the cells analysed, but increased in a time- and shear-stress-dependent manner. These data are supported by much other work in which other GPCRs were found to be regulated by FSS, suggesting that GPCRs are involved in mediating primary mechanochemical signal transduction in endothelial cells (Gudi et al., 1996), (Chachisvilis et al., 2006).

4.4 Gene expression profiling in human microvascular endothelial cells over-expressing GPR30 upon fluid shear stress (FSS)

Microarrays provide a powerful method for investigating the effects of stimuli on global gene expression (Schena et al., 1995). In the study described here, microarrays were chosen for analysing the gene expression of Human Microvascular Endothelial Cells (HMEC-1), transfected with GPR30 and/or PATJ and stimulated with FSS. HMEC-1 cells are isolated from a human microvascular endothelium, the dermal tissue, and, after immortalisation by SV40 transformation, they present the same morphology, phenotype and functional characteristics of normal human microvascular endothelial cells (Ades et al., 1992). HMEC-1 cells were preferentially chosen over HUVECs since the over-expression or knock-down of GPR30 was very difficult to achieve in primary cells and further, as already mentioned before, the expression of GPR30 was found in endothelial cells of small arteries (Isensee et al., 2009). Therefore, HMEC-1 were chosen as the best cell type suitable for this experimental approach.

After stimulation with FSS the different groups of HMEC-1 cells transfected with an empty vector, GPR30 and/or PATJ were analysed in seven different comparisons, always evaluating the influence of only one parameter (i.e. the effect of the FSS or the effect of the over-expression).

The patterns of gene expression of HMEC-1 cells were compared with changes in expression induced by over-expression of GPR30 and/or PATJ upon FSS stimulation; unstimulated cells were used as controls. In general, FSS had the strongest effect on gene, expression while the effect of the over-expression was not so great. A summary of the array data is presented, using a Venn diagram representation, showing all hypothetically possible logical relations between a finite collection of sets. The Venn diagram is shown in Figure 30.

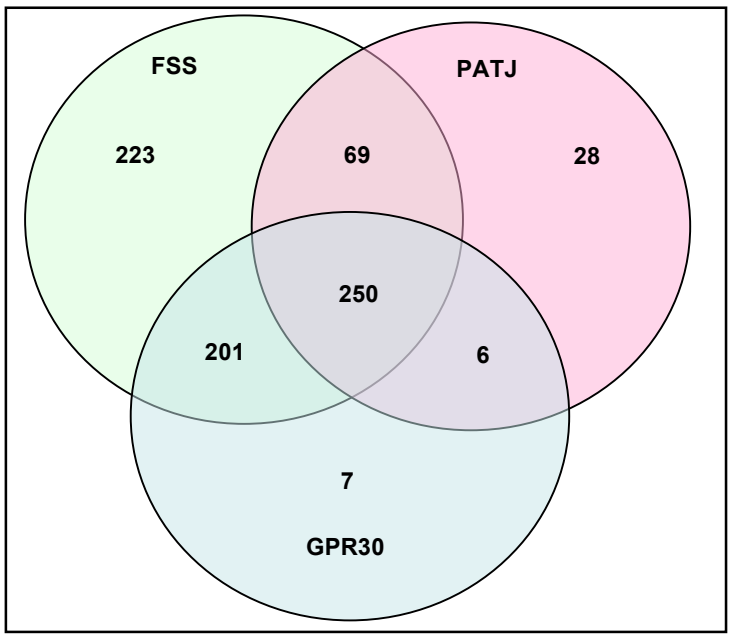

Figure 30: Venn diagram summarises number of genes of the seven different groups altered by FSS, over-expression of GPR30 and/or PATJ or both FSS and over-expression

In the control group (HMEC-1 upon FSS, Results 3.6.1) the global gene expression profile identified 217 genes up-regulated and 6 down-regulated and, as expected, the FSS alone induced the expression of a large number of genes involved in the vascular remodelling (e.g. VEGF, KLF2, JAG1) (Thi et al., 2007), (Dekker et al., 2002), (McCormick et al., 2001) while in general, the over-expression of either one of the two proteins or both together did not lead to a massive change in regulation of gene expression. In particular, in the group of HMEC-1 over-expressing GPR30 only a meagre number of deregulated genes was identified, e.g. HSPA6, MRGBP and Synaptojanin 1. One possible explanation for this low level of deregulation in gene expression could be the lack of activation of GPR30 due to the potential absence of a specific ligand. However, it is important to mention here that the whole set of microarray experiments was performed culturing the cells with 7.5% foetal bovine serum (FBS) medium and with phenol red, normally used as a pH indicator. It is well known that the serum contains traces of E2 (~18.5 pg/ml) (Santanam et al., 1998) and the presence of phenol red may interfere as a weak E2 agonist (Berthois et al., 1986).

The need of E2 for the activation of GPR30 in mediating the global gene expression has already been the object of other investigations. Indeed, in 2009 in the first microarray study aimed at characterising the transcriptional response to GPR30 signalling, human SKBr3 breast cancer cells (lacking both ERα and ERβ but expressing GPR30) were stimulated with E2 or with hydroxytamoxifen (OHT), which is an ER antagonist but a GPR30 agonist. The cells, cultured in phenol-red-free and serum-deprived media, were treated for only 1 hour to detect the primary response. The mRNA levels of 175 genes were raised by a factor of at

least 1.3 compared with uninduced control cells. Furthermore, if GPR30 expression was knocked down with an antisense RNA, a number of genes showed an at least 1.3-fold reduction in activity, demonstrating that any observed ligand-induced changes in gene expression were mediated by GPR30 (Pandey et al., 2009).
On the other hand, another study was performed with MCF-7 (ERs- and GPR30-positive) breast cancer cells to investigate the effect of E2-mediated extranuclear-initiated pathways on global gene expression. The cells treated with the E2 antagonist ICI 182,780 or knocked down for ERα, using siRNA, abolished E2-mediated gene stimulation, whereas GPR30 knock-down or treatment with the new identified selective GPR30 agonist G1 (Bologa et al., 2006) did not influence the gene expression. In this setting, it was shown that nuclear ERs and not GPR30 are the mediators of the rapid extranuclear E2 signalling (Madak-Erdogan et al., 2008).

If the over-expression itself did not affect global gene expression to a large extent, a very different situation was encountered when the aim of the comparisons was to look at the influence of FSS. Indeed, all the experiments comparing groups of unstimulated HMEC-1 cells with similar cells subjected to FSS identified a large number of deregulated genes (Results, Sections 3.6.3, 3.6.5 and 3.6.7). Surprisingly, here the effect of the shear stress in regulating the gene expression of cells differed, according to whether the cells were untransfected or over-expressing GPR30 alone or together with PATJ. For instance, many deregulated genes of the group of HMEC-1 cells over-expressing GPR30 upon FSS were not deregulated in cells transfected with empty vector upon exposure to FSS. These included genes which play an important role in vascular function and morphogenesis, e.g. plexin D1 (PLXND1) and troponin I type 3 (TNNI3).
Interestingly, when these deregulated genes of the group of HMEC-1 cells over-expressing GPR30 upon exposure to FSS were analysed with Ingenuity Pathways Analysis, one of the new networks found was Network 4, related to “Neurological disease”, “Drug metabolism” and “Endocrine system development and function”. Here a central position was occupied by E2 (Figure 3.13) which was associated with several deregulated genes, e.g. RERG (ras-related and E2-regulated growth inhibitor) and S100A13.
For RERG, it was shown that its expression was significantly decreased or lost in primary human breast tumours in an E2-dependent manner (Finlin et al., 2001). In a study aimed at identifying TFAP2C (transcription factor AP-2 gamma) regulation of physiological responses to E2 treatment in breast carcinoma, it was reported that knock-down of TFAP2C could alter the response of ERα target genes to E2 exposure; among these were RERG and GPR30 (this is in line with one of the first cloning approaches for GPR30, which was performed using ERs-positive breast carcinoma cell lines (Carmeci et al., 1997)) (Woodfield et al., 2007).

Moreover, network 4 is of particular interest, since the role of GPR30 as a new estrogen receptor is still quite controversial and, although in this experiment no E2 stimulation was applied, the over-expression of GPR30 together with the fluid shear stress induced the expression of genes involved in the endocrine system development and function. One possible reason could be the aforementioned use of medium containing FBS with traces of E2 in these microarray experiments and its eventual contribution in E2-mediated signalling. Another possible explanation could be that GPR30 is simply activated by the FSS stimulus in a ligand-independent manner.

4.5 Conclusions and outlook

GPCRs interact with, and are regulated by, several other proteins. Since to date nothing is known about the relation and interaction of GPR30 with other proteins, screening of a human heart cDNA library using the Y2H assay was performed. Several interaction partners were identified for GPR30, among them the PALS1-associated tight junction protein (PATJ) and the FUN14 domain containing 2 (FUNDC2).
In this work, these interactions were verified by co-immunoprecipitation (CoIP) experiments. For this purpose, several protocols were evaluated in order to set up conditions suitable to solubilise and immunoprecipitate GPR30. Hence, the interaction of GPR30 with PATJ was confirmed in a mammalian system (HEK293 cells over-expressing the two proteins). In addition, a partial cellular co-localisation was observed in cells overexpressing GPR30 and PATJ. However, the interaction between GPR30 and FUNDC2 could not be validated, underlining the importance of a CoIP experiment after the identification of new interaction partners for a particular protein found by Y2H, bioinformatic approaches or other methods.
The interaction GPR30-PATJ was found in yeast between the C-terminal domain of GPR30 and the last three C-terminal PDZ domains of PATJ. A further step towards a better comprehension of this interaction could be the determination of which PDZ domain of PATJ is involved, using for instance deletion mutants – i.e., removing one or the other PDZ domain either in yeast and/or in mammalian system.

Since a previous study has demonstrated the expression of GPR30 in endothelial cells of small vessels and one of the cloning approaches for GPR30 was using HUVECs exposed to FSS, the involvement of GPR30 in the vascular system was hypothesized. First, the up-regulation of GPR30 in HUVECs upon FSS was investigated and confirmed. Thereafter, GPR30 expression was analysed in other endothelial cells (HUAECs, HAoECs and HMEC-1) and was found to be up-regulated upon exposure to FSS, suggesting that GPR30 may indeed play a key role in vascular physiology.

Finally, a human cellular system to assess the potential role of GPR30 and the functional consequences of its interaction with PATJ in a vascular model was established. On this basis, the role of GPR30 and/or PATJ in the FSS response was investigated in HMEC-1 cells at the genome-wide transcript level. Interestingly, a different panel of genes was deregulated by FSS in cells over-expressing GPR30 then by FSS alone. These included genes that play an important role in vascular function and blood vessel morphogenesis (e.g. plexin D1 and troponin I type 3) and in the development and function of the endocrine system (e.g. RERG which is involved in E2 signalling).

Based on the results of this work, some questions are still to be answered. Mainly, which is the interaction domain between GPR30 and PATJ; if a dimerisation of GPR30 in endothelial cells exist and, if so, which are the molecular consequences? Can the identified downstream effectors of GPR30 upon FSS be confirmed and, if so, which are their functional relevance?

5 REFERENCES

Ades, E. W.; Candal, F. J.; Swerlick, R. A.; George, V. G.; Summers, S.; Bosse, D. C. und Lawley, T. J. (1992): HMEC-1: establishment of an immortalized human microvascular endothelial cell line, J Invest Dermatol 99 [6], Seite 683-90.

Albanito, L.; Madeo, A.; Lappano, R.; Vivacqua, A.; Rago, V.; Carpino, A.; Oprea, T. I.; Prossnitz, E. R.; Musti, A. M.; Ando, S. und Maggiolini, M. (2007): G protein-coupled receptor 30 (GPR30) mediates gene expression changes and growth response to 17beta-estradiol and selective GPR30 ligand G-1 in ovarian cancer cells, Cancer Res 67 [4], Seite 1859-66.

Alfarano, C.; Andrade, C. E.; Anthony, K.; Bahroos, N.; Bajec, M.; Bantoft, K.; Betel, D.; Bobechko, B.; Boutilier, K.; Burgess, E.; Buzadzija, K.; Cavero, R.; D'Abreo, C.; Donaldson, I.; Dorairajoo, D.; Dumontier, M. J.; Dumontier, M. R.; Earles, V.; Farrall, R.; Feldman, H.; Garderman, E.; Gong, Y.; Gonzaga, R.; Grytsan, V.; Gryz, E.; Gu, V.; Haldorsen, E.; Halupa, A.; Haw, R.; Hrvojic, A.; Hurrell, L.; Isserlin, R.; Jack, F.; Juma, F.; Khan, A.; Kon, T.; Konopinsky, S.; Le, V.; Lee, E.; Ling, S.; Magidin, M.; Moniakis, J.; Montojo, J.; Moore, S.; Muskat, B.; Ng, I.; Paraiso, J. P.; Parker, B.; Pintilie, G.; Pirone, R.; Salama, J. J.; Sgro, S.; Shan, T.; Shu, Y.; Siew, J.; Skinner, D.; Snyder, K.; Stasiuk, R.; Strumpf, D.; Tuekam, B.; Tao, S.; Wang, Z.; White, M.; Willis, R.; Wolting, C.; Wong, S.; Wrong, A.; Xin, C.; Yao, R.; Yates, B.; Zhang, S.; Zheng, K.; Pawson, T.; Ouellette, B. F. und Hogue, C. W. (2005): The Biomolecular Interaction Network Database and related tools 2005 update, Nucleic Acids Res 33 [Database issue], Seite D418-24.

Bai, M.; Trivedi, S. und Brown, E. M. (1998): Dimerization of the extracellular calcium-sensing receptor (CaR) on the cell surface of CaR-transfected HEK293 cells, J Biol Chem 273 [36], Seite 23605-10.

Bartling, B.; Tostlebe, H.; Darmer, D.; Holtz, J.; Silber, R. E. und Morawietz, H. (2000): Shear stress-dependent expression of apoptosis-regulating genes in endothelial cells, Biochem Biophys Res Commun 278 [3], Seite 740-6.

Berthois, Y.; Katzenellenbogen, J. A. und Katzenellenbogen, B. S. (1986): Phenol red in tissue culture media is a weak estrogen: implications concerning the study of estrogen-responsive cells in culture, Proc Natl Acad Sci U S A 83 [8], Seite 2496-500.

Bockaert, J.; Dumuis, A.; Fagni, L. und Marin, P. (2004): GPCR-GIP networks: a first step in the discovery of new therapeutic drugs?, Curr Opin Drug Discov Devel 7 [5], Seite 649-57.

Bockaert, J.; Marin, P.; Dumuis, A. und Fagni, L. (2003): The 'magic tail' of G protein-coupled receptors: an anchorage for functional protein networks, FEBS Lett 546 [1], Seite 65-72.

Bologa, C. G.; Revankar, C. M.; Young, S. M.; Edwards, B. S.; Arterburn, J. B.; Kiselyov, A. S.; Parker, M. A.; Tkachenko, S. E.; Savchuck, N. P.; Sklar, L. A.; Oprea, T. I. und Prossnitz, E. R. (2006): Virtual and biomolecular screening converge on a selective agonist for GPR30, Nat Chem Biol 2 [4], Seite 207-12.

Boudin, H.; Doan, A.; Xia, J.; Shigemoto, R.; Huganir, R. L.; Worley, P. und Craig, A. M. (2000): Presynaptic clustering of mGluR7a requires the PICK1 PDZ domain binding site, Neuron 28 [2], Seite 485-97.

Carmeci, C.; Thompson, D. A.; Ring, H. Z.; Francke, U. und Weigel, R. J. (1997): Identification of a gene (GPR30) with homology to the G-protein-coupled receptor superfamily associated with estrogen receptor expression in breast cancer, Genomics 45 [3], Seite 607-17.

Chachisvilis, M.; Zhang, Y. L. und Frangos, J. A. (2006): G protein-coupled receptors sense fluid shear stress in endothelial cells, Proc Natl Acad Sci U S A 103 [42], Seite 15463-8.

Chen, S. C.; Liu, Y. C.; Shyu, K. G. und Wang, D. L. (2008): Acute hypoxia to endothelial cells induces activating transcription factor 3 (ATF3) expression that is mediated via nitric oxide, Atherosclerosis 201 [2], Seite 281-8.

Chevesich, J.; Kreuz, A. J. und Montell, C. (1997): Requirement for the PDZ domain protein, INAD, for localization of the TRP store-operated channel to a signaling complex, Neuron 18 [1], Seite 95-105.

Cho, J. S.; Ouriel, K.; DeWeese, J. A.; Green, R. M.; Chen, G. Y. und Stoughton, J. (1995): Thrombus formation on polytetrafluoroethylene surfaces: the importance of von Willebrand factor, Cardiovasc Surg 3 [6], Seite 645-51.

Chung, S.; Funakoshi, T. und Civelli, O. (2008): Orphan GPCR research, Br J Pharmacol 153 Suppl 1, Seite S339-46.

Civelli, O.; Saito, Y.; Wang, Z.; Nothacker, H. P. und Reinscheid, R. K. (2006): Orphan GPCRs and their ligands, Pharmacol Ther 110 [3], Seite 525-32.

Dekker, R. J.; van Soest, S.; Fontijn, R. D.; Salamanca, S.; de Groot, P. G.; VanBavel, E.; Pannekoek, H. und Horrevoets, A. J. (2002): Prolonged fluid shear stress induces a distinct set of endothelial cell genes, most specifically lung Kruppel-like factor (KLF2), Blood 100 [5], Seite 1689-98.

Dennis, G., Jr.; Sherman, B. T.; Hosack, D. A.; Yang, J.; Gao, W.; Lane, H. C. und Lempicki, R. A. (2003): DAVID: Database for Annotation, Visualization, and Integrated Discovery, Genome Biol 4 [5], Seite P3.

Deschamps, A. M. und Murphy, E. (2009): Activation of a novel estrogen receptor, GPER, is cardioprotective in male and female rats, Am J Physiol Heart Circ Physiol 297 [5], Seite H1806-13.

Devost, D. und Zingg, H. H. (2003): Identification of dimeric and oligomeric complexes of the human oxytocin receptor by co-immunoprecipitation and bioluminescence resonance energy transfer, J Mol Endocrinol 31 [3], Seite 461-71.

DeWire, S. M.; Ahn, S.; Lefkowitz, R. J. und Shenoy, S. K. (2007): Beta-arrestins and cell signaling, Annu Rev Physiol 69, Seite 483-510.

Edinger, A. L.; Cinalli, R. M. und Thompson, C. B. (2003): Rab7 prevents growth factor-independent survival by inhibiting cell-autonomous nutrient transporter expression, Dev Cell 5 [4], Seite 571-82.

Erlandsson, M. C.; Ohlsson, C.; Gustafsson, J. A. und Carlsten, H. (2001): Role of oestrogen receptors alpha and beta in immune organ development and in oestrogen-mediated effects on thymus, Immunology 103 [1], Seite 17-25.

Ernkvist, M.; Luna Persson, N.; Audebert, S.; Lecine, P.; Sinha, I.; Liu, M.; Schlueter, M.; Horowitz, A.; Aase, K.; Weide, T.; Borg, J. P.; Majumdar, A. und Holmgren, L. (2009):

The Amot/Patj/Syx signaling complex spatially controls RhoA GTPase activity in migrating endothelial cells, Blood 113 [1], Seite 244-53.

Feng, Y. und Gregor, P. (1997): Cloning of a novel member of the G protein-coupled receptor family related to peptide receptors, Biochem Biophys Res Commun 231 [3], Seite 651-4.

Filardo, E. J. (2002): Epidermal growth factor receptor (EGFR) transactivation by estrogen via the G-protein-coupled receptor, GPR30: a novel signaling pathway with potential significance for breast cancer, J Steroid Biochem Mol Biol 80 [2], Seite 231-8.

Filardo, E. J.; Quinn, J. A.; Bland, K. I. und Frackelton, A. R., Jr. (2000): Estrogen-induced activation of Erk-1 and Erk-2 requires the G protein-coupled receptor homolog, GPR30, and occurs via trans-activation of the epidermal growth factor receptor through release of HB-EGF, Mol Endocrinol 14 [10], Seite 1649-60.

Filardo, E.; Quinn, J.; Pang, Y.; Graeber, C.; Shaw, S.; Dong, J. und Thomas, P. (2007): Activation of the novel estrogen receptor G protein-coupled receptor 30 (GPR30) at the plasma membrane, Endocrinology 148 [7], Seite 3236-45.

Finlin, B. S.; Gau, C. L.; Murphy, G. A.; Shao, H.; Kimel, T.; Seitz, R. S.; Chiu, Y. F.; Botstein, D.; Brown, P. O.; Der, C. J.; Tamanoi, F.; Andres, D. A. und Perou, C. M. (2001): RERG is a novel ras-related, estrogen-regulated and growth-inhibitory gene in breast cancer, J Biol Chem 276 [45], Seite 42259-67.

Fredriksson, R.; Lagerstrom, M. C.; Lundin, L. G. und Schioth, H. B. (2003): The G-protein-coupled receptors in the human genome form five main families. Phylogenetic analysis, paralogon groups, and fingerprints, Mol Pharmacol 63 [6], Seite 1256-72.

Funakoshi, T.; Yanai, A.; Shinoda, K.; Kawano, M. M. und Mizukami, Y. (2006): G protein-coupled receptor 30 is an estrogen receptor in the plasma membrane, Biochem Biophys Res Commun 346 [3], Seite 904-10.

Garcia-Cardena, G. und Gimbrone, M. A., Jr. (2006): Biomechanical modulation of endothelial phenotype: implications for health and disease, Handb Exp Pharmacol [176 Pt 2], Seite 79-95.

Gether, U. (2000): Uncovering molecular mechanisms involved in activation of G protein-coupled receptors, Endocr Rev 21 [1], Seite 90-113.

Gobeil, F.; Fortier, A.; Zhu, T.; Bossolasco, M.; Leduc, M.; Grandbois, M.; Heveker, N.; Bkaily, G.; Chemtob, S. und Barbaz, D. (2006): G-protein-coupled receptors signalling at the cell nucleus: an emerging paradigm, Can J Physiol Pharmacol 84 [3-4], Seite 287-97.

Gudi, S. R.; Clark, C. B. und Frangos, J. A. (1996): Fluid flow rapidly activates G proteins in human endothelial cells. Involvement of G proteins in mechanochemical signal transduction, Circ Res 79 [4], Seite 834-9.

Haas, E.; Bhattacharya, I.; Brailoiu, E.; Damjanovic, M.; Brailoiu, G. C.; Gao, X.; Mueller-Guerre, L.; Marjon, N. A.; Gut, A.; Minotti, R.; Meyer, M. R.; Amann, K.; Ammann, E.; Perez-Dominguez, A.; Genoni, M.; Clegg, D. J.; Dun, N. J.; Resta, T. C.; Prossnitz, E. R. und Barton, M. (2009): Regulatory role of G protein-coupled estrogen receptor for vascular function and obesity, Circ Res 104 [3], Seite 288-91.

Haas, E.; Meyer, M. R.; Schurr, U.; Bhattacharya, I.; Minotti, R.; Nguyen, H. H.; Heigl, A.; Lachat, M.; Genoni, M. und Barton, M. (2007): Differential effects of 17beta-estradiol

on function and expression of estrogen receptor alpha, estrogen receptor beta, and GPR30 in arteries and veins of patients with atherosclerosis, Hypertension 49 [6], Seite 1358-63.

Hahn, C. und Schwartz, M. A. (2009): Mechanotransduction in vascular physiology and atherogenesis, Nat Rev Mol Cell Biol 10 [1], Seite 53-62.

Harmar, A. J.; Hills, R. A.; Rosser, E. M.; Jones, M.; Buneman, O. P.; Dunbar, D. R.; Greenhill, S. D.; Hale, V. A.; Sharman, J. L.; Bonner, T. I.; Catterall, W. A.; Davenport, A. P.; Delagrange, P.; Dollery, C. T.; Foord, S. M.; Gutman, G. A.; Laudet, V.; Neubig, R. R.; Ohlstein, E. H.; Olsen, R. W.; Peters, J.; Pin, J. P.; Ruffolo, R. R.; Searls, D. B.; Wright, M. W. und Spedding, M. (2009): IUPHAR-DB: the IUPHAR database of G protein-coupled receptors and ion channels, Nucleic Acids Res 37 [Database issue], Seite D680-5.

Harvey, V.; Jones, J.; Misra, A.; Knight, A. R. und Quirk, K. (2001): Solubilisation and immunoprecipitation of rat striatal adenosine A(2A) receptors, Eur J Pharmacol 431 [2], Seite 171-7.

Hay, D. L.; Poyner, D. R. und Sexton, P. M. (2006): GPCR modulation by RAMPs, Pharmacol Ther 109 [1-2], Seite 173-97.

Hebert, T. E.; Moffett, S.; Morello, J. P.; Loisel, T. P.; Bichet, D. G.; Barret, C. und Bouvier, M. (1996): A peptide derived from a beta2-adrenergic receptor transmembrane domain inhibits both receptor dimerization and activation, J Biol Chem 271 [27], Seite 16384-92.

Hsieh, Y. C.; Yu, H. P.; Frink, M.; Suzuki, T.; Choudhry, M. A.; Schwacha, M. G. und Chaudry, I. H. (2007): G protein-coupled receptor 30-dependent protein kinase A pathway is critical in nongenomic effects of estrogen in attenuating liver injury after trauma-hemorrhage, Am J Pathol 170 [4], Seite 1210-8.

Huang, H. und Bader, J. S. (2009): Precision and recall estimates for two-hybrid screens, Bioinformatics 25 [3], Seite 372-8.

Hudlicka, O. (1994): Mechanical factors involved in the growth of the heart and its blood vessels, Cell Mol Biol Res 40 [2], Seite 143-52.

Isensee, J.; Meoli, L.; Zazzu, V.; Nabzdyk, C.; Witt, H.; Soewarto, D.; Effertz, K.; Fuchs, H.; Gailus-Durner, V.; Busch, D.; Adler, T.; de Angelis, M. H.; Irgang, M.; Otto, C. und Noppinger, P. R. (2009): Expression pattern of G protein-coupled receptor 30 in LacZ reporter mice, Endocrinology 150 [4], Seite 1722-30.

Jalink, K. und Moolenaar, W. H. G protein-coupled receptors: the inside story, Bioessays 32 [1], Seite 13-6.

Jassal, B.; Jupe, S.; Caudy, M.; Birney, E.; Stein, L.; Hermjakob, H. und D'Eustachio, P. The systematic annotation of the three main GPCR families in Reactome, Database (Oxford) 2010, Seite baq018.

Jones, D. W. und Peterson, E. D. (2008): Improving hypertension control rates: technology, people, or systems?, Jama 299 [24], Seite 2896-8.

Jordan, B. A. und Devi, L. A. (1999): G-protein-coupled receptor heterodimerization modulates receptor function, Nature 399 [6737], Seite 697-700.

Kang, L.; Zhang, X.; Xie, Y.; Tu, Y.; Wang, D.; Liu, Z. und Wang, Z. Y. Involvement of estrogen receptor variant ER-alpha36, not GPR30, in nongenomic estrogen signaling, Mol Endocrinol 24 [4], Seite 709-21.

Kimura, M.; Mizukami, Y.; Miura, T.; Fujimoto, K.; Kobayashi, S. und Matsuzaki, M. (2001): Orphan G protein-coupled receptor, GPR41, induces apoptosis via a p53/Bax pathway during ischemic hypoxia and reoxygenation, J Biol Chem 276 [28], Seite 26453-60.

Korenaga, R.; Ando, J.; Tsuboi, H.; Yang, W.; Sakuma, I.; Toyo-oka, T. und Kamiya, A. (1994): Laminar flow stimulates ATP- and shear stress-dependent nitric oxide production in cultured bovine endothelial cells, Biochem Biophys Res Commun 198 [1], Seite 213-9.

Kristiansen, K. (2004): Molecular mechanisms of ligand binding, signaling, and regulation within the superfamily of G-protein-coupled receptors: molecular modeling and mutagenesis approaches to receptor structure and function, Pharmacol Ther 103 [1], Seite 21-80.

Kroeze, W. K.; Sheffler, D. J. und Roth, B. L. (2003): G-protein-coupled receptors at a glance, J Cell Sci 116 [Pt 24], Seite 4867-9.

Krupnick, J. G. und Benovic, J. L. (1998): The role of receptor kinases and arrestins in G protein-coupled receptor regulation, Annu Rev Pharmacol Toxicol 38, Seite 289-319.

Kvingedal, A. M. und Smeland, E. B. (1997): A novel putative G-protein-coupled receptor expressed in lung, heart and lymphoid tissue, FEBS Lett 407 [1], Seite 59-62.

Langer, G.; Bader, B.; Meoli, L.; Isensee, J.; Delbeck, M.; Noppinger, P. R. und Otto, C. A critical review of fundamental controversies in the field of GPR30 research, Steroids 75 [8-9], Seite 603-10.

Lebesgue, D.; Chevaleyre, V.; Zukin, R. S. und Etgen, A. M. (2009): Estradiol rescues neurons from global ischemia-induced cell death: multiple cellular pathways of neuroprotection, Steroids 74 [7], Seite 555-61.

Leeb-Lundberg, L. M.; Marceau, F.; Muller-Esterl, W.; Pettibone, D. J. und Zuraw, B. L. (2005): International union of pharmacology. XLV. Classification of the kinin receptor family: from molecular mechanisms to pathophysiological consequences, Pharmacol Rev 57 [1], Seite 27-77.

Lehoux, S.; Tronc, F. und Tedgui, A. (2002): Mechanisms of blood flow-induced vascular enlargement, Biorheology 39 [3-4], Seite 319-24.

Lemmers, C.; Medina, E.; Delgrossi, M. H.; Michel, D.; Arsanto, J. P. und Le Bivic, A. (2002): hINADl/PATJ, a homolog of discs lost, interacts with crumbs and localizes to tight junctions in human epithelial cells, J Biol Chem 277 [28], Seite 25408-15.

Levick, J. R. (1995): Introduction to Cardiovascular Physiology 3rd Edition, ISBN 0-340-76376-0, Arnold, a member of the Hodder Headline Group, London, 2000.

Levoye, A.; Dam, J.; Ayoub, M. A.; Guillaume, J. L. und Jockers, R. (2006): Do orphan G-protein-coupled receptors have ligand-independent functions? New insights from receptor heterodimers, EMBO Rep 7 [11], Seite 1094-8.

Lloyd-Jones, D.; Adams, R.; Carnethon, M.; De Simone, G.; Ferguson, T. B.; Flegal, K.; Ford, E.; Furie, K.; Go, A.; Greenlund, K.; Haase, N.; Hailpern, S.; Ho, M.; Howard, V.; Kissela, B.; Kittner, S.; Lackland, D.; Lisabeth, L.; Marelli, A.; McDermott, M.; Meigs, J.; Mozaffarian, D.; Nichol, G.; O'Donnell, C.; Roger, V.; Rosamond, W.; Sacco, R.; Sorlie, P.; Stafford, R.; Steinberger, J.; Thom, T.; Wasserthiel-Smoller, S.; Wong, N.; Wylie-Rosett, J. und Hong, Y. (2009): Heart disease and stroke statistics--2009 update: a report from the American Heart Association Statistics Committee and Stroke Statistics Subcommittee, Circulation 119 [3], Seite 480-6.

Madak-Erdogan, Z.; Kieser, K. J.; Kim, S. H.; Komm, B.; Katzenellenbogen, J. A. und Katzenellenbogen, B. S. (2008): Nuclear and extranuclear pathway inputs in the regulation of global gene expression by estrogen receptors, Mol Endocrinol 22 [9], Seite 2116-27.

Maggiolini, M.; Vivacqua, A.; Fasanella, G.; Recchia, A. G.; Sisci, D.; Pezzi, V.; Montanaro, D.; Musti, A. M.; Picard, D. und Ando, S. (2004): The G protein-coupled receptor GPR30 mediates c-fos up-regulation by 17beta-estradiol and phytoestrogens in breast cancer cells, J Biol Chem 279 [26], Seite 27008-16.

Martensson, U. E.; Salehi, S. A.; Windahl, S.; Gomez, M. F.; Sward, K.; Daszkiewicz-Nilsson, J.; Wendt, A.; Andersson, N.; Hellstrand, P.; Grande, P. O.; Owman, C.; Rosen, C. J.; Adamo, M. L.; Lundquist, I.; Rorsman, P.; Nilsson, B. O.; Ohlsson, C.; Olde, B. und Leeb-Lundberg, L. M. (2009): Deletion of the G protein-coupled receptor 30 impairs glucose tolerance, reduces bone growth, increases blood pressure, and eliminates estradiol-stimulated insulin release in female mice, Endocrinology 150 [2], Seite 687-98.

McCormick, S. M.; Eskin, S. G.; McIntire, L. V.; Teng, C. L.; Lu, C. M.; Russell, C. G. und Chittur, K. K. (2001): DNA microarray reveals changes in gene expression of shear stressed human umbilical vein endothelial cells, Proc Natl Acad Sci U S A 98 [16], Seite 8955-60.

McDowall, M. D.; Scott, M. S. und Barton, G. J. (2009): PIPs: human protein-protein interaction prediction database, Nucleic Acids Res 37 [Database issue], Seite D651-6.

Milligan, G. (2009): G protein-coupled receptor hetero-dimerization: contribution to pharmacology and function, Br J Pharmacol 158 [1], Seite 5-14.

Moore, D.; Chambers, J.; Waldvogel, H.; Faull, R. und Emson, P. (2000): Regional and cellular distribution of the P2Y(1) purinergic receptor in the human brain: striking neuronal localisation, J Comp Neurol 421 [3], Seite 374-84.

Morawietz, H.; Talanow, R.; Szibor, M.; Rueckschloss, U.; Schubert, A.; Bartling, B.; Darmer, D. und Holtz, J. (2000): Regulation of the endothelin system by shear stress in human endothelial cells, J Physiol 525 Pt 3, Seite 761-70.

Morita, T.; Yoshizumi, M.; Kurihara, H.; Maemura, K.; Nagai, R. und Yazaki, Y. (1993): Shear stress increases heparin-binding epidermal growth factor-like growth factor mRNA levels in human vascular endothelial cells, Biochem Biophys Res Commun 197 [1], Seite 256-62.

Nagamatsu, S.; Kornhauser, J. M.; Burant, C. F.; Seino, S.; Mayo, K. E. und Bell, G. I. (1992): Glucose transporter expression in brain. cDNA sequence of mouse GLUT3, the brain facilitative glucose transporter isoform, and identification of sites of expression by in situ hybridization, J Biol Chem 267 [1], Seite 467-72.

Nagel, T.; Resnick, N.; Atkinson, W. J.; Dewey, C. F., Jr. und Gimbrone, M. A., Jr. (1994): Shear stress selectively upregulates intercellular adhesion molecule-1 expression in cultured human vascular endothelial cells, J Clin Invest 94 [2], Seite 885-91.

Nguyen, K. T.; Eskin, S. G.; Patterson, C.; Runge, M. S. und McIntire, L. V. (2001): Shear stress reduces protease activated receptor-1 expression in human endothelial cells, Ann Biomed Eng 29 [2], Seite 145-52.

Nourry, C.; Grant, S. G. und Borg, J. P. (2003): PDZ domain proteins: plug and play!, Sci STKE 2003 [179], Seite RE7.

O'Dowd, B. F.; Nguyen, T.; Marchese, A.; Cheng, R.; Lynch, K. R.; Heng, H. H.; Kolakowski, L. F., Jr. und George, S. R. (1998): Discovery of three novel G-protein-coupled receptor genes, Genomics 47 [2], Seite 310-3.

Oh, D. Y.; Kim, K.; Kwon, H. B. und Seong, J. Y. (2006): Cellular and molecular biology of orphan G protein-coupled receptors, Int Rev Cytol 252, Seite 163-218.

Okuma, Y. und Reisine, T. (1992): Immunoprecipitation of alpha 2a-adrenergic receptor-GTP-binding protein complexes using GTP-binding protein selective antisera. Changes in receptor/GTP-binding protein interaction following agonist binding, J Biol Chem 267 [21], Seite 14826-31.

Otto, C.; Fuchs, I.; Kauselmann, G.; Kern, H.; Zevnik, B.; Andreasen, P.; Schwarz, G.; Altmann, H.; Klewer, M.; Schoor, M.; Vonk, R. und Fritzemeier, K. H. (2009): GPR30 does not mediate estrogenic responses in reproductive organs in mice, Biol Reprod 80 [1], Seite 34-41.

Otto, C.; Rohde-Schulz, B.; Schwarz, G.; Fuchs, I.; Klewer, M.; Brittain, D.; Langer, G.; Bader, B.; Prelle, K.; Nubbemeyer, R. und Fritzemeier, K. H. (2008): G protein-coupled receptor 30 localizes to the endoplasmic reticulum and is not activated by estradiol, Endocrinology 149 [10], Seite 4846-56.

Owman, C.; Blay, P.; Nilsson, C. und Lolait, S. J. (1996): Cloning of human cDNA encoding a novel heptahelix receptor expressed in Burkitt's lymphoma and widely distributed in brain and peripheral tissues, Biochem Biophys Res Commun 228 [2], Seite 285-92.

Pandey, D. P.; Lappano, R.; Albanito, L.; Madeo, A.; Maggiolini, M. und Picard, D. (2009): Estrogenic GPR30 signalling induces proliferation and migration of breast cancer cells through CTGF, Embo J 28 [5], Seite 523-32.

Papaioannou, T. G. und Stefanadis, C. (2005): Vascular wall shear stress: basic principles and methods, Hellenic J Cardiol 46 [1], Seite 9-15.

Patel, V. H.; Chen, J.; Ramanjaneya, M.; Karteris, E.; Zachariades, E.; Thomas, P.; Been, M. und Randeva, H. S. G-protein coupled estrogen receptor 1 expression in rat and human heart: Protective role during ischaemic stress, Int J Mol Med 26 [2], Seite 193-9.

Pedram, A.; Razandi, M. und Levin, E. R. (2006): Nature of functional estrogen receptors at the plasma membrane, Mol Endocrinol 20 [9], Seite 1996-2009.

Pierce, K. L.; Premont, R. T. und Lefkowitz, R. J. (2002): Seven-transmembrane receptors, Nat Rev Mol Cell Biol 3 [9], Seite 639-50.

Prior, B. M.; Yang, H. T. und Terjung, R. L. (2004): What makes vessels grow with exercise training?, J Appl Physiol 97 [3], Seite 1119-28.

Prossnitz, E. R.; Arterburn, J. B. und Sklar, L. A. (2007): GPR30: A G protein-coupled receptor for estrogen, Mol Cell Endocrinol 265-266, Seite 138-42.

Prossnitz, E. R.; Arterburn, J. B.; Smith, H. O.; Oprea, T. I.; Sklar, L. A. und Hathaway, H. J. (2008): Estrogen signaling through the transmembrane G protein-coupled receptor GPR30, Annu Rev Physiol 70, Seite 165-90.

Revankar, C. M.; Cimino, D. F.; Sklar, L. A.; Arterburn, J. B. und Prossnitz, E. R. (2005): A transmembrane intracellular estrogen receptor mediates rapid cell signaling, Science 307 [5715], Seite 1625-30.

Rey, S. und Semenza, G. L. Hypoxia-inducible factor-1-dependent mechanisms of vascularization and vascular remodelling, Cardiovasc Res 86 [2], Seite 236-42.

Riess, N. P.; Milward, K.; Lee, T.; Adams, M.; Askham, J. M. und Morrison, E. E. (2005): Trapping of normal EB1 ligands in aggresomes formed by an EB1 deletion mutant, BMC Cell Biol 6 [1], Seite 17.

Risau, W. (1997): Mechanisms of angiogenesis, Nature 386 [6626], Seite 671-4.

Ritter, S. L. und Hall, R. A. (2009): Fine-tuning of GPCR activity by receptor-interacting proteins, Nat Rev Mol Cell Biol 10 [12], Seite 819-30.

Roh, M. H.; Fan, S.; Liu, C. J. und Margolis, B. (2003): The Crumbs3-Pals1 complex participates in the establishment of polarity in mammalian epithelial cells, J Cell Sci 116 [Pt 14], Seite 2895-906.

Roh, M. H.; Liu, C. J.; Laurinec, S. und Margolis, B. (2002): The carboxyl terminus of zona occludens-3 binds and recruits a mammalian homologue of discs lost to tight junctions, J Biol Chem 277 [30], Seite 27501-9.

Roh, M. H.; Makarova, O.; Liu, C. J.; Shin, K.; Lee, S.; Laurinec, S.; Goyal, M.; Wiggins, R. und Margolis, B. (2002): The Maguk protein, Pals1, functions as an adapter, linking mammalian homologues of Crumbs and Discs Lost, J Cell Biol 157 [1], Seite 161-72.

Romano, C.; Yang, W. L. und O'Malley, K. L. (1996): Metabotropic glutamate receptor 5 is a disulfide-linked dimer, J Biol Chem 271 [45], Seite 28612-6.

Rondou, P.; Haegeman, G.; Vanhoenacker, P. und Van Craenenbroeck, K. (2008): BTB Protein KLHL12 targets the dopamine D4 receptor for ubiquitination by a Cul3-based E3 ligase, J Biol Chem 283 [17], Seite 11083-96.

Ross, R. (1993): Atherosclerosis: current understanding of mechanisms and future strategies in therapy, Transplant Proc 25 [2], Seite 2041-3.

Rozen, S. und Skaletsky, H. (2000): Primer3 on the WWW for general users and for biologist programmers, Methods Mol Biol 132, Seite 365-86.

Ruscher, K.; Freyer, D.; Karsch, M.; Isaev, N.; Megow, D.; Sawitzki, B.; Priller, J.; Dirnagl, U. und Meisel, A. (2002): Erythropoietin is a paracrine mediator of ischemic tolerance in the brain: evidence from an in vitro model, J Neurosci 22 [23], Seite 10291-301.

Santanam, N.; Shern-Brewer, R.; McClatchey, R.; Castellano, P. Z.; Murphy, A. A.; Voelkel, S. und Parthasarathy, S. (1998): Estradiol as an antioxidant: incompatible with its physiological concentrations and function, J Lipid Res 39 [11], Seite 2111-8.

Schaper, W. (2009): Collateral circulation: past and present, Basic Res Cardiol 104 [1], Seite 5-21.

Schaper, W.; Flameng, W.; Winkler, B.; Wusten, B.; Turschmann, W.; Neugebauer, G.; Carl, M. und Pasyk, S. (1976): Quantification of collateral resistance in acute and chronic experimental coronary occlusion in the dog, Circ Res 39 [3], Seite 371-7.

Schena, M.; Shalon, D.; Davis, R. W. und Brown, P. O. (1995): Quantitative monitoring of gene expression patterns with a complementary DNA microarray, Science 270 [5235], Seite 467-70.

Sheng, M. und Sala, C. (2001): PDZ domains and the organization of supramolecular complexes, Annu Rev Neurosci 24, Seite 1-29.

Shin, K.; Straight, S. und Margolis, B. (2005): PATJ regulates tight junction formation and polarity in mammalian epithelial cells, J Cell Biol 168 [5], Seite 705-11.

Shin, K.; Wang, Q. und Margolis, B. (2007): PATJ regulates directional migration of mammalian epithelial cells, EMBO Rep 8 [2], Seite 158-64.

Snel, B.; Lehmann, G.; Bork, P. und Huynen, M. A. (2000): STRING: a web-server to retrieve and display the repeatedly occurring neighbourhood of a gene, Nucleic Acids Res 28 [18], Seite 3442-4.

Straight, S. W.; Pieczynski, J. N.; Whiteman, E. L.; Liu, C. J. und Margolis, B. (2006): Mammalian lin-7 stabilizes polarity protein complexes, J Biol Chem 281 [49], Seite 37738-47.

Takada, Y.; Kato, C.; Kondo, S.; Korenaga, R. und Ando, J. (1997): Cloning of cDNAs encoding G protein-coupled receptor expressed in human endothelial cells exposed to fluid shear stress, Biochem Biophys Res Commun 240 [3], Seite 737-41.

Thi, M. M.; Iacobas, D. A.; Iacobas, S. und Spray, D. C. (2007): Fluid shear stress upregulates vascular endothelial growth factor gene expression in osteoblasts, Ann N Y Acad Sci 1117, Seite 73-81.

Thomas, P.; Pang, Y.; Filardo, E. J. und Dong, J. (2005): Identity of an estrogen membrane receptor coupled to a G protein in human breast cancer cells, Endocrinology 146 [2], Seite 624-32.

Traub, O. und Berk, B. C. (1998): Laminar shear stress: mechanisms by which endothelial cells transduce an atheroprotective force, Arterioscler Thromb Vasc Biol 18 [5], Seite 677-85.

Vaccaro, P.; Brannetti, B.; Montecchi-Palazzi, L.; Philipp, S.; Helmer Citterich, M.; Cesareni, G. und Dente, L. (2001): Distinct binding specificity of the multiple PDZ domains of INADL, a human protein with homology to INAD from Drosophila melanogaster, J Biol Chem 276 [45], Seite 42122-30.

Vassilatis, D. K.; Hohmann, J. G.; Zeng, H.; Li, F.; Ranchalis, J. E.; Mortrud, M. T.; Brown, A.; Rodriguez, S. S.; Weller, J. R.; Wright, A. C.; Bergmann, J. E. und Gaitanaris, G.

A. (2003): The G protein-coupled receptor repertoires of human and mouse, Proc Natl Acad Sci U S A 100 [8], Seite 4903-8.

Vivacqua, A.; Bonofiglio, D.; Albanito, L.; Madeo, A.; Rago, V.; Carpino, A.; Musti, A. M.; Picard, D.; Ando, S. und Maggiolini, M. (2006): 17beta-estradiol, genistein, and 4-hydroxytamoxifen induce the proliferation of thyroid cancer cells through the g protein-coupled receptor GPR30, Mol Pharmacol 70 [4], Seite 1414-23.

Vivacqua, A.; Bonofiglio, D.; Recchia, A. G.; Musti, A. M.; Picard, D.; Ando, S. und Maggiolini, M. (2006): The G protein-coupled receptor GPR30 mediates the proliferative effects induced by 17beta-estradiol and hydroxytamoxifen in endometrial cancer cells, Mol Endocrinol 20 [3], Seite 631-46.

Vladusic, E. A.; Hornby, A. E.; Guerra-Vladusic, F. K.; Lakins, J. und Lupu, R. (2000): Expression and regulation of estrogen receptor beta in human breast tumors and cell lines, Oncol Rep 7 [1], Seite 157-67.

Waller, R. F.; Reed, M. B.; Cowman, A. F. und McFadden, G. I. (2000): Protein trafficking to the plastid of Plasmodium falciparum is via the secretory pathway, Embo J 19 [8], Seite 1794-802.

Wang, C.; Dehghani, B.; Magrisso, I. J.; Rick, E. A.; Bonhomme, E.; Cody, D. B.; Elenich, L. A.; Subramanian, S.; Murphy, S. J.; Kelly, M. J.; Rosenbaum, J. S.; Vandenbark, A. A. und Offner, H. (2008): GPR30 contributes to estrogen-induced thymic atrophy, Mol Endocrinol 22 [3], Seite 636-48.

Wang, Z.; Zhang, X.; Shen, P.; Loggie, B. W.; Chang, Y. und Deuel, T. F. (2005): Identification, cloning, and expression of human estrogen receptor-alpha36, a novel variant of human estrogen receptor-alpha66, Biochem Biophys Res Commun 336 [4], Seite 1023-7.

Weil, B. R.; Manukyan, M. C.; Herrmann, J. L.; Wang, Y.; Abarbanell, A. M.; Poynter, J. A. und Meldrum, D. R. Signaling via GPR30 protects the myocardium from ischemia/reperfusion injury, Surgery 148 [2], Seite 436-43.

White, J. H.; Wise, A.; Main, M. J.; Green, A.; Fraser, N. J.; Disney, G. H.; Barnes, A. A.; Emson, P.; Foord, S. M. und Marshall, F. H. (1998): Heterodimerization is required for the formation of a functional GABA(B) receptor, Nature 396 [6712], Seite 679-82.

Wilkie, T. M.; Gilbert, D. J.; Olsen, A. S.; Chen, X. N.; Amatruda, T. T.; Korenberg, J. R.; Trask, B. J.; de Jong, P.; Reed, R. R.; Simon, M. I. und et al. (1992): Evolution of the mammalian G protein alpha subunit multigene family, Nat Genet 1 [2], Seite 85-91.

Woodfield, G. W.; Horan, A. D.; Chen, Y. und Weigel, R. J. (2007): TFAP2C controls hormone response in breast cancer cells through multiple pathways of estrogen signaling, Cancer Res 67 [18], Seite 8439-43.

Zou, Y.; Akazawa, H.; Qin, Y.; Sano, M.; Takano, H.; Minamino, T.; Makita, N.; Iwanaga, K.; Zhu, W.; Kudoh, S.; Toko, H.; Tamura, K.; Kihara, M.; Nagai, T.; Fukamizu, A.; Umemura, S.; Iiri, T.; Fujita, T. und Komuro, I. (2004): Mechanical stress activates angiotensin II type 1 receptor without the involvement of angiotensin II, Nat Cell Biol 6 [6], Seite 499-506.

6 APPENDICES

6.1 Appendix result 3.6

6.1.1 GPR30 knock-down in HUVECs

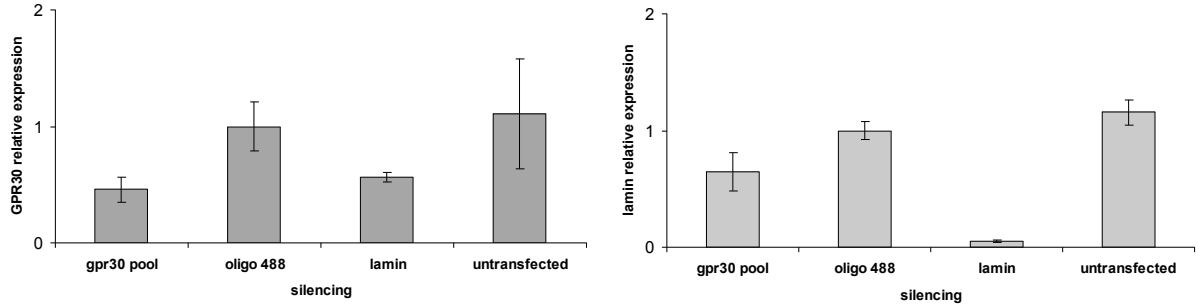

Figure 31: GPR30 knock-down in HUVECs
Relative gene expression levels of GPR30 (left panel) and lamin A/C (right panel) by real time-PCR in HUVECs transfected with different siRNAs. When the gene expression was measured using GPR30 primers, the expression of GPR30 was found to be reduced (left panel) but this was also the case for the positive control, lamin A/C. Therefore the silencing effect was considered to be an artefact. In contrast, when lamin A/C primers were used, a large reduction in the relative expression of lamin A/C was found (right panel).

6.1.2 pEGFP-C1 transfection in HUVECs

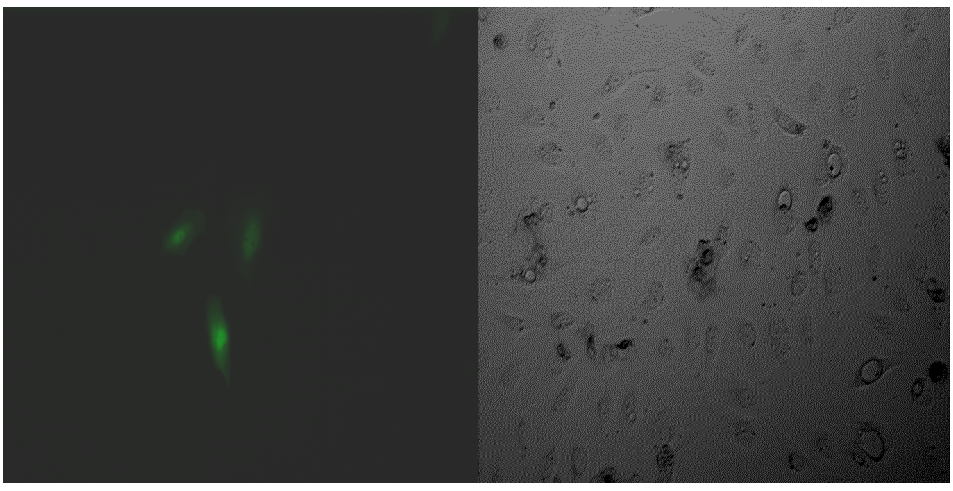

Figure 32: HUVECs transiently transfected with GPR30-EGFP

6.1.3 GPR30 knock-down in HMECs

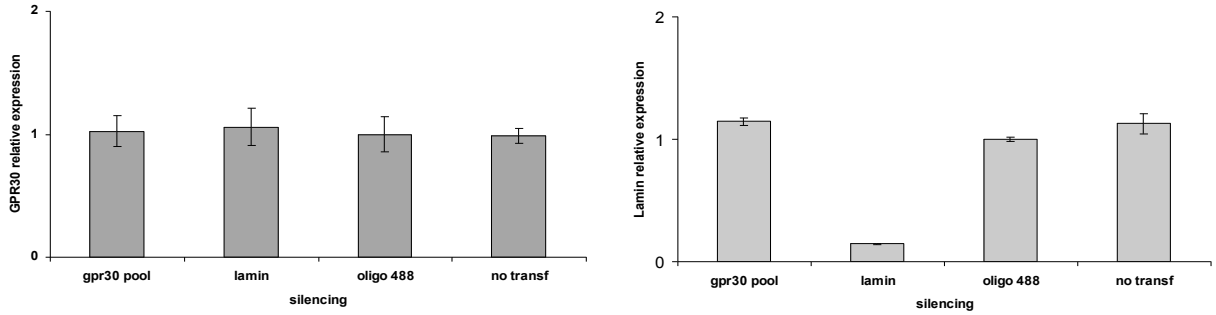

Figure 33: GPR30 knock-down in HMECs
Relative gene expression levels of GPR30 (left panel) and lamin A/C (right panel) by real time-PCR in HMECs transfected with different siRNAs. When the gene expression was measured using GPR30 primers, GPR30 was not found to be reduced (left panel). Differently, using lamin A/C primers, a high reduction of the relative expression of lamin A/C was found (right panel).

6.1.4 pEGFP-C1 transfection in HMECs

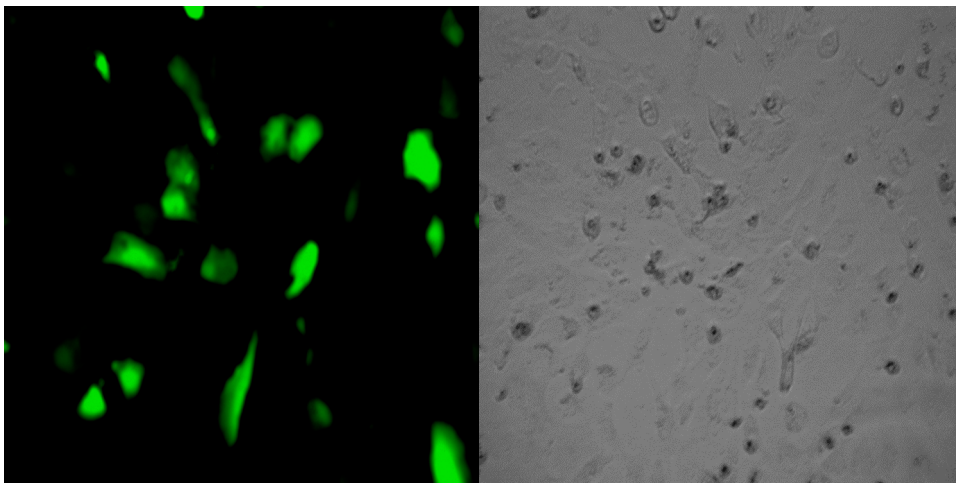

Figure 34: HMECs transiently transfected with GPR30-EGFP

6.2 Appendix table 6. Effects of FSS on HMEC-1 cells

Table 13: Deregulated genes in HMEC-1 cells upon FSS

Change ratios (*x*-fold changes) are indicated in the column Ratio and *q* values at a 'false discovery' rate (FDR) of < 5%.

ILLUMINA_ID	Gene ID	Gene Name	Ratio	q-value(%)
ILMN_2314169	PTHLH	PARATHYROID HORMONE-LIKE HORMONE	7.61	0.00
ILMN_1684306	S100A4	S100 CALCIUM BINDING PROTEIN A4 (CALCIUM PROTEIN, CALVASCULIN, METASTASIN, MURINE PLACENTAL HOMOLOG)	4.68	0.00
ILMN_1665035	KRT14	KERATIN 14 (EPIDERMOLYSIS BULLOSA SIMPLEX, DOWLING-MEARA, KOEBNER)	4.57	0.00
ILMN_1765446	EMP3	EPITHELIAL MEMBRANE PROTEIN 3	4.31	0.00
ILMN_1696048	C13orf33	HYPOTHETICAL PROTEIN FLJ14834	4.22	0.00
ILMN_1787186	NOV	NEPHROBLASTOMA OVEREXPRESSED GENE	4.12	0.00
ILMN_1811790	FOXS1	FORKHEAD-LIKE 18 (DROSOPHILA)	4.06	0.00
ILMN_1796423	CLIC3	CHLORIDE INTRACELLULAR CHANNEL 3	4.05	0.00
ILMN_1706643	COL6A3	COLLAGEN, TYPE VI, ALPHA 3	3.92	0.00
ILMN_1689431	APCDD1L	HYPOTHETICAL PROTEIN FLJ90166	3.90	0.00
ILMN_2041190	F2RL1	COAGULATION FACTOR II (THROMBIN) RECEPTOR-LIKE 1	3.87	0.00
ILMN_1802205	RHOB	RAS HOMOLOG GENE FAMILY, MEMBER B	3.81	0.00
ILMN_1763837	ANPEP	ALANYL (MEMBRANE) AMINOPEPTIDASE (AMINOPEPTIDASE N, AMINOPEPTIDASE M, MICROSOMAL AMINOPEPTIDASE, CD13, P150)	3.72	0.00
ILMN_1714170	SPSB1	SPLA/RYANODINE RECEPTOR DOMAIN AND SOCS BOX CONTAINING 1	3.66	0.00
ILMN_1800512	HMOX1	HEME OXYGENASE (DECYCLING) 1	3.62	0.00
ILMN_1738742	PLAT	PLASMINOGEN ACTIVATOR, TISSUE	3.46	0.00
ILMN_1709674	GFPT2	GLUTAMINE-FRUCTOSE-6-PHOSPHATE TRANSAMINASE 2	3.42	0.00
ILMN_2384122	GPR56	G PROTEIN-COUPLED RECEPTOR 56	3.30	0.00
ILMN_1708534	PAX8	PAIRED BOX GENE 8	3.27	0.00
ILMN_2413158	PODXL	PODOCALYXIN-LIKE	3.17	0.00
ILMN_2352097	GPR56	G PROTEIN-COUPLED RECEPTOR 56	3.07	0.00
ILMN_1791679	DNER	DELTA-NOTCH-LIKE EGF REPEAT-CONTAINING TRANSMEMBRANE	2.91	0.00
ILMN_1735930	KLF2	KRUPPEL-LIKE FACTOR 2 (LUNG)	2.83	0.00
ILMN_1803728	SLC35E4	SOLUTE CARRIER FAMILY 35, MEMBER E4	2.79	0.00
ILMN_1665792	ITGA2	INTEGRIN, ALPHA 2 (CD49B, ALPHA 2 SUBUNIT OF VLA-2 RECEPTOR)	2.71	0.00
ILMN_1807652	STRA6	STIMULATED BY RETINOIC ACID GENE 6 HOMOLOG (MOUSE)	2.69	0.00
ILMN_1760160	STX1A	SYNTAXIN 1A (BRAIN)	2.68	0.00
ILMN_1768534	BHLHB2	BASIC HELIX-LOOP-HELIX DOMAIN CONTAINING, CLASS B, 2	2.66	0.00
ILMN_1711311	PODXL	PODOCALYXIN-LIKE	2.62	0.00
ILMN_1669046	FOXQ1	FORKHEAD BOX Q1	2.62	0.00
ILMN_2137789	KLF4	KRUPPEL-LIKE FACTOR 4 (GUT)	2.59	0.00
ILMN_1657111	C14orf78	CHROMOSOME 14 OPEN READING FRAME 78	2.58	0.00
ILMN_1679929	KLF13	KRUPPEL-LIKE FACTOR 13	2.52	0.00
ILMN_1701461	TIMP3	TIMP METALLOPEPTIDASE INHIBITOR 3 (SORSBY FUNDUS DYSTROPHY, PSEUDOINFLAMMATORY)	2.52	0.00
ILMN_1760778	ENG	ENDOGLIN (OSLER-RENDU-WEBER SYNDROME 1)	2.47	0.00
ILMN_2269136	CENTG3	CENTAURIN, GAMMA 3	2.35	0.00
ILMN_1712708	TRIM47	TRIPARTITE MOTIF-CONTAINING 47	2.31	0.00
ILMN_2407703	SYN1	SYNAPSIN I	2.31	0.00
ILMN_1762803	RFXDC2	REGULATORY FACTOR X DOMAIN CONTAINING 2	2.25	0.00
ILMN_1807689	PKNOX2	PBX/KNOTTED 1 HOMEOBOX 2	2.20	0.00
ILMN_1791447	CXCL12	CHEMOKINE (C-X-C MOTIF) LIGAND 12	2.17	0.00
ILMN_1732609	KIAA1539	KIAA1539 PROTEIN	2.08	0.00

ILMN_1761425	OLFML2A	OLFACTOMEDIN-LIKE 2A	2.05	0.00
ILMN_1775501	IL1B	INTERLEUKIN 1, BETA	2.03	0.00
ILMN_1732197	MN1	MENINGIOMA (DISRUPTED IN BALANCED TRANSLOCATION) 1	2.00	0.00
ILMN_1703531	EDG3	ENDOTHELIAL DIFFERENTIATION, SPHINGOLIPID G-PROTEIN-COUPLED RECEPTOR, 3	1.99	0.00
ILMN_1756595	SH3TC1	SH3 DOMAIN AND TETRATRICOPEPTIDE REPEATS 1	1.95	0.00
ILMN_1736178	AEBP1	AE BINDING PROTEIN 1	1.94	0.00
ILMN_1785061	EPHB2	EPH RECEPTOR B2	1.94	0.00
ILMN_1753286	MYO19	MYOSIN HEAD DOMAIN CONTAINING 1	1.91	0.00
ILMN_1748124	TSC22D3	TSC22 DOMAIN FAMILY, MEMBER 3	1.91	0.00
ILMN_1751576	TEK	TEK TYROSINE KINASE, ENDOTHELIAL (VENOUS MALFORMATIONS, MULTIPLE CUTANEOUS AND MUCOSAL)	1.90	0.00
ILMN_2111237	MN1	MENINGIOMA (DISRUPTED IN BALANCED TRANSLOCATION) 1	1.90	0.00
ILMN_1787567	TSC22D1	TSC22 DOMAIN FAMILY, MEMBER 1	1.90	0.00
ILMN_1682081	RNF19B	IBR DOMAIN CONTAINING 3	1.80	0.00
ILMN_1760412	SHISA2	TRANSMEMBRANE PROTEIN 46	1.75	0.00
ILMN_1754842	DLGAP4	DISCS, LARGE (DROSOPHILA) HOMOLOG-ASSOCIATED PROTEIN 4	1.64	0.00
ILMN_1717809	RNF24	RING FINGER PROTEIN 24	1.61	0.00
ILMN_1673113	F2RL1	COAGULATION FACTOR II (THROMBIN) RECEPTOR-LIKE 1	3.96	0.91
ILMN_1844408	PLXNA2	PLEXIN A2	3.45	0.91
ILMN_2311537	HMGA1	HIGH MOBILITY GROUP AT-HOOK 1	2.97	0.91
ILMN_1713449	TBX3	T-BOX 3 (ULNAR MAMMARY SYNDROME)	2.85	0.91
ILMN_1659599	ADC	ARGININE DECARBOXYLASE	2.84	0.91
ILMN_1723971	SLC29A1	SOLUTE CARRIER FAMILY 29 (NUCLEOSIDE TRANSPORTERS), MEMBER 1	2.80	0.91
ILMN_1725852	S100A2	S100 CALCIUM BINDING PROTEIN A2	2.66	0.91
ILMN_2337058	PORCN	PORCUPINE HOMOLOG (DROSOPHILA)	2.66	0.91
ILMN_2338963	SLC29A1	SOLUTE CARRIER FAMILY 29 (NUCLEOSIDE TRANSPORTERS), MEMBER 1	2.61	0.91
ILMN_1772824	WNT5B	WINGLESS-TYPE MMTV INTEGRATION SITE FAMILY, MEMBER 5B	2.60	0.91
ILMN_2050183	MYLK2	MYOSIN LIGHT CHAIN KINASE 2, SKELETAL MUSCLE	2.51	0.91
ILMN_2401873	DUSP10	DUAL SPECIFICITY PHOSPHATASE 10	2.39	0.91
ILMN_2082585	SNAI2	SNAIL HOMOLOG 2 (DROSOPHILA)	2.35	0.91
ILMN_1652185	IL4R	INTERLEUKIN 4 RECEPTOR	2.25	0.91
ILMN_1762106	MMP2	MATRIX METALLOPEPTIDASE 2 (GELATINASE A, 72KDA GELATINASE, 72KDA TYPE IV COLLAGENASE)	2.24	0.91
ILMN_1766334	MB	MYOGLOBIN	2.18	0.91
ILMN_1706969	C6orf65	CHROMOSOME 6 OPEN READING FRAME 65	2.14	0.91
ILMN_1815130	MICALL1	MICAL-LIKE 1	2.10	0.91
ILMN_1803811	TRIB1	TRIBBLES HOMOLOG 1 (DROSOPHILA)	2.07	0.91
ILMN_1715684	LAMB3	LAMININ, BETA 3	2.05	0.91
ILMN_2127298	F2RL3	COAGULATION FACTOR II (THROMBIN) RECEPTOR-LIKE 3	2.04	0.91
ILMN_2176502	UNC5B	UNC-5 HOMOLOG B (C. ELEGANS)	2.03	0.91
ILMN_1674160	BIN1	BRIDGING INTEGRATOR 1	2.00	0.91
ILMN_1728049	S100A16	S100 CALCIUM BINDING PROTEIN A16	1.96	0.91
ILMN_1751464	TNFSF9	TUMOR NECROSIS FACTOR (LIGAND) SUPERFAMILY, MEMBER 9	1.96	0.91
ILMN_1807919	TNS1	TENSIN 1	1.94	0.91
ILMN_1772612	ANGPTL2	ANGIOPOIETIN-LIKE 2	1.93	0.91
ILMN_1751161	COL7A1	COLLAGEN, TYPE VII, ALPHA 1 (EPIDERMOLYSIS BULLOSA, DYSTROPHIC, DOMINANT AND RECESSIVE)	1.90	0.91
ILMN_2309245	BIN1	BRIDGING INTEGRATOR 1	1.89	0.91
ILMN_1771627	ZMIZ1	RETINOIC ACID INDUCED 17	1.89	0.91
ILMN_1737163	SH3BGRL3	SH3 DOMAIN BINDING GLUTAMIC ACID-RICH PROTEIN LIKE 3	1.87	0.91
ILMN_1745256	CXXC5	CXXC FINGER 5	1.87	0.91
ILMN_1699651	IL6	INTERLEUKIN 6 (INTERFERON, BETA 2)	1.86	0.91
ILMN_1701204	VEGFC	VASCULAR ENDOTHELIAL GROWTH FACTOR C	1.86	0.91
ILMN_2359287	ITGA6	INTEGRIN, ALPHA 6	1.86	0.91

ILMN_1705750	TGM2	TRANSGLUTAMINASE 2 (C POLYPEPTIDE, PROTEIN-GLUTAMINE-GAMMA-GLUTAMYLTRANSFERASE)	1.84	0.91
ILMN_1668345	OAF	OAF HOMOLOG (DROSOPHILA)	1.82	0.91
ILMN_1700384	KIAA1522	KIAA1522	1.80	0.91
ILMN_1742187	MAN1A1	MANNOSIDASE, ALPHA, CLASS 1A, MEMBER 1	1.77	0.91
ILMN_1787919	PARVB	PARVIN, BETA	1.76	0.91
ILMN_1795342	MLPH	MELANOPHILIN	1.75	0.91
ILMN_1655595	SERPINE2	SERPIN PEPTIDASE INHIBITOR, CLADE E (NEXIN, PLASMINOGEN ACTIVATOR INHIBITOR TYPE 1), MEMBER 2	1.72	0.91
ILMN_2289924	TRAK1	TRAFFICKING PROTEIN, KINESIN BINDING 1	1.69	0.91
ILMN_1682717	IER3	IMMEDIATE EARLY RESPONSE 3	1.68	0.91
ILMN_1732151	COL6A1	COLLAGEN, TYPE VI, ALPHA 1	1.63	0.91
ILMN_1734276	PMEPA1	TRANSMEMBRANE, PROSTATE ANDROGEN INDUCED RNA	5.39	1.70
ILMN_1692335	ELK3	ELK3, ETS-DOMAIN PROTEIN (SRF ACCESSORY PROTEIN 2)	2.42	1.70
ILMN_1790228	FURIN	FURIN (PAIRED BASIC AMINO ACID CLEAVING ENZYME)	2.30	1.70
ILMN_1770467	GAGE7	G ANTIGEN 5	2.22	1.70
ILMN_1714445	SLC6A9	SOLUTE CARRIER FAMILY 6 (NEUROTRANSMITTER TRANSPORTER, GLYCINE), MEMBER 9	2.03	1.70
ILMN_2066151	TEK	TEK TYROSINE KINASE, ENDOTHELIAL (VENOUS MALFORMATIONS, MULTIPLE CUTANEOUS AND MUCOSAL)	1.90	1.70
ILMN_2086077	JUNB	JUN B PROTO-ONCOGENE	2.83	1.96
ILMN_1663454	PKP1	PLAKOPHILIN 1 (ECTODERMAL DYSPLASIA/SKIN FRAGILITY SYNDROME)	2.72	1.96
ILMN_1663080	LFNG	LUNATIC FRINGE HOMOLOG (DROSOPHILA)	2.67	1.96
ILMN_2201596	CYTL1	CYTOKINE-LIKE 1	2.65	1.96
ILMN_1665865	IGFBP4	INSULIN-LIKE GROWTH FACTOR BINDING PROTEIN 4	2.27	1.96
ILMN_1728009	TMEM171	PROLINE-RICH PROTEIN PRP2	1.95	1.96
ILMN_1750711	MYO19	MYOSIN HEAD DOMAIN CONTAINING 1	1.83	1.96
ILMN_1704154	TNFRSF19	TUMOR NECROSIS FACTOR RECEPTOR SUPERFAMILY, MEMBER 19	1.81	1.96
ILMN_1677432	SRGAP1	SLIT-ROBO RHO GTPASE ACTIVATING PROTEIN 1	1.80	1.96
ILMN_1702487	SGK	SERUM/GLUCOCORTICOID REGULATED KINASE	1.76	1.96
ILMN_1761540	SEMA3F	SEMA DOMAIN, IMMUNOGLOBULIN DOMAIN (IG), SHORT BASIC DOMAIN, SECRETED, (SEMAPHORIN) 3F	1.72	1.96
ILMN_2386100	BUB3	BUB3 BUDDING UNINHIBITED BY BENZIMIDAZOLES 3 HOMOLOG (YEAST)	1.65	1.96
ILMN_1729596	C14orf151	CHROMOSOME 14 OPEN READING FRAME 151	1.59	1.96
ILMN_2309156	PMEPA1	TRANSMEMBRANE, PROSTATE ANDROGEN INDUCED RNA	5.53	2.36
ILMN_1675453	HHIP	HEDGEHOG INTERACTING PROTEIN	3.42	2.36
ILMN_1661194	CLDN14	CLAUDIN 14	3.40	2.36
ILMN_2203891	SMAD7	SMAD, MOTHERS AGAINST DPP HOMOLOG 7 (DROSOPHILA)	2.30	2.36
ILMN_1685699	PRSS3	PROTEASE, SERINE, 3 (MESOTRYPSIN)	2.16	2.36
ILMN_1744268	PLEC1	PLECTIN 1, INTERMEDIATE FILAMENT BINDING PROTEIN 500KDA	2.13	2.36
ILMN_1671142	GPR68	G PROTEIN-COUPLED RECEPTOR 68	1.78	2.36
ILMN_1792014	FAM70B	FAMILY WITH SEQUENCE SIMILARITY 70, MEMBER B	1.77	2.36
ILMN_1700690	VAT1	VESICLE AMINE TRANSPORT PROTEIN 1 HOMOLOG (T CALIFORNICA)	1.72	2.36
ILMN_1696360	CTSB	CATHEPSIN B	1.72	2.36
ILMN_1694432	CRIP2	CYSTEINE-RICH PROTEIN 2	1.67	2.36
ILMN_1666306	SRRD	SIMILAR TO SRR1-LIKE PROTEIN	1.66	2.36
ILMN_1712545	S100A3	S100 CALCIUM BINDING PROTEIN A3	3.31	2.52
ILMN_1741917	OSCAR	OSTEOCLAST-ASSOCIATED RECEPTOR	2.55	2.52
ILMN_1729455	EML1	ECHINODERM MICROTUBULE ASSOCIATED PROTEIN LIKE 1	2.28	2.52
ILMN_1666924	PINK1	PTEN INDUCED PUTATIVE KINASE 1	2.27	2.52
ILMN_1750664	PPT2	PALMITOYL-PROTEIN THIOESTERASE 2	2.19	2.52
ILMN_2308338	BMF	BCL2 MODIFYING FACTOR	1.95	2.52
ILMN_1669362	IGFBP6	INSULIN-LIKE GROWTH FACTOR BINDING PROTEIN 6	1.83	2.52
ILMN_1711566	TIMP1	TIMP METALLOPEPTIDASE INHIBITOR 1	1.83	2.52
ILMN_1656837	RBP1	RETINOL BINDING PROTEIN 1, CELLULAR	1.81	2.52

ILMN_2340052	NCOR2	NUCLEAR RECEPTOR CO-REPRESSOR 2	1.79	2.52
ILMN_2367258	SMOX	SPERMINE OXIDASE	1.73	2.52
ILMN_2082244	FOXK1	FORKHEAD BOX K1	1.50	2.52
ILMN_1658709	LAMB1	LAMININ, BETA 1	1.46	2.52
ILMN_1700448	SIM2	SINGLE-MINDED HOMOLOG 2 (DROSOPHILA)	2.13	2.65
ILMN_2111932	SERINC2	SERINE INCORPORATOR 2	1.90	2.65
ILMN_1654563	EFNB1	EPHRIN-B1	1.87	2.65
ILMN_2129161	LRRC32	LEUCINE RICH REPEAT CONTAINING 32	2.11	2.89
ILMN_2408576	FAM129B	CHROMOSOME 9 OPEN READING FRAME 88	2.04	2.89
ILMN_1713499	WISP1	WNT1 INDUCIBLE SIGNALING PATHWAY PROTEIN 1	1.91	2.89
ILMN_2365307	CD276	CD276 ANTIGEN	1.75	2.89
ILMN_1652413	UCN2	UROCORTIN 2	2.50	3.37
ILMN_1789358	ZNF628	ZINC FINGER PROTEIN 628	2.20	3.37
ILMN_1707434	LOC653778	SIMILAR TO SOLUTE CARRIER FAMILY 25, MEMBER 37	2.20	3.37
ILMN_1716265	PGM2L1	PHOSPHOGLUCOMUTASE 2-LIKE 1	2.08	3.37
ILMN_1807169	TINAGL1	TUBULOINTERSTITIAL NEPHRITIS ANTIGEN-LIKE 1	2.03	3.37
ILMN_1803686	ADA	ADENOSINE DEAMINASE	1.84	3.37
ILMN_1704353	IGSF3	IMMUNOGLOBULIN SUPERFAMILY, MEMBER 3	1.77	3.37
ILMN_2110561	IFNA8	INTERFERON, ALPHA 8	1.72	3.37
ILMN_1695432	TPST2	TYROSYLPROTEIN SULFOTRANSFERASE 2	1.72	3.37
ILMN_1661755	FAM129B	CHROMOSOME 9 OPEN READING FRAME 88	1.67	3.37
ILMN_1731736	RIN3	RAS AND RAB INTERACTOR 3	1.56	3.37
ILMN_1793302	WDR4	WD REPEAT DOMAIN 4	1.54	3.37
ILMN_1774547	M-RIP	MYOSIN PHOSPHATASE-RHO INTERACTING PROTEIN	1.39	3.37
ILMN_1687721	PROC	PROTEIN C (INACTIVATOR OF COAGULATION FACTORS VA AND VIIIA)	4.03	3.54
ILMN_2188722	GLS	GLUTAMINASE	2.75	3.54
ILMN_1743367	FZD4	FRIZZLED HOMOLOG 4 (DROSOPHILA)	2.67	3.54
ILMN_1676689	PPT2	PALMITOYL-PROTEIN THIOESTERASE 2	2.39	3.54
ILMN_1677273	TH	TYROSINE HYDROXYLASE	2.22	3.54
ILMN_2383611	PTPRE	PROTEIN TYROSINE PHOSPHATASE, RECEPTOR TYPE, E	2.15	3.54
ILMN_1743966	BCL9L	B-CELL CLL/LYMPHOMA 9-LIKE	2.13	3.54
ILMN_2098643	FADS3	FATTY ACID DESATURASE 3	1.85	3.54
ILMN_1752046	SH2B3	LYMPHOCYTE ADAPTOR PROTEIN	1.83	3.54
ILMN_1698419	NCOR2	NUCLEAR RECEPTOR CO-REPRESSOR 2	1.82	3.54
ILMN_1719236	CDH5	CADHERIN 5, TYPE 2, VE-CADHERIN (VASCULAR EPITHELIUM)	1.78	3.54
ILMN_1703955	FBXO32	F-BOX PROTEIN 32	1.77	3.54
ILMN_1796755	ITGB5	INTEGRIN, BETA 5	1.75	3.54
ILMN_2214910	EPHB4	EPH RECEPTOR B4	1.66	3.54
ILMN_2318638	TGIF1	TGFB-INDUCED FACTOR (TALE FAMILY HOMEOBOX)	1.46	3.54
ILMN_2357134	SPHK1	SPHINGOSINE KINASE 1	2.59	4.47
ILMN_1766159	MIER2	KIAA1193	2.53	4.47
ILMN_2415157	ARID5A	AT RICH INTERACTIVE DOMAIN 5A (MRF1-LIKE)	2.44	4.47
ILMN_1672295	ZC3H12A	ZINC FINGER CCCH-TYPE CONTAINING 12A	2.27	4.47
ILMN_1745964	IRAK2	INTERLEUKIN-1 RECEPTOR-ASSOCIATED KINASE 2	2.02	4.47
ILMN_1691376	JAG1	JAGGED 1 (ALAGILLE SYNDROME)	1.87	4.47
ILMN_2096719	GRK5	G PROTEIN-COUPLED RECEPTOR KINASE 5	1.85	4.47
ILMN_1758542	BMP1	BONE MORPHOGENETIC PROTEIN 1	1.83	4.47
ILMN_1702363	SULF1	SULFATASE 1	1.75	4.47
ILMN_1754660	C10orf56	CHROMOSOME 10 OPEN READING FRAME 56	1.75	4.47
ILMN_1671404	SVIL	SUPERVILLIN	1.73	4.47
ILMN_1697559	G6PD	GLUCOSE-6-PHOSPHATE DEHYDROGENASE	1.72	4.47
ILMN_1735052	ULK1	UNC-51-LIKE KINASE 1 (C. ELEGANS)	1.65	4.47
ILMN_1742450	TAPBP	TAP BINDING PROTEIN (TAPASIN)	1.54	4.47

ILMN_2374340	PLAUR	PLASMINOGEN ACTIVATOR, UROKINASE RECEPTOR	1.39	4.47
ILMN_2212878	ESM1	ENDOTHELIAL CELL-SPECIFIC MOLECULE 1	9.92	4.71
ILMN_1722726	RICS	RHO GTPASE-ACTIVATING PROTEIN	2.94	4.71
ILMN_1741404	MSC	MUSCULIN (ACTIVATED B-CELL FACTOR-1)	2.49	4.71
ILMN_1803825	CXCL12	CHEMOKINE (C-X-C MOTIF) LIGAND 12 (STROMAL CELL-DERIVED FACTOR 1)	2.31	4.71
ILMN_2376403	TSC22D3	TSC22 DOMAIN FAMILY, MEMBER 3	2.20	4.71
ILMN_1655740	SNAI2	SNAIL HOMOLOG 2 (DROSOPHILA)	2.19	4.71
ILMN_1789505	ITPR1	INOSITOL 1,4,5-TRIPHOSPHATE RECEPTOR, TYPE 1	2.12	4.71
ILMN_1659913	ISG20	INTERFERON STIMULATED EXONUCLEASE GENE 20KDA	2.08	4.71
ILMN_1656940	ABLIM3	ACTIN BINDING LIM PROTEIN FAMILY, MEMBER 3	2.01	4.71
ILMN_1714592	CDA	CYTIDINE DEAMINASE	1.93	4.71
ILMN_1687301	VCAN	CHONDROITIN SULFATE PROTEOGLYCAN 2 (VERSICAN)	1.90	4.71
ILMN_1772821	KIAA1671	KIAA1671 PROTEIN	1.77	4.71
ILMN_1756676	PHF19	PHD FINGER PROTEIN 19	1.75	4.71
ILMN_1724059	GAS2L1	GROWTH ARREST-SPECIFIC 2 LIKE 1	1.71	4.71
ILMN_1795442	LAMA4	LAMININ, ALPHA 4	1.68	4.71
ILMN_2064606	TBC1D2B	TBC1 DOMAIN FAMILY, MEMBER 2B	1.57	4.71
ILMN_1766359	GATAD2B	GATA ZINC FINGER DOMAIN CONTAINING 2B	1.52	4.71
ILMN_1803277	MVP	MAJOR VAULT PROTEIN	1.42	4.71
ILMN_1664434	TCF3	TRANSCRIPTION FACTOR 3 (E2A IMMUNOGLOBULIN ENHANCER BINDING FACTORS E12/E47)	1.42	4.71
ILMN_1794598	SCHIP1	SCHWANNOMIN INTERACTING PROTEIN 1	1.40	4.71
ILMN_1795325	ACTG2	actin, gamma 2, smooth muscle, enteric	-3.23	0.00
ILMN_1671703	ACTA2	actin, alpha 2, smooth muscle, aorta	-3.03	0.00
ILMN_2354478	CYFIP2	cytoplasmic FMR1 interacting protein 2	-1.85	1.96
ILMN_1785284	ALDH6A1	aldehyde dehydrogenase 6 family, member A1	-2.22	2.65
ILMN_1725726	DHRS2	dehydrogenase/reductase (SDR family) member 2	-2.33	2.65
ILMN_1763382	NPPB	natriuretic peptide precursor B	-3.85	2.65

6.3 Appendix table 8. Effects of over-expression of GPR30 in HMEC-1 cells upon FSS

Table 14: Deregulated genes in HMEC-1 cells over-expressing GPR30 upon FSS

Change ratios (*x*-fold changes) are indicated in the column Ratio and *q* values at a 'false discovery' rate (FDR) of < 5%.

ILLUMINA_ID	Gene ID	Gene Name	Ratio	q-value(%)
ILMN_1766264	PI16	peptidase inhibitor 16	13.61	0.00
ILMN_1787186	NOV	nephroblastoma overexpressed gene	6.25	0.00
ILMN_1802205	RHOB	ras homolog gene family, member B	4.33	0.00
ILMN_1738742	PLAT	plasminogen activator, tissue	4.25	0.00
ILMN_1696048	C13orf33	chromosome 13 open reading frame 33	3.57	0.00
ILMN_1692177	TSC22D1	TSC22 domain family, member 1	3.55	0.00
ILMN_1763837	ANPEP	alanyl (membrane) aminopeptidase	3.49	0.00
ILMN_1745132	GDF11	growth differentiation factor 11	3.46	0.00
ILMN_2150851	SERPINB2	serpin peptidase inhibitor, clade B (ovalbumin), member 2	3.40	0.00
ILMN_1844408	PLXNA2	plexin A2	3.34	0.00
ILMN_2413158	PODXL	podocalyxin-like	3.17	0.00
ILMN_2137789	KLF4	Kruppel-like factor 4 (gut)	3.13	0.00
ILMN_2276952	TSC22D3	TSC22 domain family, member 3; GRAM domain containing 4	2.03	0.00
ILMN_1807147	RC3H1	ring finger and CCCH-type zinc finger domains 1	1.82	0.00
ILMN_1681724	FPGS	folylpolyglutamate synthase	1.60	0.00
ILMN_1717101	MINK1	misshapen-like kinase 1 (zebrafish)	1.33	0.00
ILMN_1675546	KRTAP27-1	keratin associated protein 27-1	1.31	0.00
ILMN_1720243	IL25	interleukin 25	1.27	0.00
ILMN_1749304	LOC643389		1.19	0.00
ILMN_1747314	MYO5B	similar to acetyl-Coenzyme A acyltransferase 2 (mitochondrial 3-oxoacyl-Coenzyme A thiolase);	1.16	0.00
ILMN_1716857	LOC649762		1.12	0.00
ILMN_1662016	SCRN2	secernin 2	1.01	0.00
ILMN_2314169	PTHLH	parathyroid hormone-like hormone	5.47	1.05
ILMN_2376403	TSC22D3	TSC22 domain family, member 3; GRAM domain containing 4	3.63	1.05
ILMN_2189027	LIPG	lipase, endothelial	3.43	1.05
ILMN_2307861	COL6A3	collagen, type VI, alpha 3	3.10	1.05
ILMN_1684306	S100A4	S100 calcium binding protein A4	3.08	1.05
ILMN_1759787	THBD	thrombomodulin	2.94	1.05
ILMN_1765446	EMP3	epithelial membrane protein 3	2.93	1.05
ILMN_2363591	SDCBP	syndecan binding protein (syntenin)	2.91	1.05
ILMN_1709674	GFPT2	glutamine-fructose-6-phosphate transaminase 2	2.91	1.05
ILMN_1913060		chemokine-like receptor 1	2.90	1.05
ILMN_1787813	SLC5A3	solute carrier family 5 (sodium/myo-inositol cotransporter), member 3	2.85	1.05
ILMN_1726448	MMP1	matrix metallopeptidase 1 (interstitial collagenase)	2.82	1.05
ILMN_1701461	TIMP3	TIMP metallopeptidase inhibitor 3	2.80	1.05
ILMN_1708363	LOXL1	lysyl oxidase-like 1	2.77	1.05
ILMN_1791679	DNER	delta/notch-like EGF repeat containing	2.72	1.05
ILMN_1712545	S100A3	S100 calcium binding protein A3	2.70	1.05
ILMN_1665660	C11orf17	chromosome 11 open reading frame 17	2.70	1.05
ILMN_1706643	COL6A3	collagen, type VI, alpha 3	2.67	1.05
ILMN_2215119	SYNJ2	synaptojanin 2	2.61	1.05

ILMN_2384122	GPR56	G protein-coupled receptor 56	2.61	1.05
ILMN_1665449	ROBO4	roundabout homolog 4, magic roundabout (Drosophila)	2.56	1.05
ILMN_1673113	F2RL1	coagulation factor II (thrombin) receptor-like 1	2.56	1.05
ILMN_2111237	MN1	meningioma (disrupted in balanced translocation) 1	2.48	1.05
ILMN_2329927	ABCG1	ATP-binding cassette, sub-family G (WHITE), member 1	2.45	1.05
ILMN_1756595	SH3TC1	SH3 domain and tetratricopeptide repeats 1	2.42	1.05
ILMN_1657111	C14orf78	AHNAK nucleoprotein 2	2.41	1.05
ILMN_1715863	MLKL	mixed lineage kinase domain-like	2.36	1.05
ILMN_1774685	IL24	interleukin 24	2.31	1.05
ILMN_2310896	NLRP3	NLR family, pyrin domain containing 3	2.27	1.05
ILMN_1732197	MN1	meningioma (disrupted in balanced translocation) 1	2.26	1.05
ILMN_1735930	KLF2	Kruppel-like factor 2 (lung)	2.24	1.05
ILMN_1722294	CPNE8	copine VIII	2.24	1.05
ILMN_1758067	RGS4	regulator of G-protein signaling 4	2.20	1.05
ILMN_1689037	LIPG	lipase, endothelial	2.17	1.05
ILMN_1748751	NLF2	family with sequence similarity 148, member B	2.08	1.05
ILMN_1749944	DLGAP4	discs, large (Drosophila) homolog-associated protein 4	2.08	1.05
ILMN_1757825	ZNF230	zinc finger protein 230	2.03	1.05
ILMN_2169983	ATAD1	ATPase family, AAA domain containing 1	2.00	1.05
ILMN_1808537	LOC339977	leucine rich repeat containing 66	1.99	1.05
ILMN_1839422	JRK	jerky homolog (mouse)	1.98	1.05
ILMN_2313946	CPNE7	copine VII	1.94	1.05
ILMN_1801923	ATF1	activating transcription factor 1	1.91	1.05
ILMN_1662895	C14orf153	chromosome 14 open reading frame 153	1.91	1.05
ILMN_1669928	ARHGEF16	Rho guanine exchange factor (GEF) 16	1.89	1.05
ILMN_1671913	HTF9C	TRM2 tRNA methyltransferase 2 homolog A (S. cerevisiae)	1.88	1.05
ILMN_1693941	IGSF9	immunoglobulin superfamily, member 9	1.86	1.05
ILMN_1692967	AXIN1	axin 1	1.84	1.05
ILMN_2197750	LOC728137	testis specific protein, Y-linked 3; testis specific protein, Y-linked 2; testis specific protein, Y-linked 1; testis specific protein, Y-linked pseudogene 7	1.82	1.05
ILMN_2412849	SLC5A10	solute carrier family 5 (sodium/glucose cotransporter), member 10	1.80	1.05
ILMN_1657589	LOC644650		1.79	1.05
ILMN_1676844	NR1D2	nuclear receptor subfamily 1, group D, member 2	1.75	1.05
ILMN_1746359	RERG	RAS-like, estrogen-regulated, growth inhibitor	1.73	1.05
ILMN_1713813	LOC400578	keratin 16; keratin type 16-like	1.73	1.05
ILMN_1669692	IKZF3	IKAROS family zinc finger 3 (Aiolos)	1.71	1.05
ILMN_2322747	ARHGAP5	Rho GTPase activating protein 5	1.68	1.05
ILMN_1658243	PSD3	pleckstrin and Sec7 domain containing 3	1.62	1.05
ILMN_1713471	ENOX1	ecto-NOX disulfide-thiol exchanger 1	1.61	1.05
ILMN_2154115	PSD4	pleckstrin and Sec7 domain containing 4	1.58	1.05
ILMN_1689852	PAQR6	progestin and adipoQ receptor family member VI	1.54	1.05
ILMN_1800445	NEK10	NIMA (never in mitosis gene a)- related kinase 10	1.50	1.05
ILMN_2401033	GOSR1	golgi SNAP receptor complex member 1	1.49	1.05
ILMN_1762151	LOC126520	polo-like kinase 5 pseudogene	1.49	1.05
ILMN_1775423	C10orf88	chromosome 10 open reading frame 88	1.48	1.05
ILMN_1772890	C9orf57	chromosome 9 open reading frame 57	1.46	1.05
ILMN_2316278	MAGED4B	melanoma antigen family D, 4B; melanoma antigen family D, 4	1.45	1.05
ILMN_1748840	CALB2	calbindin 2	1.41	1.05
ILMN_1768600	LOC652264		1.29	1.05
ILMN_1677197	RARA	retinoic acid receptor, alpha	1.13	1.05
ILMN_1769201	ELF3	E74-like factor 3 (ets domain transcription factor, epithelial-specific)	4.58	2.52
ILMN_1810864	PMP22	peripheral myelin protein 22	3.60	2.52

ILMN_2409451	NCKAP1	NCK-associated protein 1	3.51	2.52
ILMN_1713124	AKR1C3	aldo-keto reductase family 1, member C3 (3-alpha hydroxysteroid dehydrogenase, type II)	3.48	2.52
ILMN_1665035	KRT14	keratin 14	3.19	2.52
ILMN_1676719	LOC644330	tropomyosin 3 pseudogene	3.16	2.52
ILMN_1802646	EPHB6	EPH receptor B6	2.98	2.52
ILMN_1689431	APCDD1L	adenomatosis polyposis coli down-regulated 1-like	2.91	2.52
ILMN_1669046	FOXQ1	forkhead box Q1	2.76	2.52
ILMN_1748124	TSC22D3	TSC22 domain family, member 3; GRAM domain containing 4	2.70	2.52
ILMN_1796423	CLIC3	chloride intracellular channel 3	2.65	2.52
ILMN_1794442	ZNF469	zinc finger protein 469	2.56	2.52
ILMN_2041190	F2RL1	coagulation factor II (thrombin) receptor-like 1	2.49	2.52
ILMN_1711311	PODXL	podocalyxin-like	2.46	2.52
ILMN_1724138	HTATIP	K(lysine) acetyltransferase 5	2.46	2.52
ILMN_2370976	FER1L3	myoferlin	2.44	2.52
ILMN_2348788	CD44	CD44 molecule (Indian blood group)	2.40	2.52
ILMN_1705032	SEH1L	SEH1-like (S. cerevisiae)	2.39	2.52
ILMN_1762529	SLC12A8	solute carrier family 12 (potassium/chloride transporters), member 8	2.36	2.52
ILMN_1663417	C22orf33	chromosome 22 open reading frame 33	2.34	2.52
ILMN_1693338	CYP1B1	cytochrome P450, family 1, subfamily B, polypeptide 1	2.31	2.52
ILMN_1811426	TMTC1	transmembrane and tetratricopeptide repeat containing 1	2.30	2.52
ILMN_1670215	FLJ46836	FLJ46836 protein	2.29	2.52
ILMN_2401873	DUSP10	dual specificity phosphatase 10	2.27	2.52
ILMN_1738589	MGLL	monoglyceride lipase	2.20	2.52
ILMN_1785141	MICAL2	microtubule associated monoxygenase, calponin and LIM domain containing 2	2.18	2.52
ILMN_1805466	SOX9	SRY (sex determining region Y)-box 9	2.13	2.52
ILMN_2113490	NTN4	netrin 4	2.12	2.52
ILMN_1775501	IL1B	interleukin 1, beta	2.10	2.52
ILMN_1695773	STK24	serine/threonine kinase 24 (STE20 homolog, yeast)	2.07	2.52
ILMN_2229877	PCDH18	protocadherin 18	2.04	2.52
ILMN_2066151	TEK	TEK tyrosine kinase, endothelial	2.01	2.52
ILMN_1714057	FCN2	ficolin (collagen/fibrinogen domain containing lectin) 2 (hucolin)	1.99	2.52
ILMN_1675222	PLXND1	plexin D1	1.97	2.52
ILMN_1799098	LOC652846		1.91	2.52
ILMN_2361181	C1QTNF6	C1q and tumor necrosis factor related protein 6	1.89	2.52
ILMN_2229922	C12orf35	chromosome 12 open reading frame 35	1.89	2.52
ILMN_1659856	C1orf90	family with sequence similarity 167, member B	1.82	2.52
ILMN_2387385	IGFBP1	insulin-like growth factor binding protein 1	1.74	2.52
ILMN_1693452	GAL3ST4	galactose-3-O-sulfotransferase 4	1.72	2.52
ILMN_1776656	BBS7	Bardet-Biedl syndrome 7	1.67	2.52
ILMN_2200562	LOC595101	PI-3-kinase-related kinase SMG-1 pseudogene	1.66	2.52
ILMN_1785768	PDE4A	phosphodiesterase 4A, cAMP-specific (phosphodiesterase E2 dunce homolog, Drosophila)	1.65	2.52
ILMN_1802248	RNF152	ring finger protein 152	1.65	2.52
ILMN_2358382	ZFYVE1	zinc finger, FYVE domain containing 1	1.63	2.52
ILMN_1671004	POLG2	polymerase (DNA directed), gamma 2, accessory subunit	1.62	2.52
ILMN_1742032	CCDC144A	coiled-coil domain containing 144B; coiled-coil domain containing 144A; coiled-coil domain containing 144C	1.60	2.52
ILMN_1701700	KLHL4	kelch-like 4 (Drosophila)	1.57	2.52
ILMN_1658636	MRE11A	MRE11 meiotic recombination 11 homolog A (S. cerevisiae)	1.57	2.52
ILMN_1794156	DYRK1A	dual-specificity tyrosine-(Y)-phosphorylation regulated kinase 1A	1.55	2.52
ILMN_1814002	TEAD3	TEA domain family member 3	1.52	2.52
ILMN_1805148	C2orf63	chromosome 2 open reading frame 63	1.51	2.52

ILMN_1808715	LOC389300	similar to hCG1654959	1.50	2.52
ILMN_1736068	CNOT8	CCR4-NOT transcription complex, subunit 8	1.50	2.52
ILMN_1782679	AHRR	aryl-hydrocarbon receptor repressor; programmed cell death 6	1.48	2.52
ILMN_1675687	LOC644701		1.46	2.52
ILMN_1793621	ZFYVE27	zinc finger, FYVE domain containing 27	1.44	2.52
ILMN_1706644	BDNF	brain-derived neurotrophic factor	1.42	2.52
ILMN_1710495	PAPLN	papilin, proteoglycan-like sulphated glycoprotein	1.42	2.52
ILMN_1738707	S100A13	S100 calcium binding protein A13	1.42	2.52
ILMN_1731175	XKR6	XK, Kell blood group complex subunit-related family, member 6	1.41	2.52
ILMN_1681824	LOC652294		1.41	2.52
ILMN_1678862	FUT11	fucosyltransferase 11 (alpha (1,3) fucosyltransferase)	1.41	2.52
ILMN_1730809	SLC29A2	solute carrier family 29 (nucleoside transporters), member 2	1.41	2.52
ILMN_1656647	LOC649944		1.40	2.52
ILMN_1724234	TRPV1	transient receptor potential cation channel, subfamily V, member 1	1.39	2.52
ILMN_1673129	PCDH12	protocadherin 12	1.38	2.52
ILMN_1722532	JMJD1A	lysine (K)-specific demethylase 3A	1.37	2.52
ILMN_1781656	SCGB1D1	secretoglobin, family 1D, member 1	1.35	2.52
ILMN_1807050	SHC4	SHC (Src homology 2 domain containing) family, member 4	1.34	2.52
ILMN_1736682	SPSB4	splA/ryanodine receptor domain and SOCS box containing 4	1.31	2.52
ILMN_2401770	PHF14	PHD finger protein 14	1.30	2.52
ILMN_1720452	LONRF3	LON peptidase N-terminal domain and ring finger 3	1.29	2.52
ILMN_2399016	MMP28	matrix metallopeptidase 28	1.29	2.52
ILMN_1713013	PLD3	phospholipase D family, member 3	1.29	2.52
ILMN_1655537	ING1	inhibitor of growth family, member 1	1.28	2.52
ILMN_1768637	TNNI3	troponin I type 3 (cardiac)	1.28	2.52
ILMN_1702183	LOC613266	hypothetical LOC613266	1.28	2.52
ILMN_1723004	CD72	CD72 molecule	1.27	2.52
ILMN_1675819	FAM101A	family with sequence similarity 101, member A	1.27	2.52
ILMN_2211583	KIAA1279	KIAA1279	1.24	2.52
ILMN_1729225	SORCS2	sortilin-related VPS10 domain containing receptor 2	1.23	2.52
ILMN_1802550	PCSK6	proprotein convertase subtilisin/kexin type 6	1.22	2.52
ILMN_1783827	LOC649397		1.21	2.52
ILMN_1758597	NAGS	N-acetylglutamate synthase	1.21	2.52
ILMN_1712798	ZNF608	zinc finger protein 608	1.21	2.52
ILMN_1652525	FAM125B	family with sequence similarity 125, member B	1.20	2.52
ILMN_1792635	LOC654253		1.19	2.52
ILMN_1691697	C20orf38	serine palmitoyltransferase, long chain base subunit 3	1.18	2.52
ILMN_1763673	LOC651212		1.18	2.52
ILMN_1670959	CEACAM5	carcinoembryonic antigen-related cell adhesion molecule 5	1.14	2.52
ILMN_2338038	AK3L1	adenylate kinase 3-like 2; adenylate kinase 3-like 1	1.14	2.52
ILMN_1798837	PTPN20B	protein tyrosine phosphatase, non-receptor type 20B; protein tyrosine phosphatase, non-receptor type 20A	1.14	2.52
ILMN_1893532		hypothetical protein LOC285796	1.13	2.52
ILMN_2041648	TMPRSS7	transmembrane protease, serine 7	1.12	2.52
ILMN_1793630	SLC4A3	solute carrier family 4, anion exchanger, member 3	1.11	2.52
ILMN_1729369	FGFR1	fibroblast growth factor receptor 1	1.10	2.52
ILMN_2181748	PA2G4P4	proliferation-associated 2G4, 38kDa; proliferation-associated 2G4 pseudogene 4	1.09	2.52
ILMN_1704332	LOC654147		1.08	2.52
ILMN_1659327	LOC283683	hypothetical protein LOC283683	1.08	2.52
ILMN_1796626	LOC283152	coiled-coil domain containing 153	1.08	2.52
ILMN_1764605	FGF6	fibroblast growth factor 6	1.07	2.52
ILMN_2108699	IL2RA	interleukin 2 receptor, alpha	1.07	2.52

ILMN_1690846	LOC642412		1.07	2.52
ILMN_1764496	LOC648476		1.06	2.52
ILMN_1783427	LOC641975		1.06	2.52
ILMN_1787897	CXCL1	chemokine (C-X-C motif) ligand 1 (melanoma growth stimulating activity, alpha)	1.02	2.52
ILMN_1707686	LOC646713		1.02	2.52
ILMN_1795325	ACTG2	actin, gamma 2, smooth muscle, enteric	-3.45	0
ILMN_1671703	ACTA2	actin, alpha 2, smooth muscle, aorta	-3.70	0
ILMN_1763382	NPPB	natriuretic peptide precursor B	-7.14	0

6.4 Appendix table 10. Effects of over-expression of PATJ in HMEC-1 cells upon FSS

Table 15: Deregulated genes in HMEC-1 cells over-expressing PATJ upon FSS

Change ratios (*x*-fold changes) are indicated in the column Ratio and *q* values at a 'false discovery' rate (FDR) of < 5%.

Illumina ID	Gene ID	Gene Name	Ratio	q-value(%)
ILMN_1766264	PI16	peptidase inhibitor 16	6.11	0.00
ILMN_1787186	NOV	nephroblastoma overexpressed gene	4.97	0.00
ILMN_1802205	RHOB	ras homolog gene family, member B	3.29	0.00
ILMN_2189027	LIPG	lipase, endothelial	3.21	0.00
ILMN_2307861	COL6A3	collagen, type VI, alpha 3	3.11	0.00
ILMN_1799575	IL19	interleukin 19	3.11	0.00
ILMN_1738742	PLAT	plasminogen activator, tissue	3.03	0.00
ILMN_2137789	KLF4	Kruppel-like factor 4 (gut)	3.01	0.00
ILMN_1665035	KRT14	keratin 14	2.97	0.00
ILMN_1844408	PLXNA2	plexin A2	2.94	0.00
ILMN_1763837	ANPEP	alanyl (membrane) aminopeptidase	2.80	0.00
ILMN_2314169	PTHLH	parathyroid hormone-like hormone	2.79	0.00
ILMN_2150851	SERPINB2	serpin peptidase inhibitor, clade B (ovalbumin), member 2	2.75	0.00
ILMN_1659856	C1orf90	family with sequence similarity 167, member B	2.71	0.00
ILMN_1696048	C13orf33	chromosome 13 open reading frame 33	2.69	0.00
ILMN_2043306	EPB41L5	erythrocyte membrane protein band 4.1 like 5	2.59	0.00
ILMN_1765446	EMP3	epithelial membrane protein 3	2.51	0.00
ILMN_1709674	GFPT2	glutamine-fructose-6-phosphate transaminase 2	2.45	0.00
ILMN_2413158	PODXL	podocalyxin-like	2.44	0.00
ILMN_1735930	KLF2	Kruppel-like factor 2 (lung)	2.44	0.00
ILMN_1694755	FSD1	fibronectin type III and SPRY domain containing 1	2.36	0.00
ILMN_1737406	KLF6	Kruppel-like factor 6	2.27	0.00
ILMN_1736760	KRT16	keratin 16; keratin type 16-like	2.24	0.00
ILMN_1711311	PODXL	podocalyxin-like	2.14	0.00
ILMN_2401878	DUSP10	dual specificity phosphatase 10	2.00	0.00
ILMN_1797972	C2orf65	chromosome 2 open reading frame 65	1.82	0.00
ILMN_1669046	FOXQ1	forkhead box Q1	2.49	2.31
ILMN_1657111	C14orf78	AHNAK nucleoprotein 2	2.48	2.31
ILMN_1680814	EDN2	endothelin 2	2.28	2.31
ILMN_1653504	EDG1	sphingosine-1-phosphate receptor 1	2.27	2.31
ILMN_1748881	MRAS	muscle RAS oncogene homolog	2.24	2.31
ILMN_1775501	IL1B	interleukin 1, beta	2.20	2.31
ILMN_1701461	TIMP3	TIMP metallopeptidase inhibitor 3	2.10	2.31
ILMN_1778683	RTN4RL1	reticulon 4 receptor-like 1	1.93	2.31
ILMN_1756595	SH3TC1	SH3 domain and tetratricopeptide repeats 1	1.89	2.31
ILMN_1712230	LOC731035	IQ motif and Sec7 domain 3; similar to IQ motif and Sec7 domain-containing protein 3; similar to IQ motif and SEC7 domain-containing protein 3; similar to IQ motif and Sec7 domain 3	1.67	2.31
ILMN_1670535	NDRG2	NDRG family member 2	1.31	2.31
ILMN_2376403	TSC22D3	TSC22 domain family, member 3; GRAM domain containing 4	2.85	2.44
ILMN_2276952	TSC22D3	TSC22 domain family, member 3; GRAM domain containing 4	2.34	2.44
ILMN_1695475	SEMA3C	sema domain, immunoglobulin domain (Ig), short basic domain, secreted, (semaphorin) 3C	2.21	2.44
ILMN_1802646	EPHB6	EPH receptor B6	2.20	2.44
ILMN_1693515	EGFL8	EGF-like-domain, multiple 8	2.15	2.44

ILMN_2092589	FAM5C	family with sequence similarity 5, member C	2.08	2.44
ILMN_2386040	MYO19	myosin XIX	1.96	2.44
ILMN_2329927	ABCG1	ATP-binding cassette, sub-family G (WHITE), member 1	1.96	2.44
ILMN_1732197	MN1	meningioma (disrupted in balanced translocation) 1	1.94	2.44
ILMN_1687567	CUX1	cut-like homeobox 1	1.74	2.44
ILMN_1724234	TRPV1	transient receptor potential cation channel, subfamily V, member 1	2.54	2.91
ILMN_1689431	APCDD1L	adenomatosis polyposis coli down-regulated 1-like	2.44	2.91
ILMN_1673113	F2RL1	coagulation factor II (thrombin) receptor-like 1	2.33	2.91
ILMN_2261379	SRGAP2	SLIT-ROBO Rho GTPase activating protein 2	2.26	2.91
ILMN_1665374	COL9A1	collagen, type IX, alpha 1	2.11	2.91
ILMN_1769201	ELF3	E74-like factor 3 (ets domain transcription factor, epithelial-specific)	2.02	2.91
ILMN_1772359	LAPTM5	lysosomal multispanning membrane protein 5	2.01	2.91
ILMN_1787567	TSC22D1	TSC22 domain family, member 1	2.01	2.91
ILMN_1713471	ENOX1	ecto-NOX disulfide-thiol exchanger 1	2.37	4.55
ILMN_2041190	F2RL1	coagulation factor II (thrombin) receptor-like 1	2.33	4.55
ILMN_1712545	S100A3	S100 calcium binding protein A3	2.23	4.55
ILMN_1693338	CYP1B1	cytochrome P450, family 1, subfamily B, polypeptide 1	2.17	4.55
ILMN_1811426	TMTC1	transmembrane and tetratricopeptide repeat containing 1	2.09	4.55
ILMN_2384122	GPR56	G protein-coupled receptor 56	2.04	4.55
ILMN_2215119	SYNJ2	synaptojanin 2	1.94	4.55
ILMN_1784287	TGFBR3	transforming growth factor, beta receptor III	1.88	4.55
ILMN_1778876	KIAA0423	family with sequence similarity 179, member B	1.81	4.55
ILMN_1675819	FAM101A	family with sequence similarity 101, member A	1.68	4.55
ILMN_1748614	RELT	RELT tumor necrosis factor receptor	1.54	4.55
ILMN_1692177	TSC22D1	TSC22 domain family, member 1	2.44	4.85
ILMN_2380453	USP45	ubiquitin specific peptidase 45	1.70	4.85
ILMN_1759622	G3BP2	GTPase activating protein (SH3 domain) binding protein 2	1.69	4.85

6.5 Appendix table 12. Effects of over-expression of GPR30 and PATJ in HMEC-1 cells upon FSS

Table 16: Deregulated genes in HMEC-1 cells over-expressing GPR30 and PATJ upon FSS

Change ratios (*x*-fold changes) are indicated in the column Ratio and *q* values at a 'false discovery' rate (FDR) of < 5%.

ILLUMINA ID	Gene ID	Gene Name	Ratio	q-value(%)
ILMN_1736760	KRT16	KERATIN 16 (FOCAL NON-EPIDERMOLYTIC PALMOPLANTAR KERATODERMA)	10.95	0.00
ILMN_1787186	NOV	NEPHROBLASTOMA OVEREXPRESSED GENE	6.51	0.00
ILMN_1766264	PI16	PEPTIDASE INHIBITOR 16	5.27	0.00
ILMN_1669046	FOXQ1	FORKHEAD BOX Q1	3.87	0.00
ILMN_1802205	RHOB	RAS HOMOLOG GENE FAMILY, MEMBER B	3.83	0.00
ILMN_1796423	CLIC3	CHLORIDE INTRACELLULAR CHANNEL 3	3.57	0.00
ILMN_1844408	PLXNA2	PLEXIN A2	3.55	0.00
ILMN_1799575	IL19	INTERLEUKIN 19	3.30	0.00
ILMN_2137789	KLF4	KRUPPEL-LIKE FACTOR 4 (GUT)	3.27	0.00
ILMN_1665035	KRT14	KERATIN 14 (EPIDERMOLYSIS BULLOSA SIMPLEX, DOWLING-MEARA, KOEBNER)	3.27	0.00
ILMN_1738742	PLAT	PLASMINOGEN ACTIVATOR, TISSUE	2.94	0.00
ILMN_1765446	EMP3	EPITHELIAL MEMBRANE PROTEIN 3	2.94	0.00
ILMN_1762529	SLC12A8	HYPOTHETICAL PROTEIN FLJ23188	2.90	0.00
ILMN_1712545	S100A3	S100 CALCIUM BINDING PROTEIN A3	2.90	0.00
ILMN_1708534	PAX8	PAIRED BOX GENE 8	2.88	0.00
ILMN_1684306	S100A4	S100 CALCIUM BINDING PROTEIN A4 (CALCIUM PROTEIN, CALVASCULIN, METASTASIN, MURINE PLACENTAL HOMOLOG)	2.82	0.00
ILMN_1696048	C13orf33	HYPOTHETICAL PROTEIN FLJ14834	2.74	0.00
ILMN_2327860	MAL	MAL, T-CELL DIFFERENTIATION PROTEIN	2.54	0.00
ILMN_1693338	CYP1B1	CYTOCHROME P450, FAMILY 1, SUBFAMILY B, POLYPEPTIDE 1	2.53	0.00
ILMN_2111237	MN1	MENINGIOMA (DISRUPTED IN BALANCED TRANSLOCATION) 1	2.50	0.00
ILMN_2387214	PALM	PARALEMMIN	2.35	0.00
ILMN_1657111	C14orf78	CHROMOSOME 14 OPEN READING FRAME 78	2.33	0.00
ILMN_1743367	FZD4	FRIZZLED HOMOLOG 4 (DROSOPHILA)	2.30	0.00
ILMN_1711786	NFE2	NUCLEAR FACTOR (ERYTHROID-DERIVED 2), 45KDA	2.28	0.00
ILMN_2407703	SYN1	SYNAPSIN I	2.26	0.00
ILMN_1688780	S100A4	S100 CALCIUM BINDING PROTEIN A4 (CALCIUM PROTEIN, CALVASCULIN, METASTASIN, MURINE PLACENTAL HOMOLOG)	2.26	0.00
ILMN_1714445	SLC6A9	SOLUTE CARRIER FAMILY 6 (NEUROTRANSMITTER TRANSPORTER, GLYCINE), MEMBER 9	2.25	0.00
ILMN_1763837	ANPEP	ALANYL (MEMBRANE) AMINOPEPTIDASE (AMINOPEPTIDASE N, AMINOPEPTIDASE M, MICROSOMAL AMINOPEPTIDASE, CD13, P150)	2.24	0.00
ILMN_2352097	GPR56	G PROTEIN-COUPLED RECEPTOR 56	2.23	0.00
ILMN_1769201	ELF3	E74-LIKE FACTOR 3 (ETS DOMAIN TRANSCRIPTION FACTOR, EPITHELIAL-SPECIFIC)	2.20	0.00
ILMN_2148527	H19	H19, IMPRINTED MATERNALLY EXPRESSED UNTRANSLATED MRNA	2.17	0.00
ILMN_1758067	RGS4	REGULATOR OF G-PROTEIN SIGNALLING 4	2.13	0.00
ILMN_2384122	GPR56	G PROTEIN-COUPLED RECEPTOR 56	2.12	0.00
ILMN_1701424	LAMC2	LAMININ, GAMMA 2	2.11	0.00
ILMN_1677273	TH	TYROSINE HYDROXYLASE	2.11	0.00
ILMN_1735930	KLF2	KRUPPEL-LIKE FACTOR 2 (LUNG)	2.10	0.00
ILMN_1775501	IL1B	INTERLEUKIN 1, BETA	2.06	0.00
ILMN_1714170	SPSB1	SPLA/RYANODINE RECEPTOR DOMAIN AND SOCS BOX CONTAINING 1	2.02	0.00

ILMN_1772821	KIAA1671	KIAA1671 PROTEIN	2.02	0.00
ILMN_2308903	WFDC3	WAP FOUR-DISULFIDE CORE DOMAIN 3	2.00	0.00
ILMN_2113490	NTN4	NETRIN 4	1.97	0.00
ILMN_1679929	KLF13	KRUPPEL-LIKE FACTOR 13	1.96	0.00
ILMN_1726597	C6orf32	CHROMOSOME 6 OPEN READING FRAME 32	1.95	0.00
ILMN_2150851	SERPINB2	SERPIN PEPTIDASE INHIBITOR, CLADE B (OVALBUMIN), MEMBER 2	1.95	0.00
ILMN_1774685	IL24	INTERLEUKIN 24	1.94	0.00
ILMN_1756595	SH3TC1	SH3 DOMAIN AND TETRATRICOPEPTIDE REPEATS 1	1.94	0.00
ILMN_1701461	TIMP3	TIMP METALLOPEPTIDASE INHIBITOR 3 (SORSBY FUNDUS DYSTROPHY, PSEUDOINFLAMMATORY)	1.94	0.00
ILMN_2356578	TH	TYROSINE HYDROXYLASE	1.94	0.00
ILMN_1669362	IGFBP6	INSULIN-LIKE GROWTH FACTOR BINDING PROTEIN 6	1.92	0.00
ILMN_1771627	ZMIZ1	RETINOIC ACID INDUCED 17	1.91	0.00
ILMN_1761968	PPP1R14A	PROTEIN PHOSPHATASE 1, REGULATORY (INHIBITOR) SUBUNIT 14A	1.89	0.00
ILMN_2376403	TSC22D3	TSC22 DOMAIN FAMILY, MEMBER 3	1.88	0.00
ILMN_2413158	PODXL	PODOCALYXIN-LIKE	1.85	0.00
ILMN_1668960	MID1IP1	MID1 INTERACTING PROTEIN 1 (GASTRULATION SPECIFIC G12-LIKE (ZEBRAFISH))	1.83	0.00
ILMN_2383077	SLC39A7	SOLUTE CARRIER FAMILY 39 (ZINC TRANSPORTER), MEMBER 7	1.81	0.00
ILMN_1689431	APCDD1L	HYPOTHETICAL PROTEIN FLJ90166	1.79	0.00
ILMN_1691376	JAG1	JAGGED 1 (ALAGILLE SYNDROME)	1.79	0.00
ILMN_1732197	MN1	MENINGIOMA (DISRUPTED IN BALANCED TRANSLOCATION) 1	1.78	0.00
ILMN_1657708	MGLL	MONOGLYCERIDE LIPASE	1.78	0.00
ILMN_1738589	MGLL	MONOGLYCERIDE LIPASE	1.77	0.00
ILMN_2337058	PORCN	PORCUPINE HOMOLOG (DROSOPHILA)	1.77	0.00
ILMN_1737406	KLF6	KRUPPEL-LIKE FACTOR 6	1.76	0.00
ILMN_2399174	TRAK1	TRAFFICKING PROTEIN, KINESIN BINDING 1	1.76	0.00
ILMN_1748124	TSC22D3	TSC22 DOMAIN FAMILY, MEMBER 3	1.74	0.00
ILMN_1812926	ANTXR2	ANTHRAX TOXIN RECEPTOR 2	1.74	0.00
ILMN_2314169	PTHLH	PARATHYROID HORMONE-LIKE HORMONE	1.74	0.00
ILMN_1709674	GFPT2	GLUTAMINE-FRUCTOSE-6-PHOSPHATE TRANSAMINASE 2	1.74	0.00
ILMN_1769876	TBC1D2	TBC1 DOMAIN FAMILY, MEMBER 2	1.72	0.00
ILMN_1787567	TSC22D1	TSC22 DOMAIN FAMILY, MEMBER 1	1.71	0.00
ILMN_1687978	PHLDA1	PLECKSTRIN HOMOLOGY-LIKE DOMAIN, FAMILY A, MEMBER 1	1.70	0.00
ILMN_1669376	DRAM	HYPOTHETICAL PROTEIN FLJ11259	1.70	0.00
ILMN_1735014	KLF6	KRUPPEL-LIKE FACTOR 6	1.70	0.00
ILMN_1690170	CRABP2	CELLULAR RETINOIC ACID BINDING PROTEIN 2	1.66	0.00
ILMN_1724789	CD59	CD59 ANTIGEN, COMPLEMENT REGULATORY PROTEIN	1.66	0.00
ILMN_1754842	DLGAP4	DISCS, LARGE (DROSOPHILA) HOMOLOG-ASSOCIATED PROTEIN 4	1.65	0.00
ILMN_1760412	SHISA2	TRANSMEMBRANE PROTEIN 46	1.64	0.00
ILMN_1761425	OLFML2A	OLFACTOMEDIN-LIKE 2A	1.64	0.00
ILMN_1671478	CKB	CREATINE KINASE, BRAIN	1.63	0.00
ILMN_1815023	PIM1	PIM-1 ONCOGENE	1.62	0.00
ILMN_1666893	TRIML2	HYPOTHETICAL PROTEIN FLJ25801	1.61	0.00
ILMN_1652777	CDC42EP2	CDC42 EFFECTOR PROTEIN (RHO GTPASE BINDING) 2	1.59	0.00
ILMN_2066151	TEK	TEK TYROSINE KINASE, ENDOTHELIAL (VENOUS MALFORMATIONS, MULTIPLE CUTANEOUS AND MUCOSAL)	1.58	0.00
ILMN_1673113	F2RL1	COAGULATION FACTOR II (THROMBIN) RECEPTOR-LIKE 1	1.58	0.00
ILMN_1807652	STRA6	STIMULATED BY RETINOIC ACID GENE 6 HOMOLOG (MOUSE)	1.56	0.00
ILMN_2380237	C1QTNF1	G PROTEIN COUPLED RECEPTOR INTERACTING PROTEIN, COMPLEMENT-C1Q TUMOR NECROSIS FACTOR-RELATED	1.55	0.00
ILMN_1679262	DPYSL3	DIHYDROPYRIMIDINASE-LIKE 3	1.54	0.00
ILMN_2041190	F2RL1	COAGULATION FACTOR II (THROMBIN) RECEPTOR-LIKE 1	1.54	0.00
ILMN_1672102	PTPRB	PROTEIN TYROSINE PHOSPHATASE, RECEPTOR TYPE, B	1.54	0.00

ILMN_1700001	TCTA	T-CELL LEUKEMIA TRANSLOCATION ALTERED GENE	1.53	0.00
ILMN_1784287	TGFBR3	TRANSFORMING GROWTH FACTOR, BETA RECEPTOR III (BETAGLYCAN, 300KDA)	1.51	0.00
ILMN_1670926	GALNAC4S-6ST	KIAA0598 GENE PRODUCT	1.49	0.00
ILMN_1772612	ANGPTL2	ANGIOPOIETIN-LIKE 2	1.41	0.00
ILMN_2374036	CTSL1	CATHEPSIN L	1.40	0.00
ILMN_1805466	SOX9	SRY (SEX DETERMINING REGION Y)-BOX 9 (CAMPOMELIC DYSPLASIA, AUTOSOMAL SEX-REVERSAL)	1.38	0.00
ILMN_1659316	HEPACAM	HEPATOCYTE CELL ADHESION MOLECULE	8.50	0.61
ILMN_1675453	HHIP	HEDGEHOG INTERACTING PROTEIN	2.65	0.61
ILMN_1676689	PPT2	PALMITOYL-PROTEIN THIOESTERASE 2	2.32	0.61
ILMN_2351466	HNT	NEUROTRIMIN	2.30	0.61
ILMN_2096719	GRK5	G PROTEIN-COUPLED RECEPTOR KINASE 5	2.19	0.61
ILMN_1704154	TNFRSF19	TUMOR NECROSIS FACTOR RECEPTOR SUPERFAMILY, MEMBER 19	2.15	0.61
ILMN_1809931	NDRG1	N-MYC DOWNSTREAM REGULATED GENE 1	2.10	0.61
ILMN_1793474	INSIG1	INSULIN INDUCED GENE 1	2.05	0.61
ILMN_2401822	FTSJ1	FTSJ HOMOLOG 1 (E. COLI)	1.96	0.61
ILMN_1894911		FLJ45933 PROTEIN	1.95	0.61
ILMN_1807689	PKNOX2	PBX/KNOTTED 1 HOMEOBOX 2	1.89	0.61
ILMN_1665865	IGFBP4	INSULIN-LIKE GROWTH FACTOR BINDING PROTEIN 4	1.85	0.61
ILMN_1761540	SEMA3F	SEMA DOMAIN, IMMUNOGLOBULIN DOMAIN (IG), SHORT BASIC DOMAIN, SECRETED, (SEMAPHORIN) 3F	1.84	0.61
ILMN_1700690	VAT1	VESICLE AMINE TRANSPORT PROTEIN 1 HOMOLOG (T CALIFORNICA)	1.78	0.61
ILMN_1803811	TRIB1	TRIBBLES HOMOLOG 1 (DROSOPHILA)	1.77	0.61
ILMN_1714592	CDA	CYTIDINE DEAMINASE	1.75	0.61
ILMN_2161746	TRIP10	THYROID HORMONE RECEPTOR INTERACTOR 10	1.72	0.61
ILMN_1803277	MVP	MAJOR VAULT PROTEIN	1.70	0.61
ILMN_1728049	S100A16	S100 CALCIUM BINDING PROTEIN A16	1.70	0.61
ILMN_1791447	CXCL12	CHEMOKINE (C-X-C MOTIF) LIGAND 12 (STROMAL CELL-DERIVED FACTOR 1)	1.69	0.61
ILMN_1659599	ADC	ARGININE DECARBOXYLASE	1.67	0.61
ILMN_1803818	NMNAT2	NICOTINAMIDE NUCLEOTIDE ADENYLYLTRANSFERASE 2	1.67	0.61
ILMN_1673363	CD97	CD97 ANTIGEN	1.65	0.61
ILMN_1751576	TEK	TEK TYROSINE KINASE, ENDOTHELIAL (VENOUS MALFORMATIONS, MULTIPLE CUTANEOUS AND MUCOSAL)	1.64	0.61
ILMN_1753413	TRIOBP	TRIO AND F-ACTIN BINDING PROTEIN	1.64	0.61
ILMN_1694432	CRIP2	CYSTEINE-RICH PROTEIN 2	1.64	0.61
ILMN_1688480	CCND1	CYCLIN D1	1.63	0.61
ILMN_1715684	LAMB3	LAMININ, BETA 3	1.63	0.61
ILMN_1723048	GJC2	GAP JUNCTION PROTEIN, ALPHA 12, 47KDA	1.63	0.61
ILMN_1695423	CD9	CD9 ANTIGEN (P24)	1.62	0.61
ILMN_1715969	SLC25A37	SOLUTE CARRIER FAMILY 25, MEMBER 37	1.60	0.61
ILMN_1798256	UPP1	URIDINE PHOSPHORYLASE 1	1.59	0.61
ILMN_2082585	SNAI2	SNAIL HOMOLOG 2 (DROSOPHILA)	1.59	0.61
ILMN_1803825	CXCL12	CHEMOKINE (C-X-C MOTIF) LIGAND 12 (STROMAL CELL-DERIVED FACTOR 1)	1.56	0.61
ILMN_1651799	SLC38A2	SOLUTE CARRIER FAMILY 38, MEMBER 2	1.56	0.61
ILMN_1719236	CDH5	CADHERIN 5, TYPE 2, VE-CADHERIN (VASCULAR EPITHELIUM)	1.51	0.61
ILMN_1678215	RHOJ	RAS HOMOLOG GENE FAMILY, MEMBER J	1.50	0.61
ILMN_1812031	PALM	PARALEMMIN	1.49	0.61
ILMN_1786722	ZNF385A	ZINC FINGER PROTEIN 385	1.46	0.61
ILMN_1684210	NPAL3	NIPA-LIKE DOMAIN CONTAINING 3	1.43	0.61
ILMN_1732923	SIPA1L2	SIGNAL-INDUCED PROLIFERATION-ASSOCIATED 1 LIKE 2	1.43	0.61
ILMN_2289924	TRAK1	TRAFFICKING PROTEIN, KINESIN BINDING 1	1.42	0.61
ILMN_1685580	CBLB	CAS-BR-M (MURINE) ECOTROPIC RETROVIRAL TRANSFORMING SEQUENCE B	1.42	0.61

ILMN_1750664	PPT2	PALMITOYL-PROTEIN THIOESTERASE 2	1.42	0.61
ILMN_1745223	CDC42EP4	CDC42 EFFECTOR PROTEIN (RHO GTPASE BINDING) 4	1.40	0.61
ILMN_1680738	C5orf13	CHROMOSOME 5 OPEN READING FRAME 13	1.39	0.61
ILMN_1735052	ULK1	UNC-51-LIKE KINASE 1 (C. ELEGANS)	1.39	0.61
ILMN_1812995	CTSL1	CATHEPSIN L	1.37	0.61
ILMN_1778681	EBF1	EARLY B-CELL FACTOR	1.23	0.61
ILMN_1703946	ADORA2B	ADENOSINE A2B RECEPTOR	1.23	0.61
ILMN_1680814	EDN2	ENDOTHELIN 2	2.41	1.03
ILMN_1800512	HMOX1	HEME OXYGENASE (DECYCLING) 1	2.22	1.03
ILMN_1712708	TRIM47	TRIPARTITE MOTIF-CONTAINING 47	2.15	1.03
ILMN_1717793	C19orf33	CHROMOSOME 19 OPEN READING FRAME 33	2.06	1.03
ILMN_1772074	C19orf51	SIMILAR TO HYPOTHETICAL TESTIS PROTEIN FROM MACAQUE	1.96	1.03
ILMN_1775268	HECW2	HECT, C2 AND WW DOMAIN CONTAINING E3 UBIQUITIN PROTEIN LIGASE 2	1.83	1.03
ILMN_1732609	KIAA1539	KIAA1539 PROTEIN	1.79	1.03
ILMN_1760778	ENG	ENDOGLIN (OSLER-RENDU-WEBER SYNDROME 1)	1.79	1.03
ILMN_1750101	S100A11	S100 CALCIUM BINDING PROTEIN A11 (CALGIZZARIN)	1.78	1.03
ILMN_1741404	MSC	MUSCULIN (ACTIVATED B-CELL FACTOR-1)	1.77	1.03
ILMN_1701655	SLC24A6	SOLUTE CARRIER FAMILY 24 (SODIUM/POTASSIUM/CALCIUM EXCHANGER), MEMBER 6	1.75	1.03
ILMN_1708041	PLEKHF1	PLECKSTRIN HOMOLOGY DOMAIN CONTAINING, FAMILY F (WITH FYVE DOMAIN) MEMBER 1	1.69	1.03
ILMN_1661194	CLDN14	CLAUDIN 14	1.68	1.03
ILMN_1774602	FBLN2	FIBULIN 2	1.66	1.03
ILMN_1742789	LPXN	LEUPAXIN	1.59	1.03
ILMN_1746013	SPOCK1	SPARC/OSTEONECTIN, CWCV AND KAZAL-LIKE DOMAINS PROTEOGLYCAN (TESTICAN) 1	1.43	1.03
ILMN_1756935	OSBPL6	OSBP-RELATED PROTEIN 6	1.43	1.03
ILMN_1770338	TM4SF1	TRANSMEMBRANE 4 L SIX FAMILY MEMBER 1	1.42	1.03
ILMN_2199389	VIPR1	VASOACTIVE INTESTINAL PEPTIDE RECEPTOR 1	1.39	1.03
ILMN_1700384	KIAA1522	KIAA1522	1.38	1.03
ILMN_1665510	ERRFI1	ERBB RECEPTOR FEEDBACK INHIBITOR 1	1.27	1.03
ILMN_1717809	RNF24	RING FINGER PROTEIN 24	1.23	1.03
ILMN_1756928	RTN1	RETICULON 1	8.00	1.68
ILMN_1665449	ROBO4	ROUNDABOUT HOMOLOG 4, MAGIC ROUNDABOUT (DROSOPHILA)	3.77	1.68
ILMN_1748751	NLF2	NUCLEAR LOCALIZED FACTOR 2	2.75	1.68
ILMN_1760160	STX1A	SYNTAXIN 1A (BRAIN)	2.26	1.68
ILMN_1685699	PRSS3	PROTEASE, SERINE, 3 (MESOTRYPSIN)	2.01	1.68
ILMN_1696316	CPT1A	CARNITINE PALMITOYLTRANSFERASE 1A (LIVER)	1.83	1.68
ILMN_1744268	PLEC1	PLECTIN 1, INTERMEDIATE FILAMENT BINDING PROTEIN 500KDA	1.81	1.68
ILMN_2344373	MVP	MAJOR VAULT PROTEIN	1.79	1.68
ILMN_1739238	L1CAM	L1 CELL ADHESION MOLECULE	1.79	1.68
ILMN_1671142	GPR68	G PROTEIN-COUPLED RECEPTOR 68	1.65	1.68
ILMN_1763638	BCAR3	BREAST CANCER ANTI-ESTROGEN RESISTANCE 3	1.63	1.68
ILMN_1678904	ENO3	ENOLASE 1, (ALPHA)	1.54	1.68
ILMN_1764850	HPCAL1	HIPPOCALCIN-LIKE 1	1.49	1.68
ILMN_1702171	LPCAT1	ACYLTRANSFERASE LIKE 2	1.49	1.68
ILMN_1669617	GRB10	GROWTH FACTOR RECEPTOR-BOUND PROTEIN 10	1.43	1.68
ILMN_1751656	KLF11	KRUPPEL-LIKE FACTOR 11	1.40	1.68
ILMN_2197128	OSR1	ODD-SKIPPED RELATED 1 (DROSOPHILA)	1.39	1.68
ILMN_1755364	RALA	V-RAL SIMIAN LEUKEMIA VIRAL ONCOGENE HOMOLOG A (RAS RELATED)	1.22	1.68
ILMN_1741917	OSCAR	OSTEOCLAST-ASSOCIATED RECEPTOR	1.18	1.68
ILMN_2348788	CD44	CD44 ANTIGEN (INDIAN BLOOD GROUP)	1.17	1.68
ILMN_1660942	LOC653352	SIMILAR TO EUKARYOTIC TRANSLATION INITIATION FACTOR 3, SUBUNIT 8	6.21	2.44
ILMN_2046750	PGLYRP3	PEPTIDOGLYCAN RECOGNITION PROTEIN 3	4.86	2.44

ILMN_2276952	TSC22D3	TSC22 DOMAIN FAMILY, MEMBER 3	4.48	2.44
ILMN_1686989	INSIG1	INSULIN INDUCED GENE 1	2.91	2.44
ILMN_1666924	PINK1	PTEN INDUCED PUTATIVE KINASE 1	2.44	2.44
ILMN_1803728	SLC35E4	SOLUTE CARRIER FAMILY 35, MEMBER E4	2.23	2.44
ILMN_1768391	ARL4C	ADP-RIBOSYLATION FACTOR-LIKE 4C	2.18	2.44
ILMN_1689037	LIPG	LIPASE, ENDOTHELIAL	2.00	2.44
ILMN_1689111	CXCL12	CHEMOKINE (C-X-C MOTIF) LIGAND 12 (STROMAL CELL-DERIVED FACTOR 1)	1.83	2.44
ILMN_1692177	TSC22D1	TSC22 DOMAIN FAMILY, MEMBER 1	1.83	2.44
ILMN_1801516	GPC1	GLYPICAN 1	1.73	2.44
ILMN_1815130	MICALL1	MICAL-LIKE 1	1.64	2.44
ILMN_2390919	FBLN2	FIBULIN 2	1.62	2.44
ILMN_2355225	LSP1	LYMPHOCYTE-SPECIFIC PROTEIN 1	1.51	2.44
ILMN_1725852	S100A2	S100 CALCIUM BINDING PROTEIN A2	1.50	2.44
ILMN_2315780	TACC2	TRANSFORMING, ACIDIC COILED-COIL CONTAINING PROTEIN 2	1.49	2.44
ILMN_2401873	DUSP10	DUAL SPECIFICITY PHOSPHATASE 10	1.48	2.44
ILMN_1742332	KCTD12	POTASSIUM CHANNEL TETRAMERISATION DOMAIN CONTAINING 12	1.48	2.44
ILMN_1684576	CLN8	CEROID-LIPOFUSCINOSIS, NEURONAL 8 (EPILEPSY, PROGRESSIVE WITH MENTAL RETARDATION)	1.46	2.44
ILMN_1798360	CXCR7	CHEMOKINE ORPHAN RECEPTOR 1	1.42	2.44
ILMN_1713829	PTGES	PROSTAGLANDIN E SYNTHASE	1.42	2.44
ILMN_1661755	FAM129B	CHROMOSOME 9 OPEN READING FRAME 88	1.41	2.44
ILMN_1791679	DNER	DELTA-NOTCH-LIKE EGF REPEAT-CONTAINING TRANSMEMBRANE	1.41	2.44
ILMN_1685397	ITGA3	INTEGRIN, ALPHA 3 (ANTIGEN CD49C, ALPHA 3 SUBUNIT OF VLA-3 RECEPTOR)	1.39	2.44
ILMN_1802808	LOC654103	SIMILAR TO SOLUTE CARRIER FAMILY 25, MEMBER 37	1.39	2.44
ILMN_1792495	AHNAK	AHNAK NUCLEOPROTEIN (DESMOYOKIN)	1.34	2.44
ILMN_1705144	ULK1	UNC-51-LIKE KINASE 1 (C. ELEGANS)	1.30	2.44
ILMN_1703487	LMO4	LIM DOMAIN ONLY 4	1.18	2.44
ILMN_1657077	SOCS6	SUPPRESSOR OF CYTOKINE SIGNALING 6	5.40	3.96
ILMN_1774761	CCR2	CHEMOKINE (C-C MOTIF) RECEPTOR 2	4.16	3.96
ILMN_1808777	EHD2	EH-DOMAIN CONTAINING 2	2.66	3.96
ILMN_1683607	CYP1A2	CYTOCHROME P450, FAMILY 1, SUBFAMILY A, POLYPEPTIDE 2	2.47	3.96
ILMN_1781867	FOXD4L1	FORKHEAD BOX D4-LIKE 1	2.45	3.96
ILMN_1708363	LOXL1	LYSYL OXIDASE-LIKE 1	2.35	3.96
ILMN_2129161	LRRC32	LEUCINE RICH REPEAT CONTAINING 32	2.22	3.96
ILMN_1653042	HSD3B7	HYDROXY-DELTA-5-STEROID DEHYDROGENASE, 3 BETA- AND STEROID DELTA-ISOMERASE 7	1.78	3.96
ILMN_1776395	ARMC4	ARMADILLO REPEAT CONTAINING 4	1.75	3.96
ILMN_1793729	C15orf39	DKFZP434H132 PROTEIN	1.73	3.96
ILMN_1666122	HEG1	HEG HOMOLOG 1 (ZEBRAFISH)	1.72	3.96
ILMN_2176502	UNC5B	UNC-5 HOMOLOG B (C. ELEGANS)	1.68	3.96
ILMN_1693515	EGFL8	PALMITOYL-PROTEIN THIOESTERASE 2	1.65	3.96
ILMN_1735045	A4GALT	ALPHA 1,4-GALACTOSYLTRANSFERASE (GLOBOTRIAOSYLCERAMIDE SYNTHASE)	1.64	3.96
ILMN_1706643	COL6A3	COLLAGEN, TYPE VI, ALPHA 3	1.61	3.96
ILMN_1794677	TMC6	TRANSMEMBRANE CHANNEL-LIKE 6	1.60	3.96
ILMN_1710514	BCL3	B-CELL CLL/LYMPHOMA 3	1.59	3.96
ILMN_1738558	RGS20	REGULATOR OF G-PROTEIN SIGNALLING 20	1.54	3.96
ILMN_1890614		CHROMOSOME 1 OPEN READING FRAME 183	1.53	3.96
ILMN_1661599	DDIT4	DNA-DAMAGE-INDUCIBLE TRANSCRIPT 4	1.51	3.96
ILMN_1778087	ANXA8	ANNEXIN A8	1.48	3.96
ILMN_2205999	OSMR	ONCOSTATIN M RECEPTOR	1.46	3.96
ILMN_1750338	C10orf47	CHROMOSOME 10 OPEN READING FRAME 47	1.45	3.96
ILMN_1775743	BTG1	B-CELL TRANSLOCATION GENE 1, ANTI-PROLIFERATIVE	1.39	3.96

ILMN_1680579	ATP2B4	ATPASE, CA++ TRANSPORTING, PLASMA MEMBRANE 4	1.38	3.96
ILMN_1794863	CAMK2N1	CALCIUM/CALMODULIN-DEPENDENT PROTEIN KINASE II INHIBITOR 1	1.34	3.96
ILMN_1687440	HIPK2	HOMEODOMAIN INTERACTING PROTEIN KINASE 2	1.30	3.96
ILMN_1729455	EML1	ECHINODERM MICROTUBULE ASSOCIATED PROTEIN LIKE 1	1.29	3.96
ILMN_2371458	CXCR7	CHEMOKINE ORPHAN RECEPTOR 1	1.28	3.96
ILMN_1756862	APOL3	TNF-INDUCIBLE PROTEIN CG12-1	1.22	3.96
ILMN_2307861	COL6A3	COLLAGEN, TYPE VI, ALPHA 3	1.15	3.96
ILMN_1705310	VEZF1	ZINC FINGER PROTEIN 161	1.15	3.96
ILMN_1671703	ACTA2	actin, alpha 2, smooth muscle, aorta	-2.27	0
ILMN_1725726	DHRS2	dehydrogenase/reductase (SDR family) member 2	-2.27	0
ILMN_1763382	NPPB	natriuretic peptide precursor B	-2.86	0
ILMN_1795325	ACTG2	actin, gamma 2, smooth muscle, enteric	-2.22	0

ACKNOWLEDGEMENTS

It is not possible to forget important people for something as special as my “PhD adventure”. Therefore, I would like to express my gratitude to:

Prof. Patricia Ruiz, “*mi jefa”*, for her unconditional support and our fruitful discussions about work and life matters throughout my PhD.

Ingram and Kerstin for offering me the ticket for this wonderful journey. Special thanks go to Ingram who will always remain “*il mio ex-capo*”.

The Marie Curie PhD programme, CARDIOVASC, in particular Dian and the fellows: Caterina, Nicolas, George and Catarina.

Prof. E. Prossnitz, Prof. B. Margolis and Dr. M. Ralser for supplying me with the vectors.

The Ruiz group, in particular, Luca and Jörg to be with me in this “GPR30 adventure”, especially Jörg for the knowledge transfer and for being so patient with me.

Dr. Kathleen Van Craenenbroeck for hosting me in her laboratory in Gent and for teaching me the co-IP protocol, without which I could not have performed my experiments.

The Dr. Kerstin Lehmann group for temporarily “adopting me” and introducing me to new techniques and methods. A special thanks to Philipp, Doreen, Julia, Robert and Franziska.

My Angel Alex, Kerstin, Karin, Luca, Karina and Mr. Woolley for proof-reading my work, and João for his help on formatting my thesis.

The international *“Esperanto-party-mensa”* group for the incredible time together and for the unconditional day and night support. A special thanks to Caterina, Karima, Dani and Ana.

All of my friends with special thanks to Alessandra, Enza and Valeria for always being PRESENT even though they were miles away…

The CCR for hosting me and my work. A special acknowledgment for the Christmas t-shirt gift “*Forschung ist die beste Medizin*”. A simple motto that helped me overcome some difficult research days!

My cousin Tecla for suggesting me books that helped me escape a bit from my thesis(-days)!

It is not even possible to express with words how I am grateful for the love and the support that my family showed me. *Grazie a Mamma, Papà, Francesco e Roberta*.

Last but not least, I would like to thank Henning Witt for his never ending support, and this from the very beginning of my PhD up to now. I could not have achieved this thesis without your enthusiasm and your assistance.

Valeria